TVA

Tennessee Valley Authority, 1101 Market Street, Chattanooga, TN 37402

CNL-16-162

October 21, 2016

10 CFR 2.101
10 CFR 52.15

ATTN: Document Control Desk
U.S. Nuclear Regulatory Commission
Washington, DC 20555-0001

> Clinch River Nuclear Site
> NRC Project No. 785

Subject: Submittal of Supplemental Information Related to Geologic Characterization Information, Surface Deformation, and Stability of Subsurface Materials and Foundation in Support of Early Site Permit Application for Clinch River Nuclear Site

References: 1. Letter from TVA to NRC, CNL-16-081, "Application for Early Site Permit for Clinch River Nuclear Site," dated May 12, 2016

                2. Letter from TVA to NRC, CNL-16-134, "Schedule for Submittal of Supplemental Information in Support of Early Site Permit Application for Clinch River Nuclear Site," dated August 11, 2016

By letter dated May 12, 2016 (Reference 1), Tennessee Valley Authority (TVA) submitted an application for an early site permit for the Clinch River Nuclear (CRN) Site in Oak Ridge, TN. Subsequent to the submittal of the application, and consistent with interactions with NRC staff, TVA identified certain aspects of the application that it intends to supplement. By letter dated August 11, 2016 (Reference 2), TVA provided a plan for submitting the identified supplemental information.
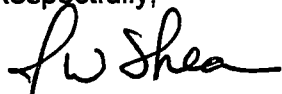
This letter provides supplemental information related to Geologic Characterization Information, Surface Deformation, and Stability of Subsurface Materials and Foundation as described in the Enclosure submitted in Reference 2. Specifically, Enclosures 1 through 3 of this letter provide specific supplemental information for each of these subject areas respectively, including markups of the affected Site Safety Analysis Report sections. Enclosure 4, a disk, provides copies of revised Site Vicinity Geologic Map Plates as discussed in the response to Enclosure 1, Geological Characterization Information, Supplemental Information A. These changes will be incorporated into a future revision of the Early Site Permit Application.

D 113
N RD

There are no new regulatory commitments associated with this submittal. If any additional information is needed, please contact Dan Stout at (423) 751-7642.

I declare under penalty of perjury that the foregoing is true and correct. Executed on this 21st day of October 2016.

Respectfully,

J. W. Shea
Vice President, Nuclear Licensing

Enclosures:

1. Supplemental Information Related to Geologic Characterization Information of the Early Site Permit Application for Clinch River Nuclear Site
2. Supplemental Information Related to Surface Deformation of the Early Site Permit Application for Clinch River Nuclear Site
3. Supplemental Information Related to Surface Deformation and Stability of Subsurface Materials and Foundation of the Early Site Permit Application for Clinch River Nuclear Site
4. CD-ROM, Revised Site Vicinity Geologic Map Plates

cc (Enclosures):

Project Manager, Division of New Reactor Licensing

cc (without Enclosures):

Executive Director of Operations
Regional Administrator, Region II
Deputy Executive Director for Reactor and Preparedness Programs
Director, Office of New Reactors
Director, Division of New Reactor Licensing
Branch Chief, Division of New Reactor Licensing
Project Manager, Division of New Reactor Licensing
Acting Assistant Secretary, Office of Nuclear Energy, Department of Energy
Deputy Assistant Secretary, Nuclear Reactor Technologies, Department of Energy
Light Water Reactor Technologies, Department of Energy
Program Manager, Licensing Technical Support Program, Department of Energy
Project Manager, Licensing Technical Support Program, Department of Energy
Regulatory Specialist, Eastern Regulatory Field Office, Nashville District,
    U.S. Army Corps of Engineers

bcc (without Enclosures):

M. A. Balduzzi
G. A. Boerschig
S. M. Bono
K. H. Bronson
D. M. Czufin
R. E. Detwiler
J. P. Grimes
P. S. Hastings
E. K. Henderson
J. M. Holcomb
J. N. Perry
J. T. Polickoski
E. D. Schrull
J. W. Shea
D. P. Stout
S. A. Vance
B. A. Wetzel
P. R. Wilson
ECM

ENCLOSURE 1

SUPPLEMENTAL INFORMATION RELATED TO
GEOLOGIC CHARACTERIZATION INFORMATION
OF THE EARLY SITE PERMIT APPLICATION FOR CLINCH RIVER NUCLEAR SITE

By letter dated May 12, 2016 (Reference 1), Tennessee Valley Authority (TVA) submitted an application for an early site permit for the Clinch River Nuclear (CRN) Site in Oak Ridge, TN. Subsequent to the submittal of the application, and consistent with interactions with NRC staff, TVA identified certain aspects of the application that it intends to supplement. By letter dated August 11, 2016 (Reference 2), TVA provided a plan for submitting the identified supplemental information.

This enclosure provides supplemental information related to Geologic Characterization Information to support the NRC staff's review. This enclosure also includes proposed changes to the affected Site Safety Analysis Report (SSAR) sections. An Early Site Permit Application (ESPA) Change Request has been initiated to incorporate these changes into a future revision of the ESPA.

Supplement Item A (Reference 2)

A. *TVA will provide a markup of the applicable Early Site Permit Application (ESPA) sections to more fully characterize the Chestnut Ridge Fault. TVA will provide sufficient data or information in the applicable ESPA sections to support age estimates or extent.*

TVA's markup will demonstrate that this fault does not represent potentially significant seismic or surface deformation hazards at the site, and will include:

- *A complete discussion of Lemiszki, et al (2013) basis for a fault interpretation,*
- *Details on structural style and kinematics that clearly relate this fault to Alleghanian orogeny or more recent tectonism,*
- *Results of a field review of Quaternary alluvial deposits and river terraces overlying the fault that demonstrate deformation, or not, and*
- *Appropriate maps and cross-sections (based on borehole data) to illustrate the final interpretation.*

Supplemental Information A

To address the information above, the following text will completely replace the existing text in Site Safety Analysis Report (SSAR) Subsections 2.5.1.2.4.2.4, "Chestnut Ridge Fault," and 2.5.3.2.5.3, "Evaluation of Terrace Profiles and Quaternary Surface Deformation." This text describes more recent mapping by Peter Lemiszki of the Tennessee Geological Survey and includes updates to the previous mapping along the Chestnut Ridge fault.

Plates 1 and 2a through 2d (included in Part 8 of the ESPA) and subsequent figures that are based on the compiled geologic maps of the CRN site vicinity and site have been updated accordingly and included as Enclosure 4 of this letter. Additionally, Figures 2.5.1-14 and 2.5.1-47 have been updated to reflect the most recent Lemiszki mapping. Copies of the updated figures are included in this enclosure.

References:

1. Letter from TVA to NRC, CNL-16-081, "Application for Early Site Permit for Clinch River Nuclear Site," dated May 12, 2016

2. Letter from TVA to NRC, CNL-16-134, "Schedule for Submittal of Supplemental Information in Support of Early Site Permit Application for Clinch River Nuclear Site," dated August 11, 2016

The following text replaces the existing SSAR Subsection 2.5.1.2.4.2.4 in its entirety:

2.5.1.2.4.2.4 Chestnut Ridge Fault

The Chestnut Ridge fault (CRF) was originally mapped by Lemiszki et al. (Reference 2.5.1-97) as a subordinate, small displacement, thrust fault approximately 1.5 miles long and located 0.5 miles west of the site and southwest of the Clinch River but within the site location (0.6-mile radius). The CRF is mapped as NE-SW trending, striking parallel to bedding and the major through-going thrust faults associated with the Alleghenian orogeny in the Valley and Ridge fold and thrust belt. The CRF is discontinuous and located based primarily on the repetition of geologic units within the Knox Group as determined by mapping loose pieces of bedrock along the ground surface (float mapping). The Kingsport Formation of the Knox Group contains an interval of thick to massive bedded chert which creates a resistant ridge parallel to bedding which makes float mapping of this unit more certain. There is no exposure of the CRF at the ground surface; thus, there are no direct observations of kinematic data from the fault plane.

This previous geologic mapping of the area around the CRF was updated in 2015 by the Tennessee Geological Survey (References 2.5.1-282 and 2.5.1-283). This recent mapping is included on Figures 2.5.1-29, 2.5.1-34, 2.5.1-37 and Plates 1 and 2 in Part 8 of the ESPA. The Tennessee Geological Survey now shows the CRF as extending farther to the northeast, approximately 2000 feet northwest of the site. The total length of the CRF is now mapped as 2.8 miles long, but is limited to the Geologic Map of the Elverton Quadrangle (Reference 2.5.1-282). The neighboring Bethel Valley Quadrangle has not been updated, but the CRF reportedly extends into this area north of the CRN Site. The recent geologic mapping bases the northeast extension of the CRF on a few geologic and geomorphic inconsistencies including; thickening of the Mascot Formation on the neighboring Bethel Valley Quadrangle, a minor topographic ridge, and some bedrock dipping angles that are steeper than the regional trend.

Based on mapping performed for the CRN Site ESPA (see Figure 2.5.1-25), the regional trend and structural style of the CRF is similar to the major through going thrust faults associated with the Alleghanian orogeny in the Valley and Ridge fold and thrust belt. However, the CRF does not juxtapose rock types with significant stratigraphic or temporal differences, nor is it associated with significant structural shortening. The CRF strikes parallel to regional bedding at approximately N50°E and is depicted in Figures 2.5.1-35, 2.5.1-37, and 2.5.1-64 as a southeast-dipping bedding plane thrust fault with relatively minor displacement. Regional mapping of the geometry of more extensively mapped faults, such as the Whiteoak Mountain fault by the Tennessee Geological Survey, suggest the dip of the CRF may steepen from approximately 35° at depth, to approximately 50° near the ground surface based on steeper bedrock dipping angles (Figure 2.5.1-64 and Plate 2 in Part 8 of the ESPA). The relatively steep dip of the CRF can be kinematically described as the result of passive rotation of the hanging wall of the Whiteoak Mountain fault as the hanging wall block climbed the footwall ramp during Alleghanian deformation of the Valley and Ridge. This suggests that the CRF may pre-date much of the motion on the Whiteoak Mountain fault and accommodated crustal shortening along bedding planes due to deformation associated with the Alleghanian orogeny. The CRF and other subordinate faults associated with Paleozoic Alleghanian orogeny in the Valley and Ridge, such as the "unnamed fault" shown on Figure 2.5.1-64 and Plate 2 in Part 8 of the ESPA (Reference 2.5.1-282), are a byproduct of the crustal shortening within the Alleghanian foreland fold-thrust belt.

As a result of the replaced text in Subsection 2.5.1.2.4.2.4, the following references are added to SSAR Subsection 2.5.1.3:

2.5.1.3   References

2.5.1-282.   Lemiszki, P. J., *Geologic Map of the Elverton Quadrangle, Tennessee*, Draft Open File Map, scale 1:24,000, 2015.

2.5.1-283.   Lemiszki, P. J., *Geologic Map of the Lovell Quadrangle, Tennessee*, Draft Open File Map, scale 1:24,000, 2013.

The following text replaces the existing SSAR Subsection 2.5.3.2.5.3 in its entirety:

2.5.3.2.5.3 Evaluation of Terrace Profiles and Quaternary Surface Deformation

Detailed mapping of fluvial terraces along the Clinch River from field reconnaissance and interpretation of recently acquired LiDAR was used to evaluate the presence or absence of Quaternary faulting at the CRN Site. Evidence for surface faulting in the Quaternary is often expressed by subtle deformation of geomorphic landforms, including river terraces, and is commonly recorded as anomalies in longitudinal stream and terrace profiles. LiDAR data allowed detailed mapping of Clinch River terraces across the Site Area (Plates 2a-2d in Part 8 of the ESPA and Figure 2.5.3-2) and evaluation of the relative ages of terrace levels using morphological correlation and longitudinal profiling (Figure 2.5.3-4). Evidence for Quaternary surface faulting in the Site Area was evaluated in two ways: (1) examination of Pleistocene terrace surfaces that directly overlie the mapped trace of faults; and (2) evaluation of longitudinal terrace profiles for systematic, along-profile irregularities that would suggest repeated fault displacements.

Fluvial terraces along the Clinch River overlie the concealed trace of each of the five mapped Alleghanian thrust faults within the site area (Plates 2a through 2d in Part 8 of the ESPA and Figure 2.5.3-2) as well as the projected trace of the shear-fracture zone feature discussed in SSAR Subsection 2.5.1.2.4.3.4. A fault surface rupture that post-dates the formation and deposition of the overlying terrace would deform the terrace surface. If these faults were reactivated in the contemporary regional stress regime of the CEUS (NE-SW principal stress axis), their orientation would predict right oblique reverse displacement. Cumulative displacement of the terrace would produce a topographic scarp or warp on the terrace surface.

Clinch River terrace surfaces overlie a portion of the concealed trace of each of the five mapped Alleghanian thrust faults within the site area (Plates 2a through 2d, Figures 2.5.3-2 and 2.5.3-6). The Copper Creek fault is directly overlain by Qht1, Qht2, and Qht3 terraces (Figure 2.5.3-3); the northeastern projection of the Chestnut Ridge fault is overlain by Qht2 within the site area and Qpt2 northeast of the 0.6-mile site radius (Figures 2.5.3-2 and 2.5.3-7); the Whiteoak Mountain fault is overlain by Qht2 and Qpt2 terraces; and two unnamed faults of Lemiszki (Reference 2.5.3-56) are overlain by Qht1, Qht2, Qht3, Qpt1, and Qpt2 terraces (Figure 2.5.3-8). The projected trace of the shear-fracture zone (in the Eidson Member of the Lincolnshire Formation) is overlain by Qpt2 (Figure 2.5.3-9). While each of these terrace surfaces have some amount of topographic erosion and anthropogenic alteration, none of them display any linear topographic features or warping of the terrace profile suggestive of surface deformation as a result of repeated faulting. Furthermore, interpretation of LiDAR data documents the absence of any geomorphic lineament, scarps, sag ponds, or other features typically associated with an active Quaternary fault within the site area.

As discussed above, absolute age data for terraces in the site area is sparse, however relative age of terrace levels was interpreted from morphological position and longitudinal profiling (Figure 2.5.3-4). The longitudinal profiles of terrace levels presented in Figure 2.5.3-4 provide another means to assess irregularities that could be associated with repeated fault surface rupture. Repeated thrust faulting and relative uplift would result in increased incision and terrace formation in the hanging wall of the faults. The consistent number of terraces levels with similar longitudinal profile slopes that can be correlated across the site area document the absence of discernible Quaternary displacement along all of the Alleghanian thrust faults in the site area.

As a result of the replaced text in Subsection 2.5.3.2.5.3, the following reference is added to SSAR Subsection 2.5.3.9:

2.5.3.9   References

2.5.3-56.   Lemiszki, P. J., *Geologic Map of the Elverton Quadrangle, Tennessee*, Draft Open File Map, scale 1:24,000, 2015

As a result of the replaced text in Subsections 2.5.1.2.4.2.4 and 2.5.3.2.5.3, the following existing Figures in SSAR Subsection 2.5.1 are revised and replaced:

Figure 2.5.1-14.   Site Vicinity Stratigraphic Columns

Figure 2.5.1-25.   Geologic Field Reconnaissance Waypoint Locations

Figure 2.5.1-29.   Site Location Geologic Map Showing Borings

Figure 2.5.1-34.   Site Area Geologic Map

Figure 2.5.1-35.   Site Are Geologic Cross Section A-A'

Figure 2.5.1-37.   (Sheet 1 of 2) Site Location Geologic Map

Figure 2.5.1-37.   (Sheet 2 of 2) Site Location Geologic Map

Figure 2.5.1-47.   Distribution of Mapped Karst Features in the Site Area

As a result of the replaced text in Subsections 2.5.3.2.5.3, the following existing Figures in SSAR Subsection 2.5.3 are revised and replaced.

Figure 2.5.3-2.   (Sheet 1 of 4) Quaternary Terrace Map Adjacent to the Clinch River Arm of the Watts Bar Reservoir Within the Clinch River Nuclear Site Area, Location

Figure 2.5.3-2.   (Sheet 2 of 4) Quaternary Terrace Map Adjacent to the Clinch River Arm of the Watts Bar Reservoir Within the Clinch River Nuclear Site Area, Location B

Figure 2.5.3-2.   (Sheet 3 of 4) Quaternary Terrace Map Adjacent to the Clinch River Arm of the Watts Bar Reservoir Within the Clinch River Nuclear Site Area, Location C

Figure 2.5.3-2.   (Sheet 4 of 4) Quaternary Terrace Map Adjacent to the Clinch River Arm of the Watts Bar Reservoir Within the Clinch River Nuclear Site Area, Location D

Copies of these revised Figures are provided on the following pages.

As a result of the replaced text in Subsections 2.5.1.2.4.2.4 and 2.5.3.2.5.3, Site Vicinity Geologic Map Plates 1 and 2a through 2d in Part 8 of the ESPA are revised and replaced.

Plate 1.   Clinch River Site Vicinity Geologic Map

Plate 2a.   Clinch River Site Vicinity Geologic Map (northwest quadrant)

Plate 2b.   Clinch River Site Vicinity Geologic Map (northeast quadrant)

Plate 2c.   Clinch River Site Vicinity Geologic Map (southwest quadrant)

Plate 2d.   Clinch River Site Vicinity Geologic Map (southeast quadrant)

Copies of these revised Plates are provided in Enclosure 4, on the disk, "Revised Site Vicinity Geologic Map Plates."
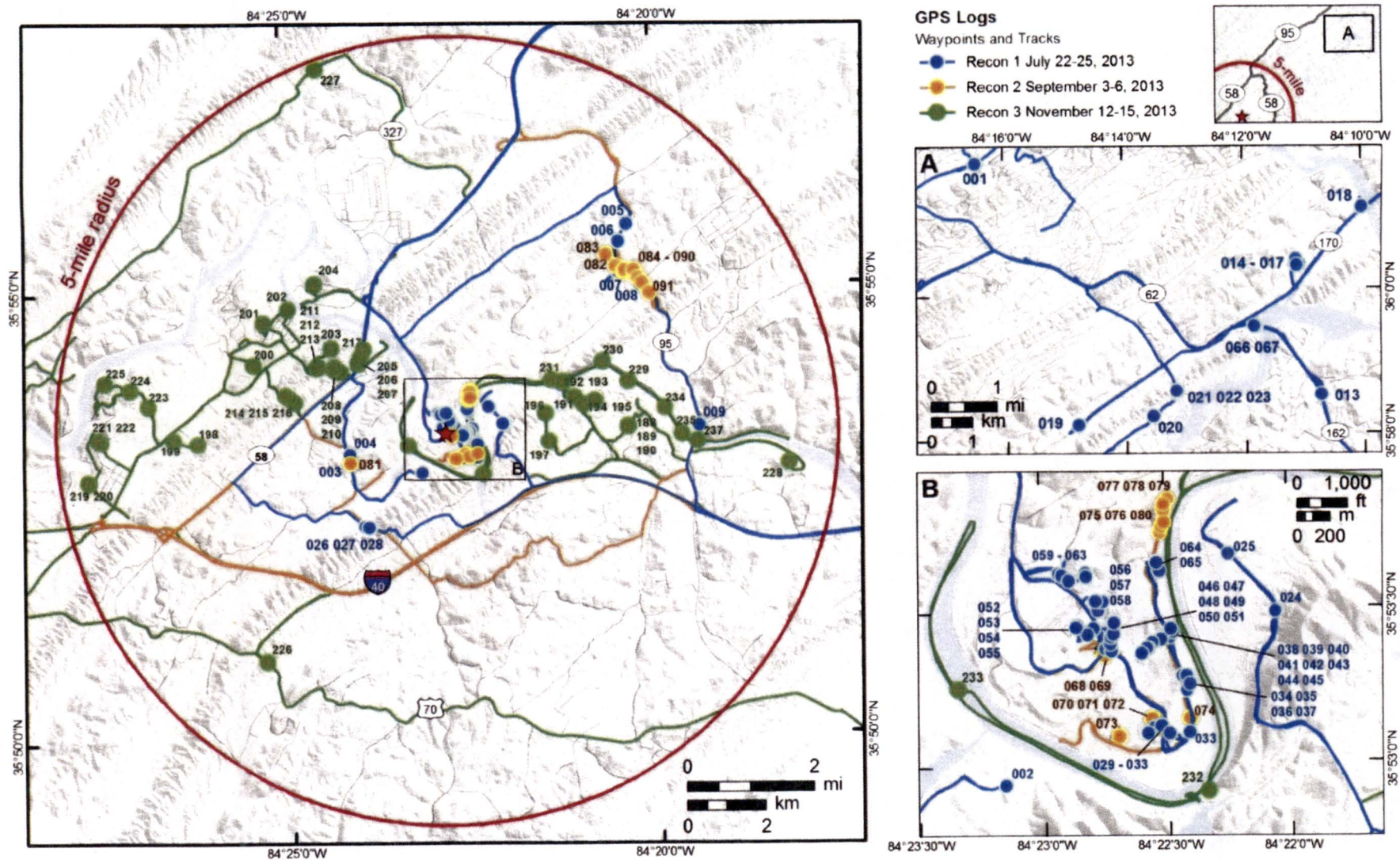
Geologic Units

Pennsylvanian Middle	Pmu	Middle Pennsylvanian - undivided
Pennsylvanian Lower	Pcf	Crooked Fork Group - undivided
	Pcg	Crab Orchard Mountains Group & Gizzard Group - undivided
	Pco	Crab Orchard Mountains Group - undivided
	Pg	Gizzard Group - undivided
Mississippian Upper	Mp	Pennington Formation
	Mn	Newman Limestone
Mississippian Lower - Devonian Upper	Mfp	Fort Payne Fm.
	MDc	Chattanooga Shale
Silurian Lower	Sr	Rockwood Fm.
Ordovician Upper	Os	Sequatchie Fm.
	Or	Reedsville Shale

Chickamauga Supergroup

Nashville Group

Ocn	Cannon Ls.
Ocyl	Catheys and Leipers Fm. - undivided
Oh	Hermitage Fm.

Ordovician Middle

Chickamauga Group

Och	Chickamauga group - undivided
Omc	Moccasin Fm.
Owi	Witten Fm.
Obw	Bowen Fm.
Obe	Benbolt Fm.
Ork	Rockdell Fm.
Ofl	Fleanor Shale
Obl	Blackford Fm. (includes Eidsen mbr.)

Obs	Bays formation
Oo	Ottosee Shale
Ocr	Chapman Ridge Sandstone
Oho	Holston Formation
Ole	Lenoir Ls.
Oa	Athens Shale

Stones River Group

Osr	Stones River Group - undivided
Oca	Carters Ls.
Olb	Lebanon Ls.
Omp	Pierce Ls. and Murfreeboro Ls. - undivided
Ops	Pong Spring Fm.
Ord	Ridley Ls.

Knox Group

OCk	Knox Group - undivided
Oma	Mascot Dolomite
Ok	Kingsport Fm.
Olv	Longview Dolomite
Oc	Chepultepec Dolomite
Ccr	Copper Ridge Dolomite

Ordovician Lower

Conasauga Group

Cc	Conasauga Group - undivided
Cmn	Marynardville Ls.
Cn	Nolichucky Shale
Cdg	Dismal Gap Fm. (Maryville Ls.)
Crg	Rogersville Shale
Cf	Friendship Fm. (Rutledge Ls.)
Cpv	Pumpkin Valley Shale

Cambrian Middle

Cambrian Lower	Cr	Rome Fm. - undivided

Geologic Structures

Syncline	*dashed where approximate*
Anticline	*dashed where approximate*
Overturned Syncline	*dashed where approximate*
– – –	Major Fault
– – –	Minor Fault
....	Contact *dashed where approximate, dotted where concealed*

Other

————	Source map boundary

Figure 2.5.1-14. Site Vicinity Stratigraphic Columns

Figure 2.5.1-25. Geologic Field Reconnaissance Waypoint Locations

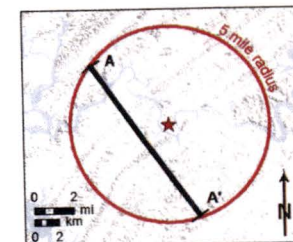**Figure 2.5.1-29. Site Location Geologic Map Showing Borings**

CNL-16-162

Groups

Pg	Gizzard Group
M	Mississippian
OS	Ordovician-Silurian
Och	Chickamauga Group
OЄk	Knox Group
Єc	Conasauga Group
Єr	Rome Formation

—— Fault

Anticline

Syncline

Overturned syncline

Notes:
Simplified geologic map of the Clinch River Nuclear site area developed by Lettis Consultants International, Inc.
See Site Area Geologic Cross Section A-A' (Figure 2.5.1-35).
See Plate 2 in Part 8 for more detailed geologic map of the site area

Figure 2.5.1-34. Site Area Geologic Map

CNL-16-162

Figure 2.5.1-35. Site Area Geologic Cross Section A-A'

Notes:
See site area geologic map for cross-section location (Plate 2).
Cross section developed by Lettis Consultants International, Inc. No vertical exaggeration.
Geologic cross-section through the site area projected to Precambrian basement

CNL-16-162
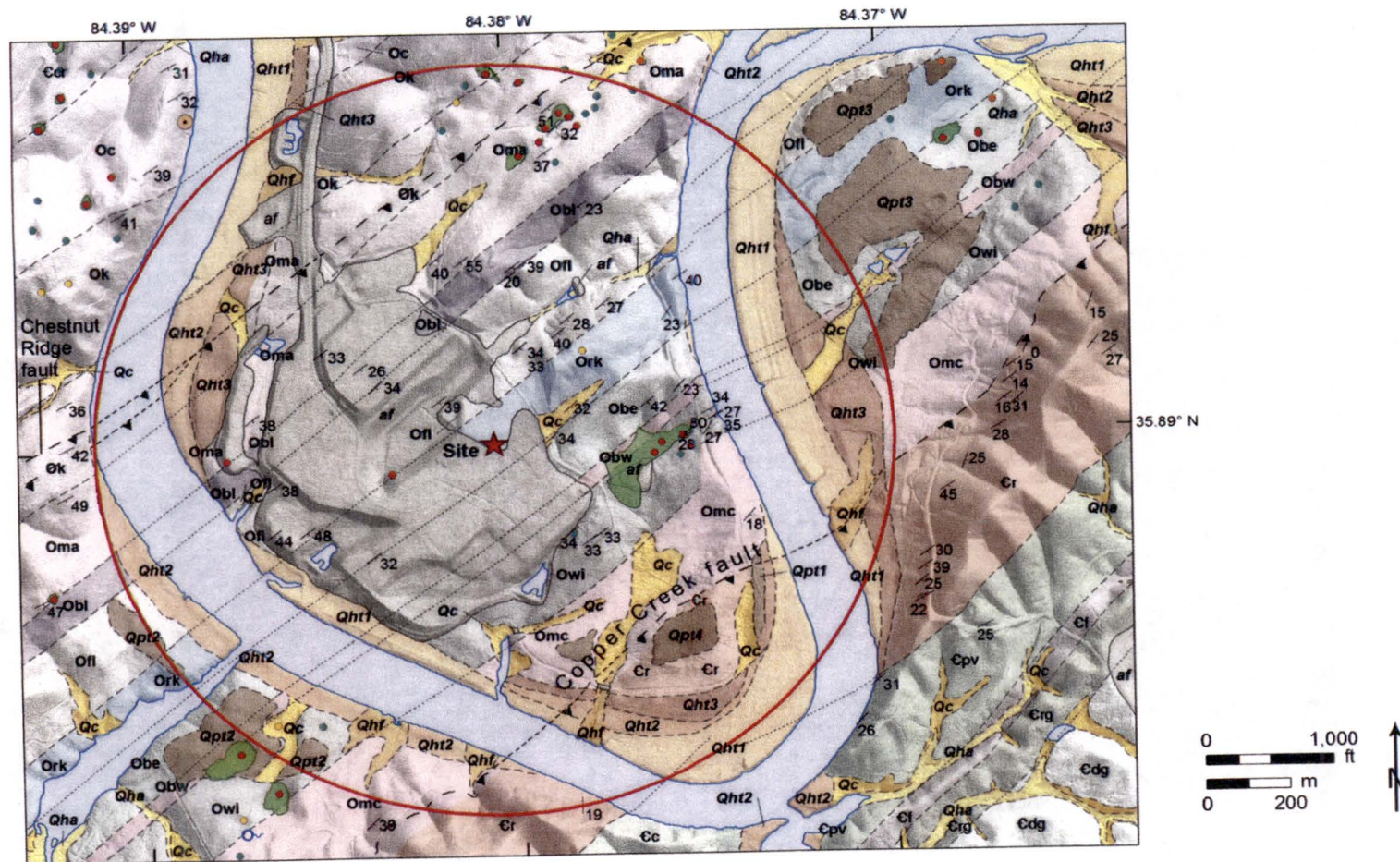
Note: Simplified geologic map of the Clinch River Nuclear site area

Figure 2.5.1-37. (Sheet 1 of 2) Site Location Geologic Map

Quaternary Units

Quaternary

af		Artificial Fill
Qha		Alluvium
Qc		Colluvium
Qhf		Alluvial Fan
Qht1	*Qht2*	Holocene Clinch River Terraces
Qht3		
Qpt1	*Qpt2*	Pleistocene Clinch River Terraces
Qpt3	*Qpt4*	
Qpt5		

Geologic Structures

—▲— ▲— **Thrust Fault**
dashed where approximate, dotted where concealed

·········─ ─ ── **Contact**
dashed where approximate, dotted where concealed

28 ╲ **Structure Measurement**

Karst Features

- ◉ Cave
- ● Closed depression ≥ 2 ft deep and 100 sq ft area
- ○ Three-sided depression
- ● Two-sided depression
- ● Shallow closed depression < 2 ft deep
- ○ᵥ Spring
- ▭ Closed depression ≥ 2 ft deep and 2000 sq ft area

Bedrock Units

Chickamauga Group

Middle Ordovician

Omc	Moccasin Fm.	*siltstone with limestone interbeds*
Owi	Witten Fm.	*limestone with shale interbeds*
Obw	Bowen Fm.	*siltstone with limestone interbeds*
Obe	Benbolt Fm.	*limestone with siltstone interbeds*
Ork	Rockdell Fm.	*limestone with siltstone interbeds*
Ofl	Fleanor Shale mbr. of the Lincolnshire Fm.	*shale and siltstone with limestone*
Obl	Blackford Fm. (includes Eidsen mbr.)	*limestone and siltstone*

Knox Group

Lower Ordovician

Oma	Mascot Dolomite	*dolomite with chert, limestone and sandstone*
Ok	Kingsport Fm.	*dolomite with chert, limestone and sandstone*
Olv	Longview Dolomite	*dolomite and chert*
Oc	Chepultepec Dolomite	*dolomite with chert, limestone and sandstone*

Upper Cambrian

Єcr	Copper Ridge Dolomite	*dolomite with chert, limestone and sandstone*

Conasauga Group

Єc	Conasauga Group - undivided	

Middle Cambrian

Єdg	Dismal Gap Fm. (Maryville Ls.)	*shale and limestone with dolomite and siltstone*
Єrg	Rogersville Shale	*shale with mudstone and siltstone interbeds*
Єf	Friendship Fm. (Rutledge Ls.)	*limestone, dolomite, siltstone and shale*
Єpv	Pumpkin Valley Shale	*shale with mudstone and siltstone interbeds*

Rome Formation

Lower Cambrian

Єr	Rome Fm. - undivided	*sandstone, shale and siltstone with interbeds of dolomite*

Note: Explanation for geologic map shown in (A)

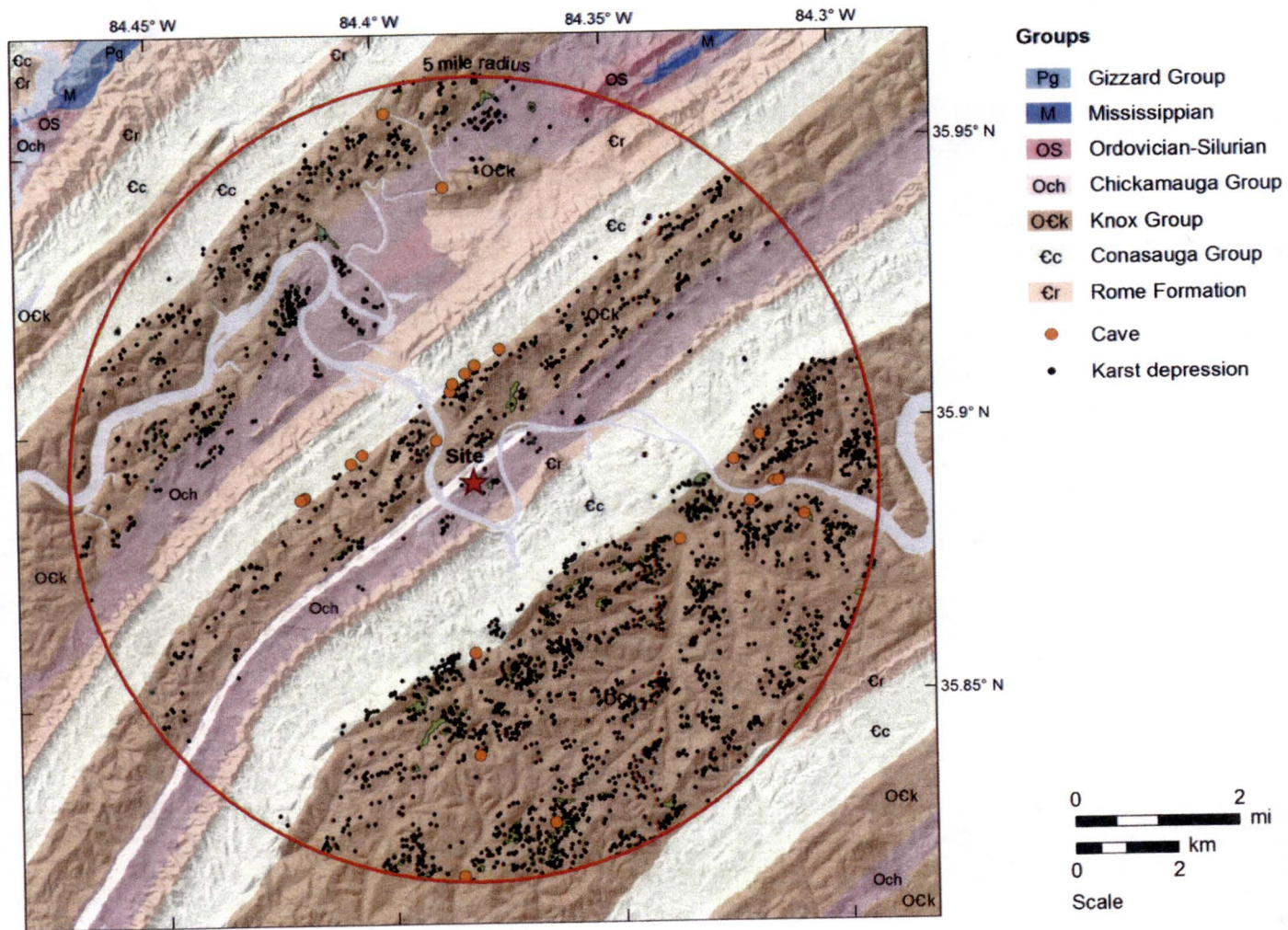**Figure 2.5.1-37. (Sheet 2 of 2) Site Location Geologic Map**

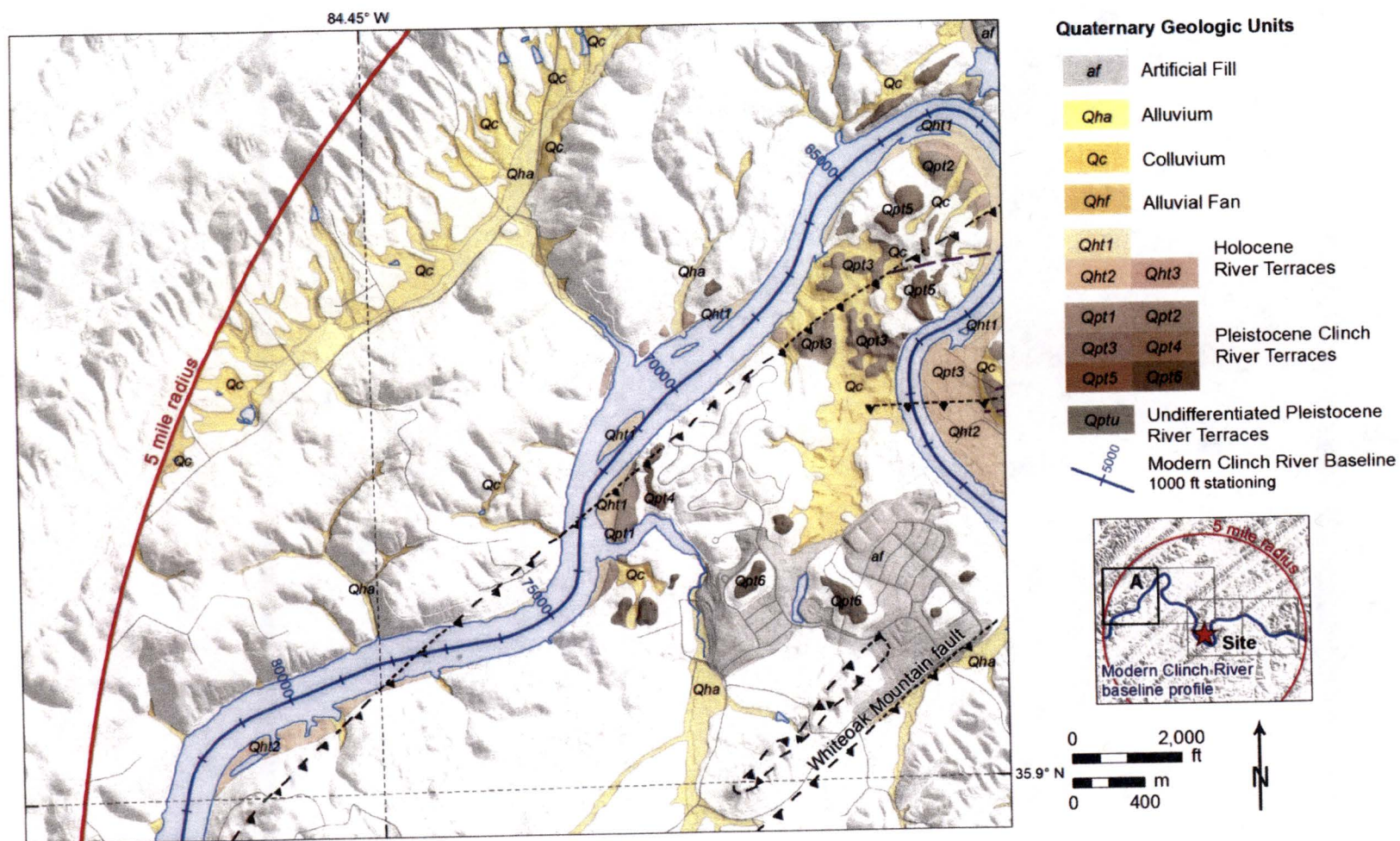Figure 2.5.1-47. Distribution of Mapped Karst Features in the Site Area

CNL-16-162

Quaternary Geologic Units

af	Artificial Fill
Qha	Alluvium
Qc	Colluvium
Qhf	Alluvial Fan
Qht1 / Qht2 / Qht3	Holocene River Terraces
Qpt1 / Qpt2 / Qpt3 / Qpt4 / Qpt5 / Qpt6	Pleistocene Clinch River Terraces
Qptu	Undifferentiated Pleistocene River Terraces

Modern Clinch River Baseline 1000 ft stationing

Figure 2.5.3-2, (Sheet 1 of 4). Quaternary Terrace Map Adjacent to the Clinch River Arm of the Watts Bar Reservoir Within the Clinch River Nuclear Site Area, Location A

Figure 2.5.3-2, (Sheet 2 of 4). Quaternary Terrace Map Adjacent to the Clinch River Arm of the Watts Bar Reservoir Within the Clinch River Nuclear Site Area, Location B

Figure 2.5.3-2, (Sheet 3 of 4). Quaternary Terrace Map Adjacent to the Clinch River Arm of the Watts Bar Reservoir Within the Clinch River Nuclear Site Area, Location C

Quaternary Geologic Units

af	Artificial Fill
Qha	Alluvium
Qc	Colluvium
Qhf	Alluvial Fan

Qht1		Holocene River Terraces
Qht2	Qht3	

Qpt1	Qpt2	Pleistocene Clinch River Terraces
Qpt3	Qpt4	
Qpt5	Qpt6	

Qptu — Undifferentiated Pleistocene River Terraces

Modern Clinch River Baseline 1000 ft stationing
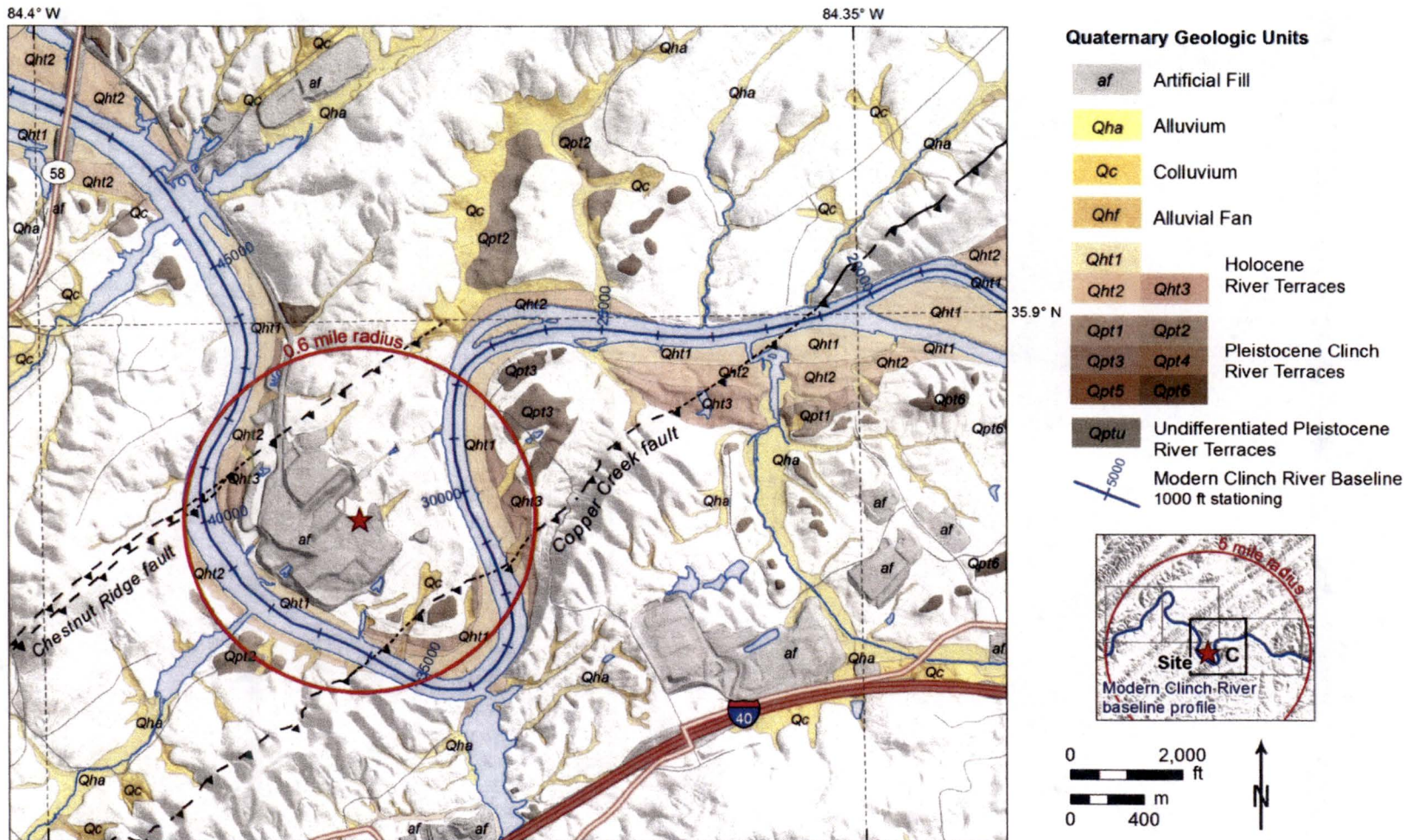
Figure 2.5.3-2, (Sheet 4 of 4). Quaternary Terrace Map Adjacent to the Clinch River Arm of the Watts Bar Reservoir Within the Clinch River Nuclear Site Area, Location D

As a result of the replaced text in Subsection 2.5.1.2.4.2.4, the following Figure is added to SSAR Subsection 2.5.1:

Figure 2.5.1-64.   Geologic Map and Cross Section B-B'

As a result of the replaced text in Subsection 2.5.3.2.5.3, the following Figures are added to SSAR Subsection 2.5.3:

Figure 2.5.3-6.   Location Map of Topographic Profiles Across Quaternary Fluvial Terraces and Mapped Faults

Figure 2.5.3-7.   (Sheet 1 of 2) Geologic Map and Topographic Profile C-C' of Quaternary Fluvial Terraces and Northeastern Projection of Chestnut Ridge Fault

Figure 2.5.3-7.   (Sheet 2 of 2) Geologic Map and Topographic Profile D-D' of Quaternary Fluvial Terraces and Chestnut Ridge Fault

Figure 2.5.3-8.   (Sheet 1 of 3) Geologic Map Location and Topographic Profile E-E' of Quaternary Fluvial Terraces and Unnamed Fault

Figure 2.5.3-8.   (Sheet 2 of 3) Geologic Map and Topographic Profile F-F' of Quaternary Fluvial Terraces and Unnamed Fault

Figure 2.5.3-8.   (Sheet 3 of 3) Geologic Map and Topographic Profile G-G' of Quaternary Fluvial Terraces and Unnamed Fault

Figure 2.5.3-9.   Geologic Map and Topographic Profile H-H' of Quaternary Fluvial Terraces and Surface Projection of the Shear Fracture Zone

Copies of the new Figures are provided on the following pages.

Source: Reference 2.5.1-282

Figure 2.5.1-64. Geologic Map and Cross Section B-B'

CNL-16-162
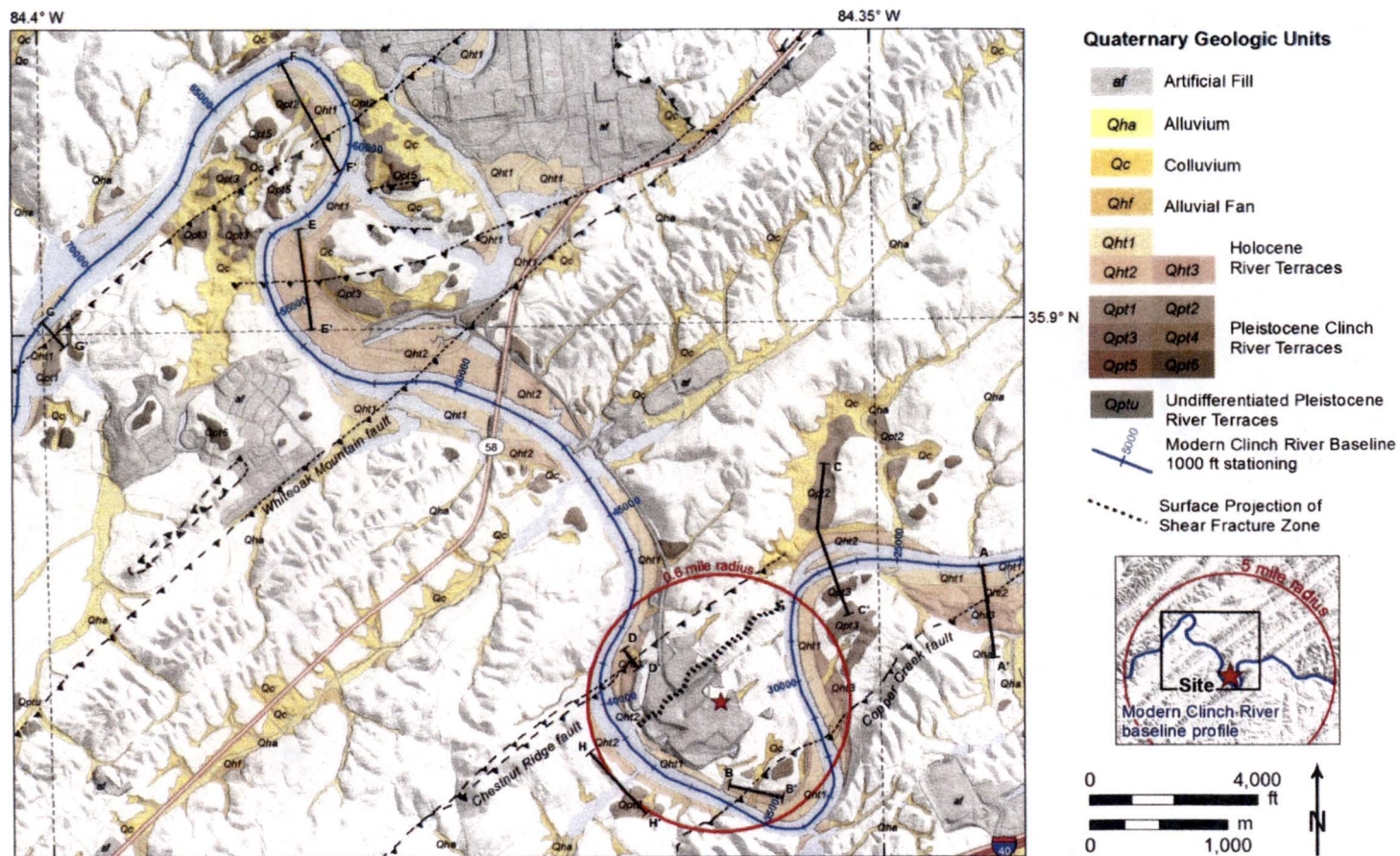
Note: Topographic profiles are shown on Figures 2.5.3-7 through 2.5.3-9

Figure 2.5.3-6. Location Map of Topographic Profiles Across Quaternary Fluvial Terraces and Mapped Faults
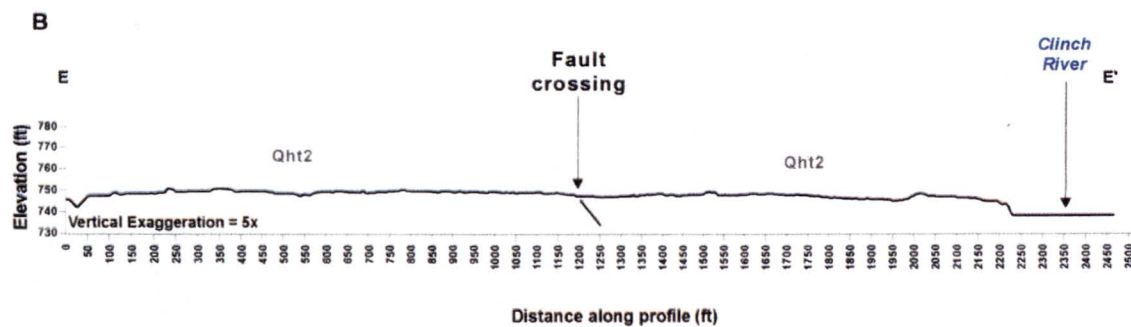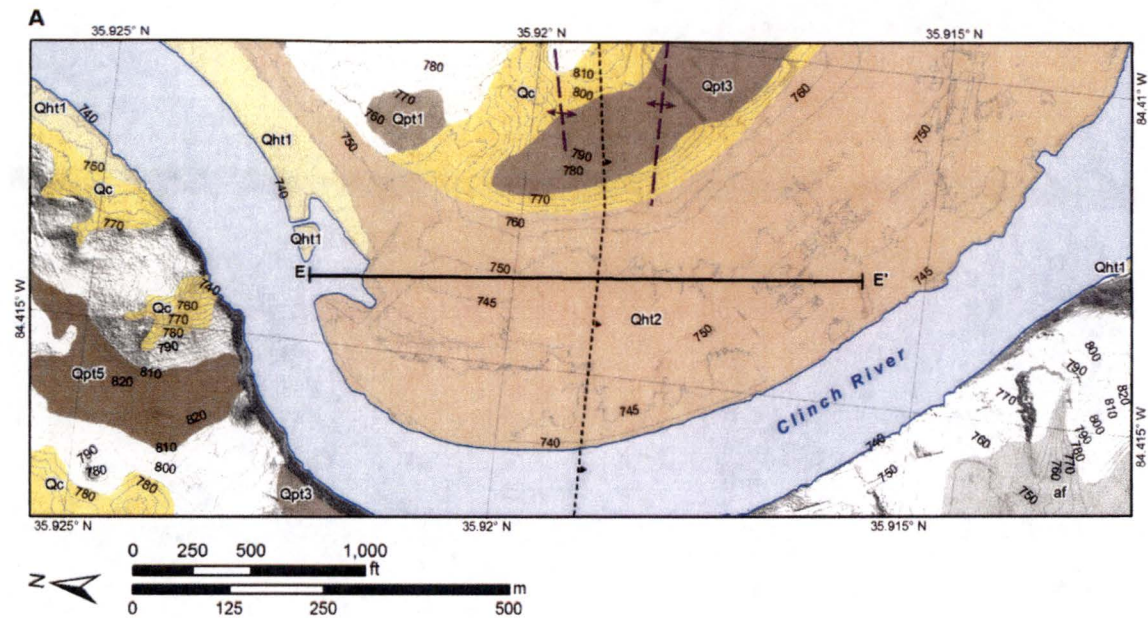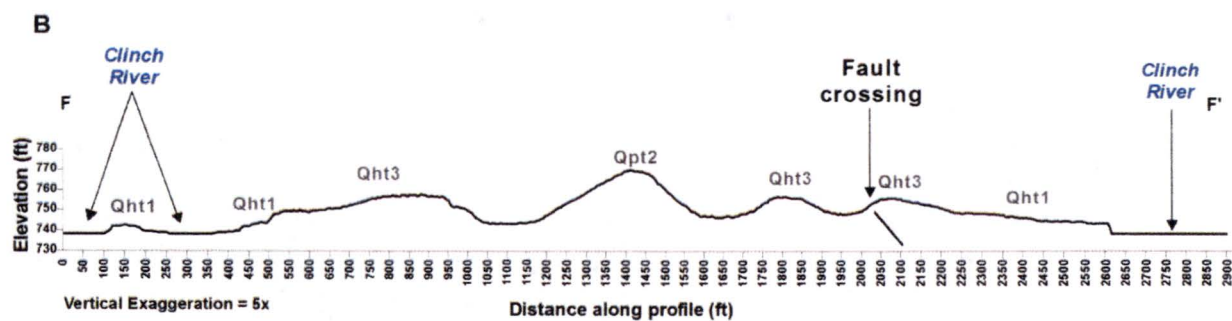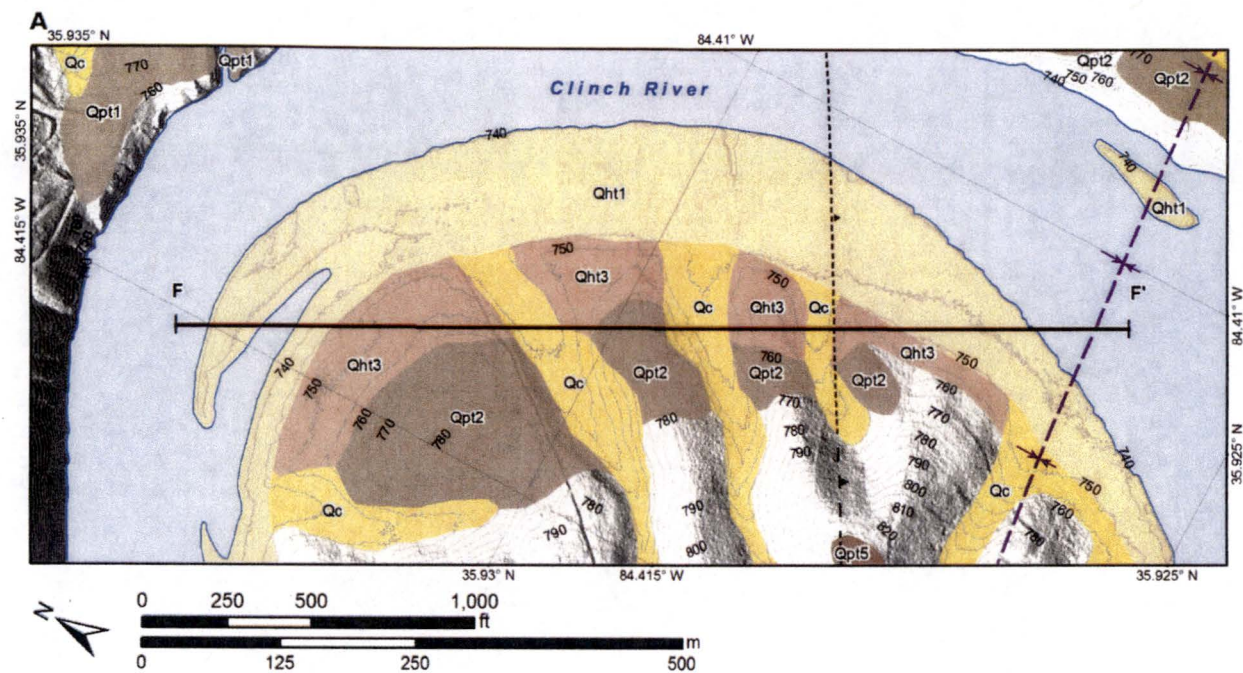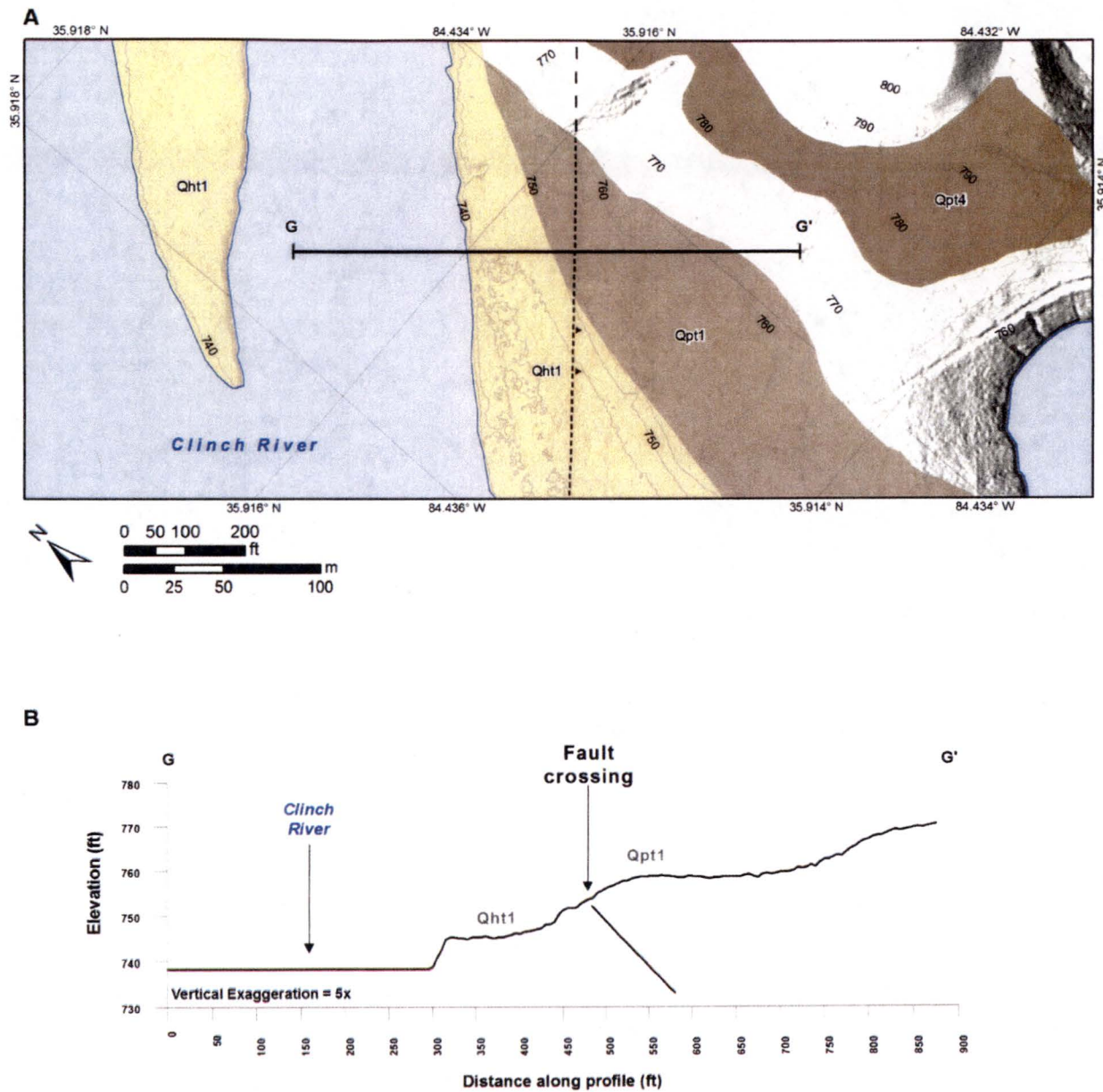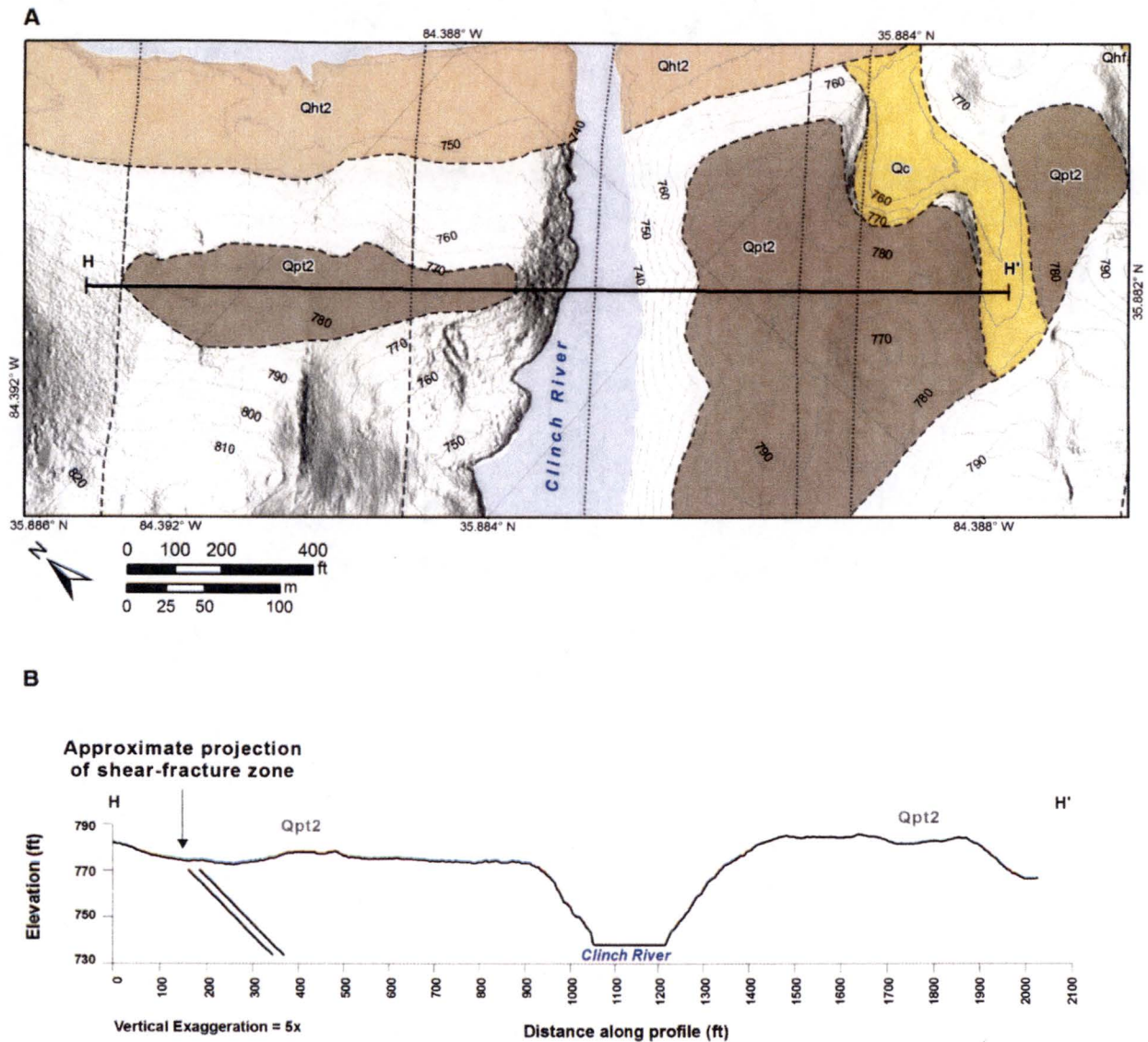
A

B
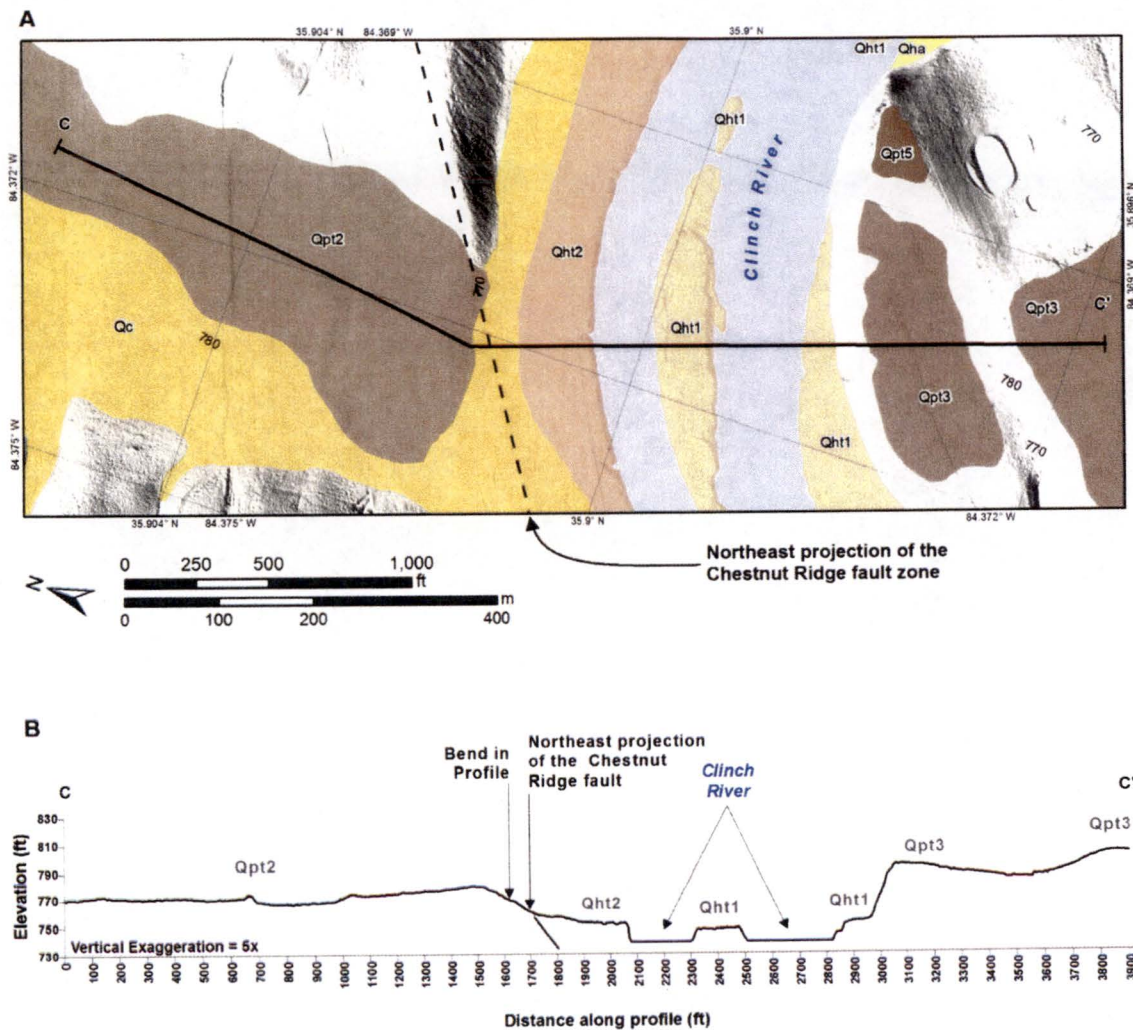
Note: Location of profile is shown on Figure 2.5.3-6
Source: Reference 2.5.3-56
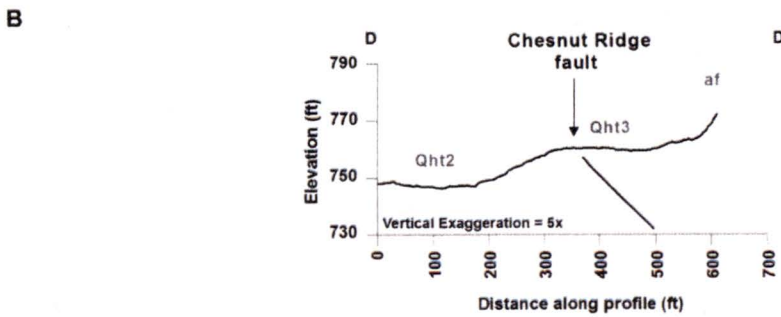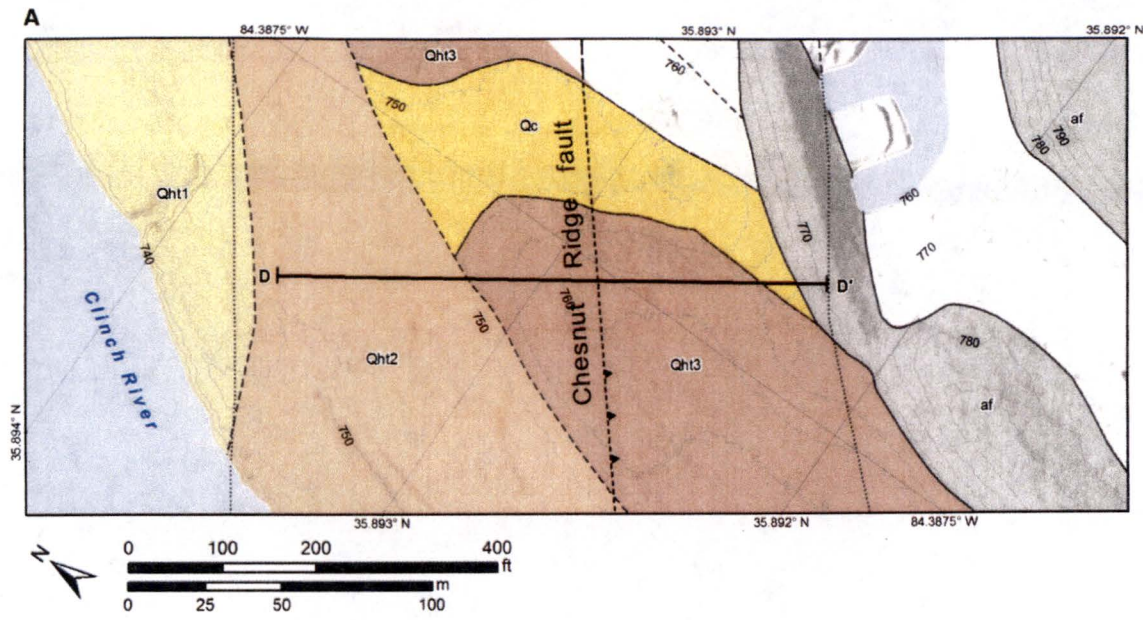
Figure 2.5.3-7. (Sheet 1 of 2), Geologic Map and Topographic Profile C-C' of Quaternary Fluvial Terraces and Northeastern Projection of Chestnut Ridge Fault

Note: Location of profile is shown on Figure 2.5.3-6
Source: Reference 2.5.3-56

Figure 2.5.3-7. (Sheet 2 of 2), Geologic Map and Topographic Profile D-D' of Quaternary Fluvial Terraces and Chestnut Ridge Fault

CNL-16-162

A

B

Note: Location of profile is shown on Figure 2.5.3-6
Source: Reference 2.5.3-56

Figure 2.5.3-8., (Sheet 1 of 3), Geologic Map Location and Topographic Profile E-E' of Quaternary Fluvial Terraces and Unnamed Fault

A

B

Note: Location of profile is shown on Figure 2.5.3-6
Source: Reference 2.5.3-56

Figure 2.5.3-8. (Sheet 2 of 3), Geologic Map and Topographic Profile F-F' of Quaternary Fluvial Terraces and Unnamed Fault

A

B

Note: Location of profile is shown on Figure 2.5.3-6
Source: Reference 2.5.3-56

Figure 2.5.3-8. (Sheet 3 of 3), Geologic Map and Topographic Profile G-G' of Quaternary Fluvial Terraces and Unnamed Fault

A

B

Note: Location of profile is shown on Figure 2.5.3-6

Figure 2.5.3-9. Geologic Map and Topographic Profile H-H' of Quaternary Fluvial Terraces and Surface Projection of the Shear Fracture Zone

CNL-16-162

By letter dated May 12, 2016 (Reference 1), Tennessee Valley Authority (TVA) submitted an application for an early site permit for the Clinch River Nuclear (CRN) Site in Oak Ridge, TN. Subsequent to the submittal of the application, and consistent with interactions with NRC staff, TVA identified certain aspects of the application that it intends to supplement. By letter dated August 11, 2016 (Reference 2), TVA provided a plan for submitting the identified supplemental information.

This enclosure provides supplemental information related to Geologic Characterization Information to support the NRC staff's review. This enclosure also includes proposed changes to the affected Site Safety Analysis Report (SSAR) sections. An Early Site Permit Application (ESPA) Change Request has been initiated to incorporate these changes into a future revision of the ESPA.

Supplement Item B (Reference 2)

B. *TVA will provide a markup of the applicable ESPA sections to more fully characterize and analyze the Shear Fracture Zone at the site location to demonstrate that this zone does not represent a potentially significant hazard for surface deformation at the site. TVA will:*

- *Include maps and cross-sections to illustrate location, geometry and stratigraphic position.*
- *Provide a conceptual model or illustration to clarify cross-cutting relationships between structural elements, addressing how the latest styolites might be related to Cenozoic compressional stress directions.*
- *Clarify with greater detail how this feature should be considered analogous to Foreman and Dunne's (SSAR Ref. 2.5.3-19) or Lemiszki's (SSAR Ref. 2.5.1-215) features.*
- *Assess cross-cutting relationship with Quaternary age river terraces and alluvium/colluvium stratigraphic units that overly or are in contact with the Shear Fracture Zone.*
- *Provide an assessment of the age of the Shear Fracture Zones in support of TVA's conclusion of Alleghanian age.*

Supplemental Information B

To address the information above, the following text will completely replace the existing text in SSAR Subsections 2.5.1.2.4.3.4, "Shear-Fracture Zones," and 2.5.3.2.5.3, "Evaluation of Terrace profiles and Quaternary Surface Deformation." The replaced text and figures provide additional background and further characterization of the shear-fracture zones described in the current investigation. The replacement also provides a review of possibly analogous nearby features, an assessment of the relationship between the shear-fracture zones and Quaternary river terraces, and an assessment of the relationship between stylolites and shear-fracture zones at the site.

Additional characterization and assessment of the shear-fracture zone involved re-evaluation of borehole logs, construction of borehole-constrained cross-sections and map, and literature review. A brief conceptual model is presented to describe the temporal development of various features described in the text and to support an age assessment of the shear-fracture zones.

In addition, an analysis of the crosscutting relationships between the shear-fracture zone and Quaternary age river terraces has been added to SSAR Subsection 2.5.3.2.5.3, "Evaluation of Terrace Profiles and Quaternary Surface Deformation." This information is presented in the response to Supplemental Information A of this enclosure.

References:

1. Letter from TVA to NRC, CNL-16-081, "Application for Early Site Permit for Clinch River Nuclear Site," dated May 12, 2016

2. Letter from TVA to NRC, CNL-16-134, "Schedule for Submittal of Supplemental Information in Support of Early Site Permit Application for Clinch River Nuclear Site," dated August 11, 2016

The following text replaces the existing SSAR Subsection 2.5.1.2.4.3.4 in its entirety:

2.5.1.2.4.3.4   Shear-Fracture Zones

During the CRBR site investigation, a structure was identified in the Unit A Limestone (Eidson Member of the Lincolnshire Formation) that was described as an ancient rehealed shear zone (Reference 2.5.1-100). The shear zone was encountered in 39 boreholes during that investigation, and a surface exposure in the northeastern portion of the site was described in the CRBR PSAR (Reference 2.5.1-238) (Figure 2.5.1-65). This zone was described as 19 to 46 ft thick, and is on average approximately 35 ft thick (Reference 2.5.1-100). The zone, including slickensides, is conformable with bedding (Reference 2.5.1-238). It is characterized as "a zone of interbed slippage characterized by a combination of slickensides, calcite veins, and 1-in. to 1-ft segments that are either severely warped or brecciated" (Reference 2.5.1-100). The authors concluded that the shear zone is a zone of interbed slippage that developed during Alleghanian Valley and Ridge shortening, based on the truncation of calcite-filled fractures by stylolites (Reference 2.5.1-238). Interbed slippage in the zone is estimated to be on the order of inches (Reference 2.5.1-238), although no evidence is provided to support that statement.

Similar structures identified in boreholes in the Lincolnshire (Eidson Member), Rockdell, and Benbolt Formations are termed as shear-fracture zones in the current subsurface investigation (see Subsection 2.5.1.2.6) (Reference 2.5.1-214). The Lincolnshire Formation (Eidson Member) and the Unit A Limestone are equivalent. These shear-fracture zones are located and characterized in 18 of the 100-, 200-, and 400-series boreholes (Table 2.5.1-17), and are described in more detail in Subsection 2.5.1.2.6.4. Shear-fracture zones consist of intensely fractured, calcite-healed zones that are conformable with bedding, with thicknesses that mostly range from about 1 ft to 22 ft (Table 2.5.1-17) (see Subsections 2.5.1.2.4 and 2.5.1.2.6). The thickest zone encountered in the current investigation is approximately 35 ft, and occurs in the Eidson Member of the Lincolnshire Formation (Table 2.5.1 17) (Reference 2.5.1-214).

The shear-fracture zone within the lower Eidson Member of the Lincolnshire Formation is shown on two cross-sections through the site in Figures 2.5.1-66 and 2.5.1-67. These cross-sections show that the shear-fracture zone is conformable to bedding and is laterally continuous across the site. Similarly, the strike-parallel extent of the shear-fracture zone based on boreholes that encountered the shear-fracture zone also suggests a high degree of lateral continuity, although a few boreholes that penetrated the lower Eidson Member of the Lincolnshire Formation did not encounter the shear-fracture zone (Figure 2.5.1-65). Within the Eidson Member, the shear-fracture zone is recognized in boreholes for a distance of about 500 ft parallel to dip direction, and for a distance of about 2,700 ft parallel to strike.

As noted above, additional discrete shear-fracture zone features were also observed up-section in boreholes during this investigation further to the southeast within the Benbolt and Rockdell Formations (Figure 2.5.1-65). These less well defined shear-fracture zones were not observed in the three boreholes completed for the CRBRP that penetrated these units (References 2.5.1-100 and 2.5.1-238). These shear-fracture zone features share similar characteristics with the shear-fracture zone features in the Eidson Member of the Lincolnshire Formation (Table 2.5.1-17). Within the Rockdell and Benbolt Formations, the shear-fracture zone features are located in the approximately middle third of each unit (Figure 2.5.1-67). The features in the Rockdell Formation define a discrete zone that is roughly conformable with bedding, while the features in the Benbolt Formation are not dense or extensive enough to define a zone (Figure 2.5.1-67). As depicted in map view (Figure 2.5.1-65) and cross-section view (Figure 2.5.1-67), neither the Benbolt nor the Rockdell Formation shear-fracture zone features define laterally continuous zones through multiple borings parallel to dip or strike.

Instead, the shear-fracture zone features in the Benbolt and Rockdell Formations appear to comprise local zones of shearing that do not extend continuously for more than a few hundred feet in either the dip-parallel or strike-parallel directions.

The descriptions of the shear-fracture zone features at the site (References 2.5.1-100, 2.5.1-214 and 2.5.1-238) are similar to the descriptions of veins and fractures studied by Foreman and Dunne (Reference 2.5.1-237) in the nearby Upper Cambrian Nolichucky Shale. Their study was conducted at the Oak Ridge National Laboratory and on the Whiteoak Mountain thrust sheet, the same regional structure element that the CRN Site is located on. Foreman and Dunne (Reference 2.5.1-237) observed in limestones and shales four sets of bed-normal calcite veins that are offset 0.8 in. or less by bed-parallel veins. The bed-parallel veins are characterized by slickensides oriented parallel to Alleghanian thrusting. On the basis of calcite twinning, fluid inclusions and cross-cutting relationships, Foreman and Dunne (Reference 2.5.1-237) conclude that the development of the bed-normal veins occurred in the middle Mississippian during the onset of the Ouachita and Alleghanian orogenies. The bed-parallel veins, which offset the bed-normal veins, developed during the Alleghanian orogeny. Slickensides, oriented parallel to the thrusting direction, formed during movement of the Whiteoak Mountain thrust sheet. Features similar to the bed-normal veins are common throughout borehole logs of the current investigation (Reference 2.5.1-214), which describe calcite healed tensional fractures oriented orthogonal to bedding. Given the similarity in geologic setting, tectonic history, and fracture characteristics, the slickensided, bed-parallel shear-fracture zone features observed at the site likely share the same Alleghanian origin and development as the slickensided, bed-parallel veins described by Foreman and Dunne (Reference 2.5.1-237).

Lemiszki (Reference 2.5.1-215) observed and briefly described local "shear fractures" that are most common in, but not exclusive to the K-25 site area of the Oak Ridge National Laboratory. The shear fractures are described as single, discrete fractures to wide zones of en echelon fractures and tension gashes with left- and right-lateral shears based on offset of chert marker beds and mineral-filling geometries. That study describes the shears as "commonly perpendicular to bedding," which is not consistent with descriptions of the shear-fracture zone observed in the CRBRP (Reference 2.5.1-100 and 2.5.1-238), the bed-parallel veins described by Foreman and Dunne (Reference 2.5.1-237), or the shear-fracture zones as described in the current study (Reference 2.5.1-214). However, the "shear fractures" described by Lemiszki (Reference 2.5.1-215) could be related to the bed-normal veins observed by Foreman and Dunne (Reference 2.5.1-237) and in the current study (Reference 2.5.1-214).

The CRBRP study noted that the shear-fracture zone features are truncated by stylolites, and concludes the shear-fracture zones formed before or during rock lithification (Reference 2.5.1-238). Stylolites are sedimentary structures that form in response to lithostatic-driven pressure dissolution (Reference 2.5.1-284). The term is typically used to describe horizontal "seams" in carbonate rocks that developed diagenetically during burial due to lithostatic pressure (Reference 2.5.1-285). Several studies have shown that stylolite "seams" develop perpendicular to maximum compressive stress (e.g., References 2.5.1-285 and 2.5.1-286) and that vertical stylolites can develop in active compressive margins in response to horizontal compressive stress (References 2.5.1-285, 2.5.1-286, 2.5.1-287 and 2.5.1-288). These vertical stylolites are referred to as tectonic stylolites. The stylolites observed in the current investigation are generally described as bedding joints that dip between 20 to 40° conformable with bedding (Reference 2.5.1-214). The bedding-conformable nature of the stylolites indicates that they developed diagenetically during active deposition and lithification of sediments deposited in the Appalachian foreland basin.

In summary, the minimum age of development of the shear-fracture zone is constrained by (1) local truncation by stylolites that formed during active deposition of the Appalachian foreland basin (Figure 2.5.1-68) indicating an Alleghanian orogeny age, and (2) analogy to the nearby bed-parallel veins described by Foreman and Dunne (Reference 2.5.1-237) that formed during Alleghanian thrusting in the Whiteoak Mountain thrust sheet. Quaternary terrace profiles (presented and discussed in SSAR Subsection 2.5.3.2.5.3) across the projected trace of the shear fracture zone show no evidence of any linear topographic features or warping of the terrace profile suggestive of surface deformation as a result of movement along the shear-fracture zone. These age constraints are mutually consistent and support the conclusion reached in the CRBRP that the shear-fracture zone represents a Paleozoic rehealed shear zone (References 2.5.1-100 and 2.5.1-238).

As a result of the replaced text in Subsection 2.5.1.2.4.3.4, the following references are added to SSAR Subsection 2.5.1.3:

2.5.1.3   References

2.5.1-284.   Boggs, Jr., S., *Principles of Sedimentology and Stratigraphy*, Fifth Edition, Prentice Hall, New Jersey, 2001.

2.5.1-285.   Ebner, M., R. Toussaint, J. Schmittbuhl, D. Koehn, and R. Bons, *Anisotropic scaling of tectonic stylolites: A fossilized signature of the stress field?*, Journal of Geophysical Research: Solid Earth, Vol. 115, No. B6, 2010.

2.5.1-286.   Railsback, L. B., and L.M. Andrews, *Tectonic stylolites in the 'undeformed' Cumberland Plateau of southern Tennessee*, Journal of Structural Geology, Vol. 17, No. 6, pp. 911-915, 1995.

2.5.1-287.   Lavenu, A.P.C., J. Lamarche, A. Gallois, and B.D.M. Gauthier, *Tectonic versus diagenetic origin of fractures in a naturally fractured carbonate reservoir analog (Nerthe anticline, southeastern France)*, AAPG Bulletin, Vol. 97, No. 12, pp. 2207-2232, 2013.

2.5.1-288.   Rolland, A., R. Toussaint, P. Baud, N. Conil, and P. Landrein, *Morphological analysis of stylolites for paleostress estimation in limestones*, International Journal of Rock Mechanics and Mining Sciences, Vol. 67, pp. 212-225, 2014.

The following SSAR Subsection 2.5.1.2.6.4 is revised as indicated: (Note - deletions are shown as "~~strike-through~~" text and additions are shown as "underlined" text.)

2.5.1.2.6.4   Deformational Zones

Borings drilled at the CRN Site indicate the presence of shear-fracture (fractures where differential movement has taken place along a surface, characterized by striations and/or slickensides) zones within the stratigraphic units. The development of these shear-fracture zones at the site is considered to be closely related to folding and faulting in the area reflecting a long and varied stress history (Subsection 2.5.1.2.4) and are often associated with fracture zones (SZ/FZ) or occur as single shear fractures (SH) (noted as joints on the boring logs).

A summary of the shear-fracture zones (greater than or equal to approximately 0.9 ft thick (apparent thickness along boring axis)) encountered in the 100-, ~~and~~ 200-, and 400-series borings drilled at the CRN Site are contained in Table 2.5.1-17 and shown on Figure 2.5.1-60 (see Subsection 2.5.1.2.4). Shear-fracture zones are encountered in the Rockdell and Benbolt Formations (in the 100-series borings) between depths of about 50 and 350 ft below the ground surface. The shear-fracture zones range in thickness from about 1 to 7 ft with an average apparent thickness of about 3 ft. Shear-fracture zones are encountered in the Eidson Member (200- and 400-series borings) between depths of about 115 and 280 ft below the ground surface. These zones range in thickness from about 1 to ~~18~~22 ft with an average apparent thickness of approximately 4 ft. ~~The 18-ft-thick shear-fracture zone is encountered in MP-201 at a depth of approximately 150 ft below the ground surface.~~ Descriptions from the 100-, ~~and~~ 200-, and 400-series borings logs indicate that the shear-fracture zones are typically zones of multiple, closely spaced, tightly healed, calcite filled shear fractures with occasional, primarily discrete, fracture zones and the fractures commonly form orthogonal to bedding. The quality of the rock within these zones is generally high, unless associated with fracture zones (Reference 2.5.1-214).

A shear zone is reported to have been encountered during the subsurface investigation for the CRBRP. Thirty-nine ~~seven~~ borings drilled as part of the CRBRP investigation encountered the shear zone in the lower portion of the Eidson Member, which ranges in thickness from 19 to 46 ft. The shear zone outcrops to the northeast of the CRBRP along the right bank of the Clinch River arm of the Watts Bar Reservoir and strikes parallel to the strike of the bedding planes. The shear zone is described as a hard, re-healed, cemented zone characterized by continuous, thin to medium bedded gray limestone with 1 to 6 inch layers of maroon and gray calcareous siltstone and gray-white chert. The results of the subsurface investigation on the shear zone for the CRBRP reveal that it is not a fault breccia or fault zone (Reference 2.5.1-100).

Shear-fracture zones are incorporated in the average GSI rating for each of the stratigraphic units, so bearing capacity based on GSI considers these zones in the foundation rock mass. During excavation for the power block area, detailed geologic mapping of the foundations for the safety-related structures provides further characterization of shear-fracture zones, if found present in those foundations.

Characterization of the shear-fracture zones is based on the 100-, ~~and~~ 200-, and 400-series borings drilled at the CRN Site. Further evaluation of these zones may be required in support of the COLA, when a reactor technology has been selected.

The following SSAR Subsection 2.5.3.2.2 is revised as indicated: (Note - deletions are shown as "~~strike-through~~" text and additions are shown as "<u>underlined</u>" text.)

2.5.3.2.2   Shear Fracture Zones

As discussed in Subsections 2.5.1.2.4 and 2.5.1.2.6, a structure loosely described as a shear zone was identified in the Eidson Member of the Lincolnshire Formation in the CRBRP PSAR (References 2.5.3-5 and 2.5.3-6). The shear zone was penetrated in ~~37~~<u>39</u> boreholes during the CRBRP investigation, and a surface exposure in the northeastern portion of the site was described in the CRBRP PSAR (Reference 2.5.3-6). This zone ranges from 19 to 46 ft thick and is, on average, approximately 35 ft thick (Reference 2.5.3-6). The zone, including slickensides, is roughly parallel to bedding and occurs in the same stratigraphic position where encountered (Reference 2.5.3-5). It is characterized as "a zone of interbed slippage characterized by a combination of slickensides, calcite veins, and 1-inch to 1-foot segments that are either severely warped or brecciated" (Reference 2.5.3-5). Interbed slippage in the zone is estimated to be on the order of inches (Reference 2.5.3-6), as no stratigraphic offset is demonstrable.

Similar structures identified in the Lincolnshire (Eidson Member), Rockdell, and Benbolt Formations are defined as shear fracture zones in the current subsurface investigation (see Subsections 2.5.1.2.4 and 2.5.1.2.6). These shear fracture zones are located and characterized in ~~15~~<u>18</u> of the 100-<u>,</u> ~~and~~200-<u>, and 400-</u>series boreholes (Table 2.5.1-17; Figure 2.5.1-60). Shear fracture zones consist of intensely fractured, calcite-healed zones that form parallel to bedding, with thicknesses that range from 1 to ~~18~~<u>22</u> ft (see Subsections 2.5.1.2.4 and 2.5.1.2.6). These shear fracture zones are interpreted to be the same structures that were encountered and described as shear zones in the CRBRP PSAR (References 2.5.3-5 and 2.5.3-6).

~~Fifteen~~<u>Eighteen</u> boreholes penetrated shear-fracture zones during the subsurface investigation (Reference 2.5.3-3; see Table 2.5.1-17). Core recovered from 100-<u>,</u> ~~and~~200-<u>, and 400-</u>series borings in shear-fracture zones is commonly described as calcite-healed, with rock quality generally described as high with moderate to high core recovery (Reference 2.5.3-3; see Subsection 2.5.1.2.6.4). Shear fracture zones do not appear to be loci for accelerated dissolution relative to adjacent rock.

Foreman and Dunne (Reference 2.5.3-19) describe the occurrence of bed-parallel slickensided veins in a detailed fracture analysis in eastern Tennessee. These veins are calcite-filled and appear to be similar structures as those identified as shear zones in the CRBR investigation.

Elsewhere in the site vicinity, Lemiszki (Reference 2.5.3-20) reported mesoscopic shear zones that offset extensional fractures. These are described as both left- and right-lateral shears based on offset of chert marker beds and mineral-filling geometries (Reference 2.5.3-20).

Lemiszki (Reference 2.5.3-20) indicates the development of these shear zones is closely related to faulting and folding in the area, although the report provides no technical basis for that conclusion.

The following SSAR Subsection 2.5.4.1.3.2 is revised as indicated: (Note - deletions are shown as "~~strike-through~~" text and additions are shown as "underlined" text.)

2.5.4.1.3.2   Shear-Fracture Zones

A detailed discussion on the shear-fracture zones encountered in the 100- and 200-series borings (Locations A and B, respectively) at the CRN Site is provided in Subsections 2.5.1.2.4 and 2.5.1.2.6.4. Descriptions from the borings indicate that the shear-fracture zones are typically zones of multiple, closely spaced, tightly healed, calcite filled shear fractures (Reference 2.5.4.1). A summary of the shear-fracture zones (greater than or equal to approximately 0.9 ft thick [apparent thickness along boring axis]) encountered in the 100- and 200-series borings is contained in Table 2.5.1-17 and shown on Figure 2.5.1-60. The shear fracture zones are encountered in the Rockdell and Benbolt Formations (100-series borings) and the Eidson Member (200- and 400-series borings) between elevations of about 750 and 450 ft. The zones range in thickness from about 1 to ~~18~~22 ft with an average apparent thickness of about 4 ft. The shear-fracture zones encountered are considered to be similar to the shear zone encountered during the CRBRP (Reference 2.5.4-3), as discussed in Subsection 2.5.1.2.6.4.

Shear-fracture zones are likely to be encountered at or below the foundation level. For this reason, the shear-fracture zones are incorporated in the average Geological Strength Index (GSI) rating for each stratigraphic unit for rock mass characterization (See Subsection 2.5.1.2.6). During excavation for the power block area, detailed geologic mapping provides further characterization of any shear-fracture zones encountered.

Characterization of the shear-fracture zones are based on the 100-, ~~and~~200-, and 400-series borings drilled at the CRN Site. Further evaluation of these zones is performed at COLA, when a reactor technology has been selected.

As a result of the replaced text in Subsection 2.5.1.2.4.3.4, Table 2.5.1-17, "Summary of Shear-Fracture Zones," is revised as indicated to provide additional information:
(Note - deletions are shown as "~~strike-through~~" text and additions are shown as "underlined" text.)

Table 2.5.1-17
Summary of Shear-Fracture Zones (> approximately 0.9 ft. thick) using 100-, 200-, and 400-series Borehole Data

Boring Number	Stratigraphic Unit	Ground Surface Elevation (ft)	Drilled Depth		Elevation (NAVD88)		Apparent Thickness (ft)	Run No.	RQD (%)	Boring Log Description [d]
			From (ft)	To (ft)	From (ft)	To (ft)				
MP-101	Rockdell Formation	800.5	246.6	253.4	553.9	547.1	6.8	47, 48	100	SZ/FZ, multiple shears at 45° and parallel to bedding, intensely fractured and healed with calcite (intact), some folding/rotation of bedding observed; SZ/FZ, several healed fractures at 80°, VT, A, I, with calcite
			259.2	263.3	541.3	537.2	4.1	49, 50	96, 94	SZ/FZ intensely fractured, 60-80°, PL-PR, VT, A, I-Intact and healed with calcite.
			280.6	282.0	519.9	518.5	1.4	54	100	SH, 40-50°, PL, VT, A, I, with calcite (intact)
			287.1	290.1	513.4	510.4	3	55	92	BJ/SH, 30-40°, PL-PR, PO-T, C, III, with calcite
			291.0	294.9	509.5	505.6	3.9	56	70	BJ/SH, 30-35°, SL, VT, A, III, with calcite
			311.7	315.0	488.8	485.5	3.3	60	82	BJ/SH, 30-40°, PL, VT-T, C, II
MP-102	Rockdell Formation	797.9	322.8	324.5	475.1	473.4	1.7	65	90	SH, 30-35°, VT, A, I, with calcite
			326.9	332.6	471.0	465.3	5.7	66, 67	84, 94	SH, 20-30°, VT, A, I, with calcite; BJ/SH, 30°, PL, T-PO, C, III, with calcite; SH, 60°, PL, PO, C, III, with calcite; SH, 30°, VT, A, I, with calcite; SZ, 15-25°, PL, T-PO, C, II, with calcite containing brecciated siltstone
			346.8	350.3	451.1	447.6	3.5	70	84	SH, 35-20°, PL, T-PO, C, II-III, with calcite; SH, 30-70°, VT, A, I, with calcite (intact)
MP-103	Rockdell Formation	800.6	125.3	129.0	675.3	671.6	3.7	22	60	SH/BJ, 40°, PL-SL, VT-T, C, II, with calcite; SH/BJ, 40°, PL-SL, VT-T, C, II, with calcite

Boring Number	Stratigraphic Unit	Ground Surface Elevation (ft)	Drilled Depth From (ft)	Drilled Depth To (ft)	Elevation (NAVD88) From (ft)	Elevation (NAVD88) To (ft)	Apparent Thickness (ft)	Run No.	RQD (%)	Boring Log Description [d]
			146.8	149.5	653.8	651.1	2.7	26	46	SH/BJ, 30°, PL-PR, T, C, II with calcite
			160.0	162.4	640.6	638.2	2.4	29	92	SH/BJ, 30-35°, PL-PR, VT-T, B, II with trace calcite
			164.6	168.8	636.0	631.8	4.2	30, 31	50, 98	SH/BJ, 25-30°, SL-SR, VT-PO, C, II with calcite; SH/BJ, 25-35°, SL-SR, VT-PO, C, II with calcite
MP-107	Rockdell Formation	801.6	171.9	173.0	629.7	628.6	1.1	27	90	SH, 20-30°, PL, T-PO, B-C, II, with calcite
MP-108	Benbolt Formation	798.5	131.9	133.5	666.6	665.0	1.6	26	92	SH, 30°, PL, T-PO, C, II, with calcite; SH, 30-50°, PL-UL, VT-T, A-B, I-II, with calcite; SZ, 30-50°, PL-UL, VT-T, A-B, C, I-II, with calcite
MP-114	Benbolt Formation	797.2	164.0	165.9	633.2	631.3	1.9	31, 32	100, 94	SH, 30-35°, PL, T, B, II with calcite; SZ, 35-55°, PL-UL, VT, A, I with calcite; SH, 35°, PL, T, B, II with calcite
MP-120	Rockdell Formation	800.1	281.8	283.2	518.3	516.9	1.4	52	62	SH, 30°, PL, T, B, II; SH, 30°, PL, VT, A, I, intact with calcite
			287.3	290.7	512.8	509.4	3.4	53, 54	64, 68	SH, 30-35°, PL, T-PO, B, II, most with calcite; SH, 25-30°, PL, T, B, II
			293.3	299.0	506.8	501.1	5.7	54, 55	68, 98	SH, 25-30°, PL, T, B, II; SZ, 30°, PL, O, C, II, with calcite, 0.1' loss of core; SZ, 30-50°, PL, VT/T/O, A-C, I-II, mostly intact with calcite and irregular healed fractures around chert nodules; SH, 30°, PL, T, B, II, most with calcite; SZ, 0°, US, VT, A, I-II, mostly intact-tensional shears; SH, 30°, PL, VT, A, I, intact with calcite
			341.7	342.7	458.4	457.4	1	64	82	SH, 30°, PL, T, B, II with calcite; SZ, 10-80°, UL, VT-T, A-B, I-II, mostly intact, intense calcite mineralization along multiple cross-cutting shears

CNL-16-162

Boring Number	Stratigraphic Unit	Ground Surface Elevation (ft)	Drilled Depth From (ft)	Drilled Depth To (ft)	Elevation (NAVD88) From (ft)	Elevation (NAVD88) To (ft)	Apparent Thickness (ft)	Run No.	RQD (%)	Boring Log Description [d]
MP-121	Benbolt Formation	797.6	47.0	48.8	750.6	748.8	1.8	6	66	SZ/FZ, 30°, PL, T, B, II; SZ/FZ, 45-60° and 90°, VT, A, I, with calcite and spaced at about 0.1'; SH, 40-45°, PL, T-PO, B, II
			51.6	53.6	746.0	744.0	2	7	62	SZ/FZ, 30-40°, PL, T, B, II, with calcite
			56.1	58.0	741.5	739.6	1.9	8	92	SH, 30-45°, PL, T, B-C, II-III, with calcite
MP-201	Eidson Member	790.9	146.7	164.3	644.2	626.6	17.6	27, 28, 29, 30	70, 22, 74, 72	SZ, 30°, PL, PO-MO, A-C, I-II, with calcite healed gouge; SH, 20-30°, PL, T-PO, A-C, I-II, with calcite; SZ, 30°, PL, T-PO, B, I, with calcite; BJ/SH (10), 35-40°, PL, T-PO, A-D, I-III; SZ, 20-30°, PL, PO, C-D, II-III, with calcite; SZ, 35°, PL, T-PO, A-D, II-III, with calcite; SZ, 30°, PL, PO-O, C, III, with calcite; SH, 30°, PL, T-PO, A-C, I-II, with calcite; SZ, 30°, PL, T-PO, A-C, I-II; SH, 30°, PL, T-PO, C, I; SZ, 30°, PL, T-PO, A-C, I-II, with calcite
MP-202	Eidson Member	811.8	276.9	282.2	534.9	529.6	5.3	57, 58	46, 72	SHEAR ZONE, intense shearing with calcite mineralization
	Blackford Formation		366.3	367.2	445.5	444.6	0.9	75	94	SH, 80°, VT, A, I with calcite
MP-205	Eidson Member	810.9	202.6	203.5	608.3	607.4	0.9	38	78	SZ, 30°, US-UL-PL
			206.3	212.1	604.6	598.8	5.8	39, 40	52, 67	SZ, core loss 1.2'; SZ, PR, MO, C, II, core loss of 0.4'; FZ/SZ, core loss of 1.0'
MP-207	Eidson Member	779.7	116.8	119.5	662.9	660.2	2.7	21	60	SZ, 70-80°, PL-PR, C-K, II with calcite
			123.2	124.4	656.5	655.3	1.2	22	82	SZ, 30°, PL, PO-O, C, II with calcite
MP-209	Eidson Member	807.7	207.7	208.7	600.0	599.0	1	42	72	SZ, 30°, SL, VT-T
MP-211	Eidson Member	779.8	112.8	113.9	667.0	665.9	1.1	22	96	SZ, 30-80°, US-UL, VT, I
MP-219A	Eidson Member	808.6	175.8	177.2	632.8	631.4	1.4	35	88	SZ, 30-40°, VT-T, C, I, with calcite

Boring Number	Stratigraphic Unit	Ground Surface Elevation (ft)	Drilled Depth		Elevation (NAVD88)		Apparent Thickness (ft)	Run No.	RQD (%)	Boring Log Description [d]
			From (ft)	To (ft)	From (ft)	To (ft)				
MP-417	Eidson Member	772.7	228.9	233.5	543.8	539.2	4.6	38, 39	60, 88	SHEAR ZONE, multiple calcite healed shears at 40-65° to core axis; BJ/SH, 35°, PL, T, C, II; SHEAR ZONE, multiple calcite healed shears at 20-30° to core axis
MP-418A	Eidson Member	811.1	88.9	90.8	722.2	720.3	1.9	4	48	SZ, 45-50°, PR-PL, T-PO, C, III; SZ, 45-50°, UR-PR/PL, O-PO, B, III, with calcite
			94.4	95.9	716.7	715.2	1.5	5	80	BJ/SH 40-50°, PR-PL, T-PO, B-C, II-III; SZ, 50°, PL, PO, H-C, III, calcite
MP-423	Eidson Member	799.0	80.1	101.9	718.9	697.1	21.8	13,14, 15,16, 17,18, 19	89, 74, 33, 0, 70, 60, 84	FZ/SZ, 40-75°, PR, VT-T, A, I, with calcite; FZ-SZ, 50-80°, calcite-healed fractures; SZ-FZ, 50-90°, VT-PO, A-B, I; SH/BJ, 30°, PL-SL, T, C, II; FZ/SZ, 35-85°; SH, 35-40°, SL/PL, T-PO, B, II; SZ, 30-85°, with calcite-healed limestone breccia
			109.8	118.2	689.2	680.8	8.4	21, 22	80, 85	SH, 30°, PL-SL, T-PO, B, II; SZ, 30-35°, VT, A, I, calcite-healed shears closely spaced; SH, 30°, PL-SL, T-PO, B II; SH, 30-35°, PL/UR/PR, TP-O, D-B, II; FZ/SZ, 40-60° and 30°, VT, A, I, with calcite; BJ/SH, 35°, PL, PO, B, II

Notes:

(a) Shear-fracture zones include one or a cluster of SZ's or SH's ≥ 0.9 ft (and/or BJ/SH) with average frequencies per cluster of ≤ 0.5 ft.
(b) Shear-fracture zones include one or a cluster of SZ's or SH's ≥ 0.9 ft (and/or BJ/SH) with average frequencies per cluster of ≤ 0.5 ft.
(c) Thickness of the shear-fracture zones is apparent as not measured perpendicular to the bounding discontinuity.
(d) Explanation of abbreviations is contained in Table B.1.1 in Appendix B in Reference 2.5.1-214.

Source: Reference 2.5.1-214

CNL-16-162

As a result of the replaced text in Subsection 2.5.1.2.4.3.4, the following Figures are added to SSAR Subsection 2.5.1:
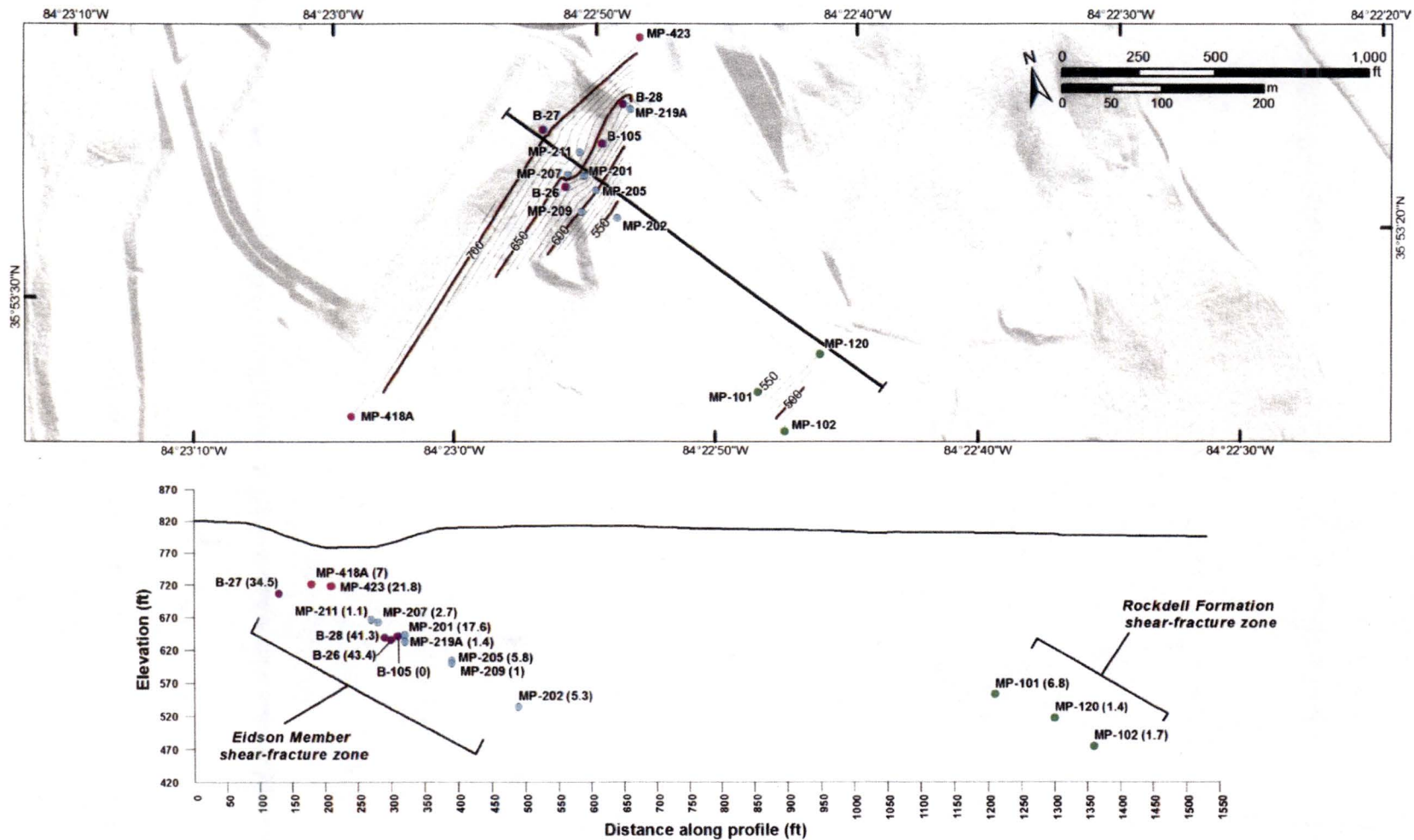
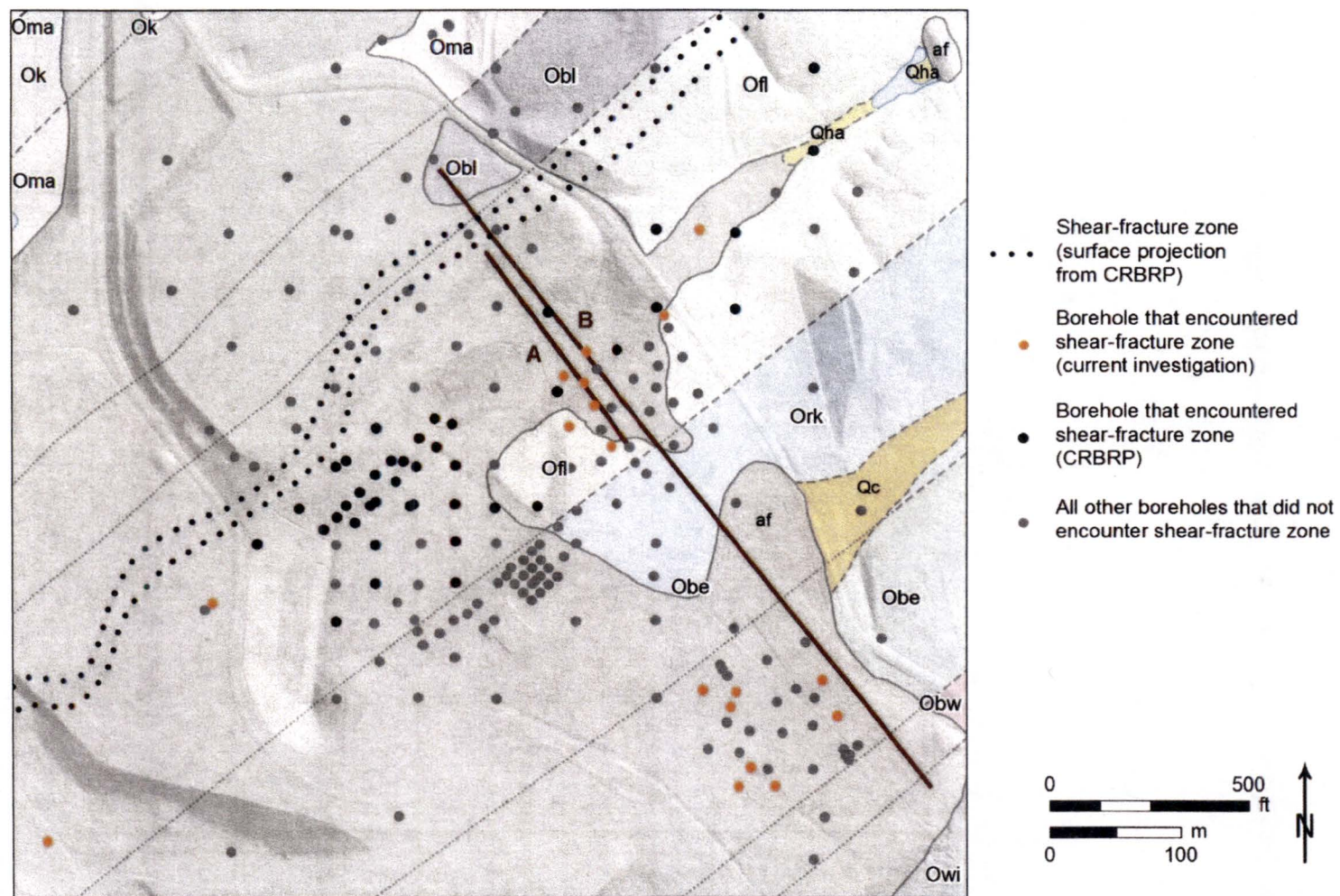Figure 2.5.1-65.   (Sheet 1 of 2) Structure Contour Map of Shear Fracture Zones

Figure 2.5.1-65.   (Sheet 2 of 2) Map of Cross-Section Locations and Boreholes that Encountered Shear Fracture Zones
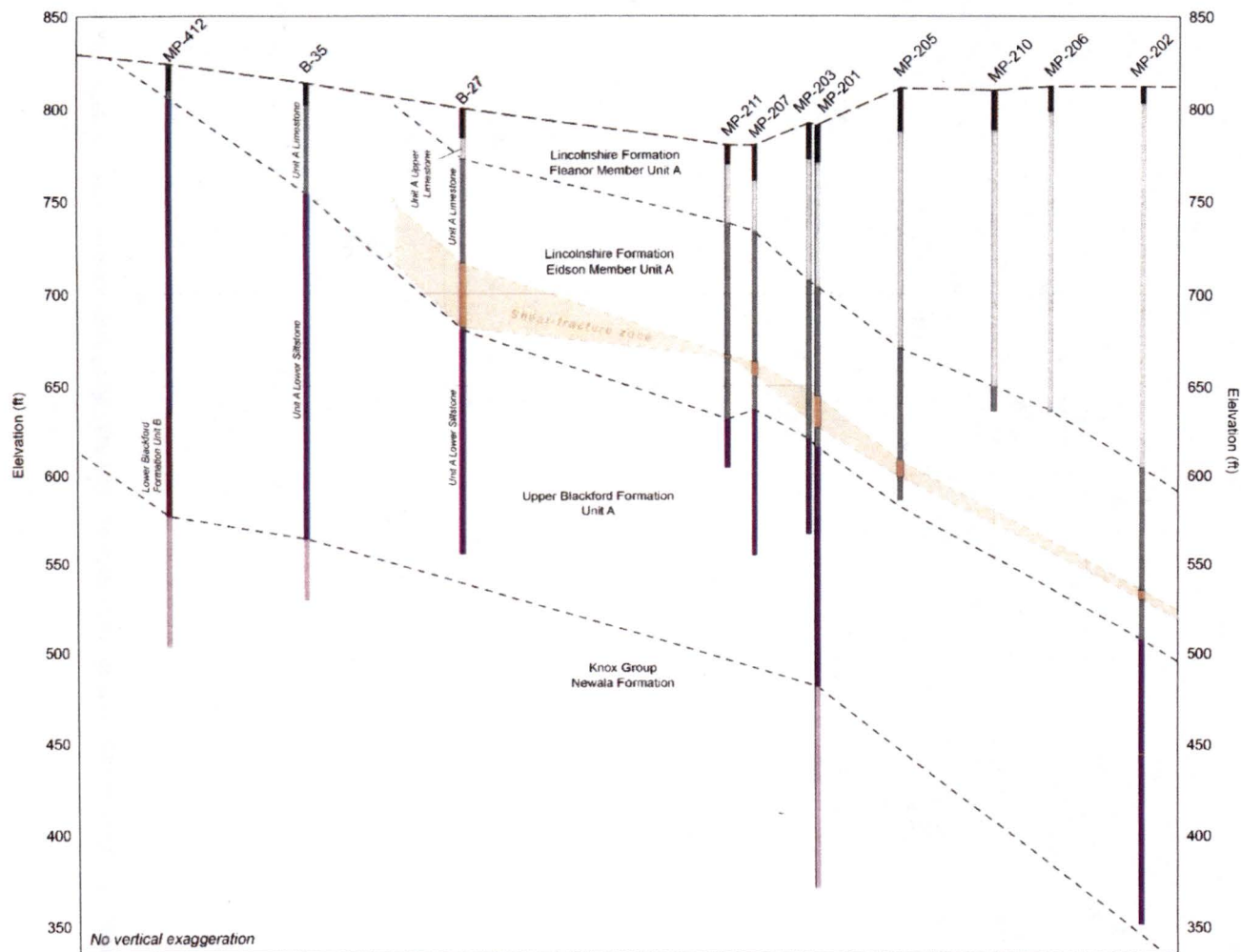
Figure 2.5.1-66.   Cross-Section through the Shear-Fracture Zone within the Eidson Member of the Lincolnshire Formation (Cross Section Line A in Figure 2.5.1-65)
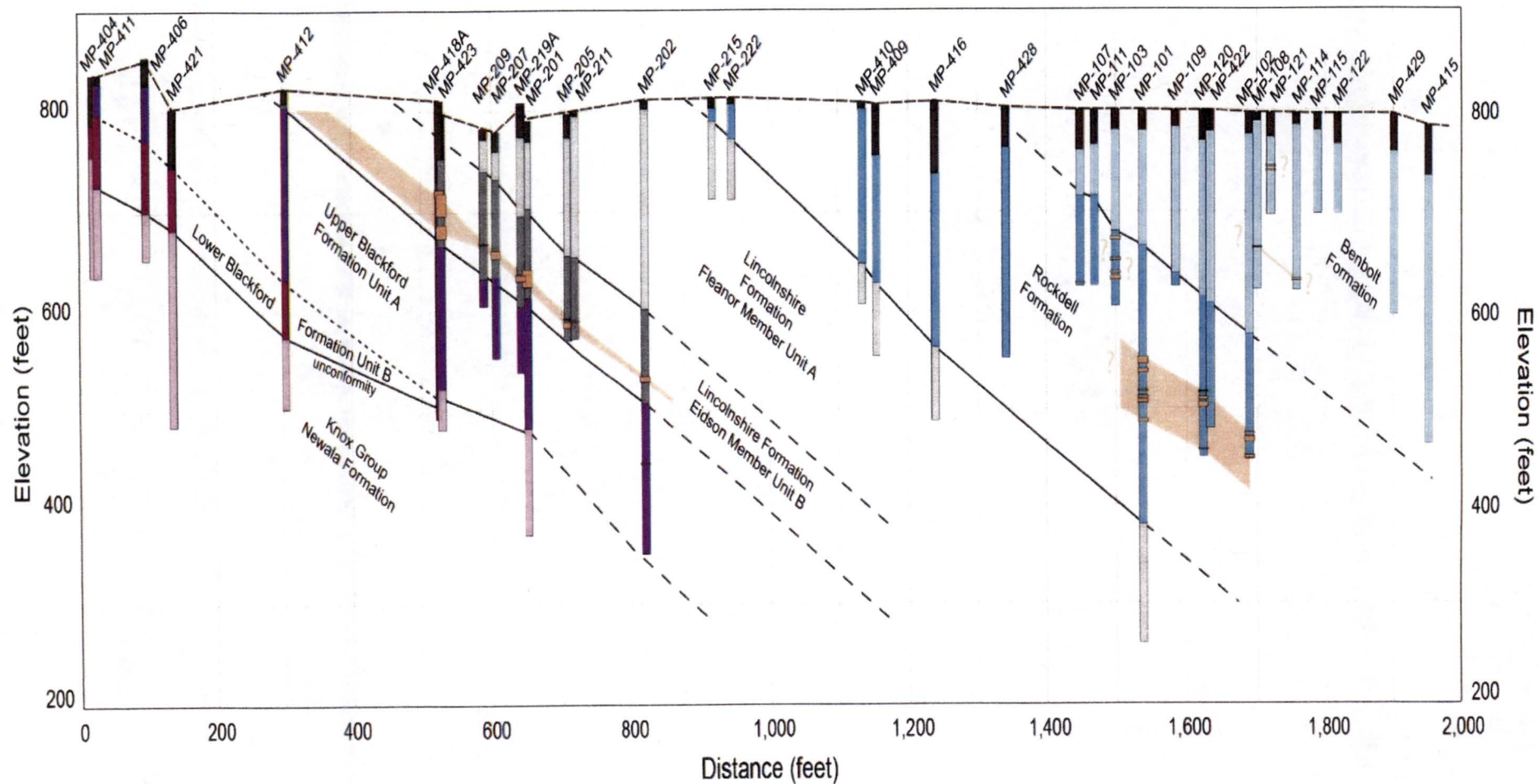
Figure 2.5.1-67.   Cross-Section Through All Shear-Fracture Zone Features (Cross Section Line B in Figure 2.5.1-65)

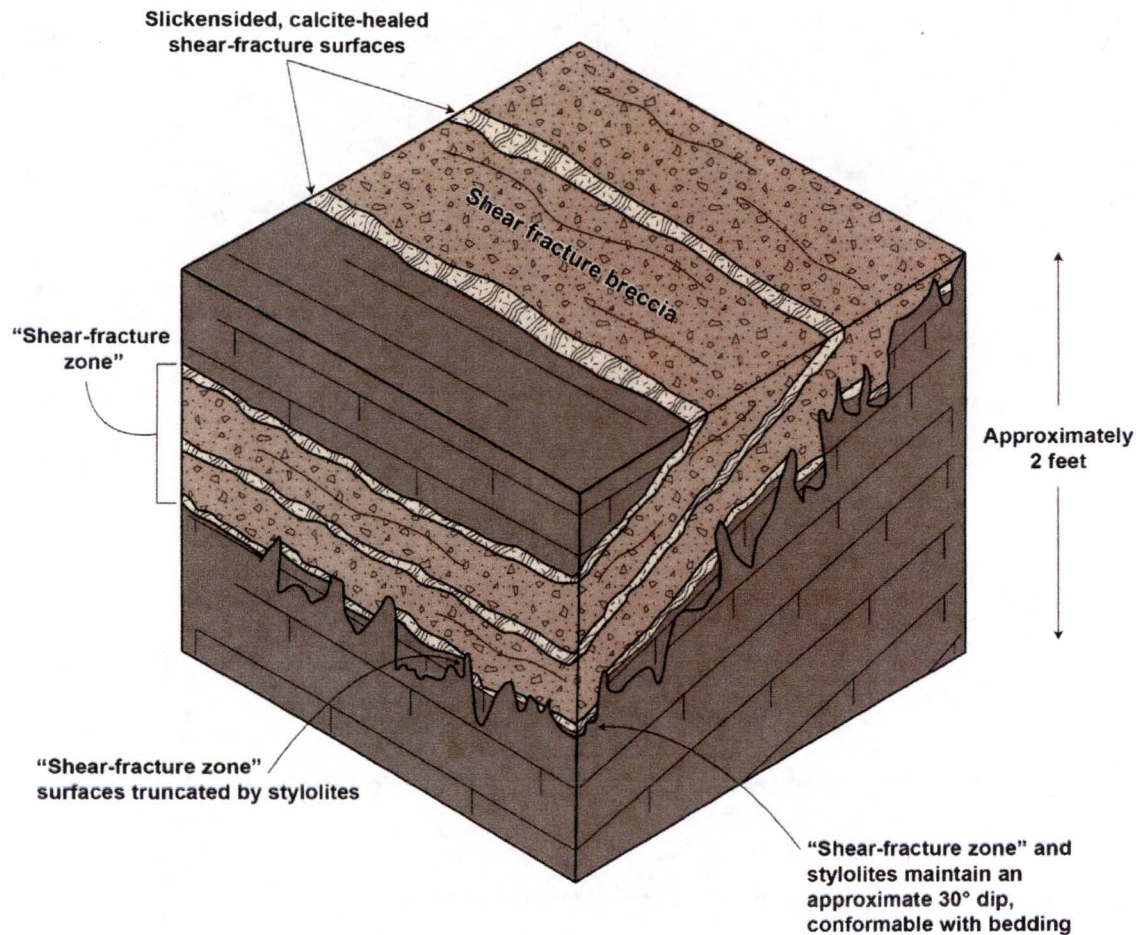Figure 2.5.1-68.   Schematic Diagram of the Crosscutting Relationships Between Bedding, Stylolites, and Shear-Fracture Zone Features

Copies of the new Figures are provided on the following pages.

Figure 2.5.1-65. (Sheet 1 of 2), Structure Contour Map of Shear Fracture Zones

Figure 2.5.1-65. (Sheet 2 of 2), Map of Cross-Section Locations and Boreholes that Encountered Shear Fracture Zones

Figure 2.5.1-66. Cross-Section through the Shear-Fracture Zone within the Eidson Member of the Lincolnshire Formation (Cross Section Line A in Figure 2.5.1-65)

Figure 2.5.1-67. Cross-Section Through All Shear-Fracture Zone Features (Cross Section Line B in Figure 2.5.1-65)

Schematic diagram of the "shear-fracture zone"

Slickensided, calcite-healed
shear-fracture surfaces

Shear fracture breccia

"Shear-fracture
zone"

Approximately
2 feet

"Shear-fracture zone"
surfaces truncated by stylolites

"Shear-fracture zone" and
stylolites maintain an
approximate 30° dip,
conformable with bedding

Figure 2.5.1-68. Schematic Diagram of the Crosscutting Relationships Between Bedding,
Stylolites, and Shear-Fracture Zone Features

By letter dated May 12, 2016 (Reference 1), Tennessee Valley Authority (TVA) submitted an application for an early site permit for the Clinch River Nuclear (CRN) Site in Oak Ridge, TN. Subsequent to the submittal of the application, and consistent with interactions with NRC staff, TVA identified certain aspects of the application that it intends to supplement. By letter dated August 11, 2016 (Reference 2), TVA provided a plan for submitting the identified supplemental information.

This enclosure provides supplemental information related to Geologic Characterization Information to support the NRC staff's review. This enclosure also includes proposed changes to the affected Site Safety Analysis Report (SSAR) sections. An Early Site Permit Application (ESPA) Change Request has been initiated to incorporate these changes into a future revision of the ESPA.

Supplement Item C (Reference 2)

C. *TVA will provide a markup of the applicable ESPA sections to more fully characterize and analyze the East Tennessee Seismic Zone (ETSZ) to demonstrate that it does not represent a potentially significant seismic hazard for the site, including:*

- *Results of the field work and re-excavated trenches in the ETSZ that were completed by TVA.*
- *Discussion of the bases of alternative hypotheses.*
- *Detailed documentation on the Senior Seismic Hazard Analysis Committee (SSHAC) Level 2 study, including how alternative data and interpretations were considered in the seismic hazard analysis.*

Supplemental Information C

To address the information in the first two bullets above, a new Subsection 2.5.3.2.6, "Proposed Quaternary Deformation Features Along Douglas Reservoir, TN," will be added to the ESPA. This new Section includes results of previously performed field work and re-excavated trenches in the ETSZ completed by TVA and a discussion of the bases of alternative hypotheses.

To address the third bullet above, a description of the SSHAC Level 2 process and how it was implemented during the CRN Site ESPA investigation will be added to Subsection 2.5.2.2.5, "Post-CEUS SSC Studies." This SSHAC Level 2 summary will be submitted under separate cover in the response to Supplemental Information, Supplemental Information B to the area of Vibratory Ground Motion as described in the Enclosure to Reference 2.

References:

1. Letter from TVA to NRC, CNL-16-081, "Application for Early Site Permit for Clinch River Nuclear Site," dated May 12, 2016

2. Letter from TVA to NRC, CNL-16-134, "Schedule for Submittal of Supplemental Information in Support of Early Site Permit Application for Clinch River Nuclear Site," dated August 11, 2016

The following new Subsection 2.5.3.2.6 is added to the ESPA.

2.5.3.2.6   Proposed Quaternary Deformation Features Along Douglas Reservoir, TN

The CEUS SSC (Reference 2.5.3-1) includes a paleoliquefaction database developed from earlier compilations of paleoliquefaction data of the New Madrid seismic zone and surrounding area. The ETSZ was discussed in general terms by the CEUS SSC modelers as a zone of elevated seismicity and noted:

> "At locations east to northeast of Knoxville, Tennessee, with late Quaternary terrace deposits, Vaughn et al. [Reference 2.5.3-11] report the occurrence of outcrop-scale strike-slip, reverse, and normal faults and prevalent fractures; minor paleoliquefaction features; and anomalous fractured and disrupted features attributed to liquefaction and forceful expulsion of groundwater during one or more major late Quaternary earthquakes. These preliminary observations suggest that the ETSZ has produced surface faulting and generated one or more strong earthquakes during late Quaternary time. However, these preliminary results could not qualify that RLMEs had occurred in the ETSZ, and were therefore insufficient to determine whether the ETSZ could be considered an RLME zone and treated accordingly in the CEUS SSC Project." (Reference 2.5.3-1, Section 7.3.4.4).

The elevated seismicity rate that defines the ETSZ was included in the CEUS SSC model as part of the Paleozoic Extended Crust (PEZ) areal source zone. Spatial smoothing was used to retain the elevated rate of seismicity in the ETSZ region.

Since publication of the CEUS SSC report more recent published research formally presents the earlier findings from Vaughn et al. (Reference 2.5.3-11) as well as additional evidence for possible paleoseismic features within the ETSZ (References 2.5.3-12, 2.5.3-13, and 2.5.3-57). Guidance from the CEUS SSC (Reference 2.5.3-1, Appendix E) is used to evaluate the recently reported paleoseismic evidence in these new publications on the ETSZ (References 2.5.3-11, 2.5.3-12, 2.5.3-13, and 2.5.3-57).

2.5.3.2.6.1   Established Criteria for Evaluating Evidence for Paleoliquefaction and Other Paleoseismic Features

2.5.3.2.6.1.1   CEUS SSC Paleoliquefaction Database

For inclusion in the CEUS SSC paleoliquefaction database and consideration in the seismic source characterization as earthquake-induced liquefaction features, features are required to satisfy specific, well-established criteria as defined in References 2.5.3-58 and 2.5.3-59. These criteria are listed below:

1. Sedimentary characteristics consistent with case histories of earthquake-induced liquefaction.

2. Sedimentary characteristics indicative of sudden, strong, upwardly directed hydraulic force of short duration.

3. Occurrence of more than one type of liquefaction feature and of similar features at multiple locations.

4. Occurrence in geomorphic settings where hydraulic conditions described in (2) would not develop under nonseismic conditions.

5. Age data to support both contemporaneous and episodic formation of features over a large area.

These well-established criteria are adopted to maintain consistency between datasets considered for the paleoliquefaction database. The CEUS SSC Report (Reference 2.5.3-1, Appendix E) also describes the types of liquefaction features used to identify paleoearthquakes in regional studies that are consistent with the above criteria. Potential paleoliquefaction features include sand blows or sand-blow craters (with feeder dikes), sand dikes, sand sills, ball-and-pillow structures, basal erosion and sand diapirs, dish structures, load casts, and pseudo-nodules (Reference 2.5.3-1, Appendix E).

Sedimentary characteristics of paleoliquefaction described in Reference 2.5.3-1 (Appendix E) that are consistent with the criteria outlined above include:

- Sand blows or sand-blow craters (with feeder dikes)

    o Typically elliptical or linear, sometimes circular, in plan view

    o Connected to feeder dikes below

    o Often characterized by "cut-and-fill" structure and flow structures, and/or lineations, above the feeder dike

    o Vented sediment is typically fine to coarse sand, may include some silt and clay

    o Often becomes finer-grained up-section and laterally away from feeder dike/vent

    o Usually thins laterally away from feeder dike/vent

    o May comprise multiple fining-up depositional units related to a sequence of earthquakes; seismites may be separated by layers of fines such as silty clay or clay that accumulated between earthquakes

    o May contain clasts of host deposit, especially near feeder dike, clast size generally decreases with distance from vent

    o Volume of vented deposit should "make sense" relative to size and number of sand dikes

    o Subsidence structures may be seen near vent, including localized downwarping of surface soil and host strata and possible vertical displacement across feeder dikes

    o Sand-blow craters often form in organic-rich soils or clay-rich host deposits

    o Sand-blow craters contain vented sand deposits and clasts of host material; overlain by crater fill deposits and/or reworked material

- Sand dikes

  - Dike sidewalls typically subparallel, usually widen downward; also may broaden upward into vent structure at the ground surface (event horizon)

  - Typically a few meters to tens of meters long (in plan view); therefore, often, but not always, exposed in both walls of a trench

  - Sand within dikes often fines upward

  - Often characterized by flow structure or lineations

  - Often contain clasts of host deposit(s)

  - Near-vertical dikes may exhibit grading, with finer material along dike margins; inclined dikes may exhibit bedding

  - May be characterized by subsidiary dikes and/or sills

  - Source layer often lacks original sedimentary structure where fluidized, may exhibit flow structure or lineations as well as soft-sediment deformation structures such as ball-and-pillow structures and dish structures.

2.5.3.2.6.1.2 Counts and Obermeier Paleoseismic Criteria

While the criteria described in Reference 2.5.3-1 broadly apply to paleoliquefaction features, Reference 2.5.3-60 presents criteria for also identifying small-scale soft-sediment deformation features. These features are often characterized by small intrusions of sand into a fine-grained host, deformed and disrupted bedding from seismic shaking, or deformation from sill intrusions. Reference 2.5.3-60 states that at least one of the following criteria should be met in order to consider a seismic origin for a feature:

1. Intrusion is the result of suddenly applied pore-water force that (a) caused hydraulic fracturing of the fine-grained host; (b) is indicated by small pinching-together dikes in the fine-grained host; (c) is indicated by clasts from overlying fine-grained stratum that have been transported downwards into underlying sand; or (d) is indicated by sand sills between fine-grained strata in which nonseismic fluidization can be eliminated.

2. Intrusion is much younger than the host and cannot be the result of external forces (e.g., wave pounding or wave shear from overlying flood waters). Wave shear is the friction exerted by flowing water on the stream bed, or in the case of flood waters, on the flood terrace. Wave shear can result in the injection of bedload sediment into the underlying material.

3. Multiple sites with proximal features are documented and their regional pattern of occurrence cannot be explained by sedimentary characteristics. Small-scale features found proximal to large-scale, more readily apparent seismically induced features are ideal.

Reference 2.5.3-60 also presents additional criteria to consider when identifying ground fractures, including:

1. Above liquefied sediment: fractures cannot be explained by lithologic properties or geologic anisotropies of the host sediments, are found at multiple proximal sites, occur in a regional pattern, and are parallel locally and across a larger area. Reference 2.5.3-60 stated that nonparallel fractures can be caused by seismic shaking; however, such features require additional evidence supporting a seismic origin.

2. Above nonliquefied sediment: fractures extend for meters in length and depth can be parallel or not, cannot be explained by characteristics of the sediments or bedrock (e.g., jointing at depth, desiccation, weathering, slumping), are found at multiple proximal sites, and occur in a regional pattern.

2.5.3.2.6.1.3 Criteria to Evaluate the Origin of Clastic Dikes

Clastic dikes are sedimentary dikes in soil or rock consisting of clastic material such as sand or gravels. Clastic dikes are cited as either resulting from paleoearthquakes (References 2.5.3-60 and 2.5.3-61) or soil-forming processes (References 2.5.3-62, 2.5.3-63, and 2.5.3-64). Reference 2.5.3-62 describes problems in evaluating the development of clastic dikes, including determining the origin of the fractures, the source of the clastic material, and the method of emplacement of the dike material (whether infilling from above or liquefaction). Reference 2.5.3-61 states that, in order for a clastic dike to be considered a liquefaction feature resulting from a paleoearthquake, the following criteria must be met:

1. Details of individual clastic dikes conform with those of known seismic origin.
2. Both the pattern and location of dikes in plan view conform with a seismic origin, on a scale of tens to thousands of meters.

3. The size of dikes on a regional scale identifies a central "core region" of widest dikes, which conforms with severity of effects expected in the energy source region (the meizoseismal zone).

4. Other possible causes for the dikes are ruled out (References 2.5.3-61, 2.5.3-65).

2.5.3.2.6.2   Douglas Reservoir Terrace Mapping

In order to better constrain the relative ages of terraces along Douglas Reservoir, morphological correlation and longitudinal profiling of terrace elevations was completed along approximately 95 km of the French Broad River as part of the CRN Site investigation (Figures 2.5.3-10 and 2.5.3-11). Correlated terraces include the modern (prior to the construction of Douglas Dam) flood plain (T0) and seven older terraces (T1 to T5, including an intermediate, locally observed terrace T2.5, and an undifferentiated Pleistocene terrace designation [QPT]). Terrace surfaces mapped on the banks of tributaries of the French Broad River, including the Pigeon River, the Little Pigeon River, and the Nolichucky River, were not correlated but instead designated as uncorrelated terraces (UT) due to different development histories.

A baseline longitudinal profile was developed to represent the incised French Broad River prior to the construction of Douglas Dam (Figure 2.5.3-11). Elevation points within the study area below the dam (~13 km) and above Douglas Reservoir were extracted from the DEM, fit with a linear regression, and extrapolated along ~95 km of the mapped French Broad River. Additionally, correlated terrace surfaces' location and elevation data were linearly regressed. The linear regressions for the modern French Broad River and terraces T2 to T5 have the same slope of -5×10^{-4}, and QPT has a slightly steeper slope of -6×10^{-4} (Figure 2.5.3-11). Using these regression-derived slopes, terraces T2, T3, T4, and T5 are approximately 15 m, 25 m, 31 m,

and 37 m above the modern French Broad River, respectively. These are slightly higher average terrace elevations when compared to Hatcher et al. (Reference 2.5.3-12). Undifferentiated Pleistocene terrace, QPT, has a slightly steeper profile slope, possibly resulting from a long-term change in uplift or incision rates, or the erroneous inclusion of unrelated older terrace surfaces under a single profile (Figure 2.5.3-11). QPT is approximately 46 to 56 m above the modern French Broad River.

2.5.3.2.6.3   Field Reconnaissance of Proposed Quaternary Deformation along Douglas Reservoir

Douglas Reservoir, located on the French Broad River in Eastern Tennessee, has been the site of extensive recent study by University of Tennessee Professor Robert Hatcher and his colleagues. Douglas Reservoir is significantly drawn down each winter, exposing wave-eroded soil and weathered bedrock along the shoreline. Hatcher et al. (Reference 2.5.3-12) completed an 18-month pilot study to search for paleoseismic features in the ETSZ that included field reconnaissance with a focus on six sites (DL-1 through DL-6) along the Douglas Reservoir near Dandridge, Tennessee. In that pilot study, Hatcher et al. (Reference 2.5.3-12) identified potential paleoseismic features that include possible faults, fissures, bleached clay fractures, evidence of paleoliquefaction, shale "boils," and disturbed sediments. These features were observed at different sites within fluvial terraces of the French Broad River at Douglas Reservoir (Figures 2.5.3-10, 2.5.3-12).

Warrell (Reference 2.5.3-13) also studied potential paleoliquefaction features at the sites presented in Reference 2.5.3-12 with an emphasis on Site DL-6 and Site DL-9 (not presented in Reference 2.5.3-12; Sites DL-7 or DL-8 are not mentioned in either reference). These seven sites were visited and evaluated to support the CRN Site ESPA. Professor Robert Hatcher and Mr. James Vaughn accompanied Technical Integrator (TI) Team members during field reconnaissance of Sites DL-1, DL-3, DL-4, DL-5, DL-6, and DL-9. The results of that reconnaissance are included in the descriptions below.

2.5.3.2.6.3.1   Site DL-1

Hatcher et al. Observations and Interpretations

Site DL-1 is the farthest upstream site in the Reference 2.5.3-12 study area (Figure 2.5.3-13). Hatcher et al. (Reference 2.5.3-12) report a clastic dike that is at least 1 m long in plan view and greater than 1 m high. This dike is reported to be filled with fine- to medium-grained sand that can be traced down to an underlying sand bed with similar texture. Hatcher et al. (Reference 2.5.3-12) interpret the fine grain size of the dike fill as evidence of seismic liquefaction. Small "dikelets" (3-15 cm), and associated sills are noted by Hatcher et al. (Reference 2.5.3-12) to cut through their interpreted T1 terrace (based on the location of the site relative to their Figure 5). Hatcher et al. (Reference 2.5.3-12) conclude that these features are seismic based on the presence of microfaults, sills, and clasts close to the base of the dike.

TI Team Observations, Interpretations, and Evaluation of Previous Work

Based on the results of field reconnaissance and longitudinal profiling of fluvial terraces, Site DL-1 is located on the T2 terrace (Figures 2.5.3-10, 2.5.3-13), and has the most well-preserved and easily observable terrace deposit of the Hatcher et al. (Reference 2.5.3-12) sites. The T1 terrace of Hatcher et al. (Reference 2.5.3-12) is correlative with the T2 terrace that was delineated during terrace mapping to support the CRN Site ESPA (Figure 2.5.3-13). Several

small terraces identified by Hatcher et al. (T2 and T3, Reference 2.5.3-12) near Site DL-1 were not observed during field reconnaissance (see Figure 2.5.3-13).

Terrace deposits at Site DL-1 overlie the Sevier Shale, and consist of a fining upward sequence with coarse gravelly sand that grades upward to a silt and clay (loess?) cap. The Sevier Shale is well exposed in an approximately 12 m high bluff above the modern river level. Thin joints were observed within the Sevier Shale beds and are likely the result of volume changes or regional strain within the Sevier Shale.

The exposure of the fine to medium-grained sand dike in T2, described by Hatcher et al. (Reference 2.5.3-12) as extending downward to an underlying sand bed with very small dikelets and micro-faults, was not located during reconnaissance with Professor Hatcher and James Vaughn. Review of photographic evidence (Reference 2.5.3-12, their Figure 15) suggests the interpreted paleoseismic fracture could easily have formed as the result of slope failure. In this alternative, gravity driven block rotation along the well exposed bluff produced an extensional fracture or fissure. The fissure was infilled by medium- to fine-grained sand that is locally abundant on the ground surface, and appears to have been transported aerially, which is supported by local loess deposits. Micro-fractures with soil bleaching were observed within the terrace deposits in T2, which appear to be pedogenic cutans (Reference 2.5.3-64) or other weathering phenomenon (References 2.5.3-62, 2.5.3-63) based on: 1) the fractures do not appear to disrupt bedding at the site; 2) similarity between fracture fill and host material; and 3) their relative abundance in the upper portions of the exposure. The consensus of the TI Team is that there is not sufficient evidence to support a seismic component to the origin of any of the features observed at DL-1. All of the features observed at DL-1 can be attributed to commonly occurring geomorphic and pedogenic processes.

2.5.3.2.6.3.2   Site DL-2

Site DL-2 is the next site downstream of site DL-1. The location of this site is shown by Hatcher et al. (Reference 2.5.3-12) to be on the south side of Douglas Reservoir. However, Hatcher et al. (Reference 2.5.3-12) do not discuss the presence or lack of potential seismogenic features within the text. Professor Hatcher and James Vaughn did not accompany the TI Team to this site during their field reconnaissance.

Site DL-2 occurs on the T1 and T2 terraces (Figure 2.5.3-10). Terrace deposits consist of mottled clay with ~10% sand and few pebbles, with ~25 cm and ~10 cm of modern surficial lacustrine material on terraces T1 and T2, respectively. No bleached fractures, boils, or other potential paleoliquefaction features were located during field reconnaissance at this site.

2.5.3.2.6.3.3   Site DL-3

Hatcher et al. Observations and Interpretations

Site DL-3 is located on the south side of Douglas Reservoir near the Tennessee Highway 92 bridge (Figure 2.5.3-10). East of the bridge at Site DL-3, Hatcher et al. (Reference 2.5.3-12) report an ~80 cm long bleached fracture that includes weathered Sevier Shale clasts in the undisturbed T3 terrace. These shale clasts are interpreted by Hatcher et al. (Reference 2.5.3-12) to be carried upward by "fluid moving through the fracture as it formed (possible hydrofracture?)". Hatcher et al. (Reference 2.5.3-12) conclude that this feature is not related to any karst processes, based on their interpretation that the shale fragments were carried from below through undeformed terrace deposits.

TI Team Observations, Interpretations, and Evaluation of Previous Work

Site DL-3 is located on a wave-cut exposure of the T3 terrace and consists of predominantly reddish mottled clay with no apparent fluvial structures (Figure 2.5.3-10). Weathered Sevier Shale clasts were observed in the terrace deposit during field reconnaissance at this site. The thin fracture described by Hatcher et al. (Reference 2.5.3-12) as the conduit for shale clasts to travel upward from depth was not observed during field reconnaissance with Professor Hatcher and James Vaughn because of surficial sediment cover. Within the terrace deposit, several irregularly shaped, clay-lined fractures in contact with weathered shale clasts appear to curve around the clasts, rather than involve them. This implies the in-situ shale clasts within the terrace deposit are unrelated to the fractures. Additionally, anastomosing bleached fractures exposed at this site resemble pedogenic cutans similar to those described at Site DL-1 (Subsection 2.5.3.2.6.3.1). The consensus of the TI Team was that the bleached fractures can be more easily explained by pedogenic processes and the presence of Sevier Shale clasts is a function of deposition of the T3 terrace.

2.5.3.2.6.3.4 Site DL-4

Hatcher et al. Observations and Interpretations

Site DL-4 is located directly southwest of the Tennessee Highway 92 bridge over Douglas Reservoir (Figures 2.5.3-10, 2.5.3-14). Hatcher et al. (Reference 2.5.3-12) report bleached clay-filled fractures in their T2, T3, and T4 terraces, which are truncated by an overlying 1-2 m colluvial unit that yielded an OSL age >73.4 ka. Hatcher et al. (Reference 2.5.3-12) state that this OSL age provides a minimum age for deformation event(s) that may have involved coseismic deformation, mass movement, karst collapse or a combination of these processes. The observed fractures have various orientations, with some isolated, branching, or intersecting. The host material is oxidized alluvium that contains rounded vein quartz and quartzite pebbles derived from the Blue Ridge and locally derived Knox Group angular chert pebbles (Reference 2.5.3-12).

TI Team Observations, Interpretations, and Evaluation of Previous Work

Based on the field assessment of the TI Team, Site DL-4 is located in the T3 terrace, similar to Site DL-3 (Figures 2.5.3-10, 2.5.3-14). This terrace deposit (near DL-4b and DL-4c) contains mottled silty clay with trace sand and lenses of rounded gravel. Bleached, vertically trending clay-rich fractures described by Hatcher et al. (Reference 2.5.3-12) were observed during field reconnaissance with Professor Hatcher and James Vaughn. These bleached fractures exhibit a gradation in color, with grayish interior and darker red borders (Figure 2.5.3-14). They appear to crosscut one another and often pinch out at depth (Figure 2.5.3-14). Collectively, these attributes support the interpretation of these features as pedogenic cutans versus evidence for liquefaction or paleoseismicity.

Field reconnaissance confirms that these bleached fractures do not penetrate into the thin, overlying colluvium that was dated using OSL (>73.4 ka; Reference 2.5.3-12). Therefore, the depositional age of the colluvium represents the minimum age of the fractures (Reference 2.5.3-12). Hatcher et al. (Reference 2.5.3-12) correlate this colluvial OSL age from Site DL-5 to other sites surrounding Douglas Reservoir, and conclude that where proposed paleoseismic features penetrate the Bt horizons of ultisols in terrace deposits (specifically at Site DL-6), the proposed features represent a seismogenic event younger than 73.4 ka. The resulting conclusion that "two strong shocks occurred sometime after ~73 ka, and possibly much later than 73 ka" (Reference 2.5.3-12) is speculative based on the lack of terrace correlations. Field

reconnaissance indicates that correlation of colluvial or soil units between sites around Douglas Reservoir, with respect to age and origin, is inherently uncertain and has not been sufficiently demonstrated at this time. Reconnaissance observations indicate that colluvium exposed at DL-4 and surficial materials at DL-6 have significantly different physical properties and soil development characteristics. Therefore, not only does this stratigraphic correlation (and the resulting conclusion) remain suspect, the interpreted paleoseismic features at DL-4 are better explained by pedogenic processes.

2.5.3.2.6.3.5 Site DL-5

Hatcher et al. Observations and Interpretations

Site DL-5 is located east of the Tennessee Highway 92 bridge along Douglas Reservoir (Figure 2.5.3-15). Hatcher et al. (Reference 2.5.3-12) report shale-clay "boils" and an anastomosing bleached clay-filled fracture array in the T3 terrace that is offset ~25 cm by a sinistral fault at Site DL-5. The orientations of these fractures vary from regional joint data sets in the Valley and Ridge and the western Blue Ridge Foothills (Reference 2.5.3-12). Hatcher et al. (Reference 2.5.3-12) obtained an OSL age of >104.5 ka from alluvium in the lower part of the T3 terrace. Observed fractures at this site crosscut this alluvium, and Hatcher et al. (Reference 2.5.3-12) suggest the OSL age of >104.5 ka represents a maximum age of the fractures, and that they may be as young as Pleistocene (Wisconsin stage) or Holocene. Hatcher et al. (Reference 2.5.3-13) note the presence of Knox Group carbonates and Sevier Shale (Reference 2.5.3-66) beneath DL- 5 and suggests the features described above may be related to karst collapse.

Additionally, Warrell (Reference 2.5.3-13) identifies an outcrop of Lenoir Limestone that lies structurally above highly fractured Sevier Shale saprolite at Site DL-5c. Trenching across this contact exposed Sevier Shale and layered terrace alluvium that Warrell (Reference 2.5.3-13) interprets to be a paleolandslide deposit buttressed at its toe against an exposure of Lenoir Limestone. Warrell (Reference 2.5.3-13) concludes that a seismic or aseismic origin for this landslide could not be determined.

TI Team Observations, Interpretations, and Evaluation of Previous Work

Site DL-5 occurs on the wave cut exposure of the T3 terrace between the Tennessee Highway 92 bridge and Site DL-3 (Figures 2.5.3-10, 2.5.3-15). Along the wave cut surface, potential Quaternary alluvium landslide deposits were observed buttressed against an outcrop of Lenoir Limestone, as described in Reference 2.5.3-13. Additionally, rounded gravels and cobbles that had eroded from the overlying terrace deposits are imbedded in the soft clay-rich Sevier Shale saprolite all along the shoreline at Sites DL-3 and 5.

Examples of shale chips, shale "boils," and the anastomosing bleached clay-filled fracture array described by Hatcher et al. (Reference 2.5.3-12) were observed during field reconnaissance with Professor Hatcher and James Vaughn. The specific shale "boil" presented in Figure 10c of Hatcher et al. (Reference 2.5.3-12) was covered by lacustrine sediment and not exposed during the field reconnaissance. Reportedly similar shale chip features were observed up-river, approximately 30 m near the boat dock walkway. The shale chips are located within a mottled reddish clay matrix with little to no sand, similar to terrace deposits at Site DL-4. The shale chip "boil" reported by Hatcher et al. (Reference 2.5.3-12) occurs very close to the underlying contact with Sevier Shale and resembles classic soil mottling (redoximorphic features) described above. Another possible interpretation is that these shale "boils" are rip-up clasts that resulted from fluvial processes during terrace deposition.

No clastic dikes were observed during field reconnaissance with Professor Hatcher and James Vaughn. However, bleached fractures similar to Site DL-4 were observed. Hatcher et al. (Reference 2.5.3-12) also cites slickensides as evidence for possible displacement along fractures, although slickensides on clay-filled fractures may be related to repeated clay soil expansion and differential forces rather than tectonic microfaulting at this site. These types of slickensides are referred to as stress cutans and are the result of soil processes resulting in the concentration of particular soil constituents or in situ modification due to differential forces as described above (Reference 2.5.3-64).

Hatcher et al. (Reference 2.5.3-12) suggest that a well-developed ultisol with a very long development history (Wisconsin stage and Holocene) that contains bleached fractures is evidence for young paleoseismic activity. It is not clear if these bleached fractures postdate soil development or the secondary soil development post-dates the fractures. The relative age uncertainty described by Hatcher et al. (Reference 2.5.3-12), as well as the uncertainty regarding the formation of the fractures by either soil processes or suggested ground shaking, makes any conclusions regarding number of earthquakes or earthquake timing at Site DL-5 highly uncertain. It was the opinion of the TI Team that the features observed at Site DL-5 were most likely related to pedogenic or depositional processes.

Additionally, during field reconnaissance, Professor Hatcher and James Vaughn showed the location of an OSL sample, collected downslope of DL-5 on the T2 terrace, that yielded an age of ~200 ka. This age is inconsistent with the T2 terrace OSL age of ~27 ka near Site DL-1, which highlights (1) the uncertainty in the available terrace ages; (2) the potential limits of applying OSL dating to sites within Douglas Reservoir; and (3) the need for additional age control.

2.5.3.2.6.3.6   Site DL-6

Hatcher et al. and Warrell Observations and Interpretations

Site DL-6 is located on the north side of Douglas Reservoir, ~5 km southwest of Dandridge, Tennessee, on a partially eroded south-facing T3 terrace slope (Reference 2.5.3-12). Hatcher et al. (Reference 2.5.3-12) and Warrell (Reference 2.5.3-13) document potential paleoseismic features at this site that include: (1) thrust and sinistral faults that cut Sevier Shale and terrace alluvium; (2) alluvium filled fissures; (3) clastic dikes and sills; (4) fracture arrays; and (5) anomalous fracture-bound, elongate "boat" structures that Hatcher et al. (Reference 2.5.3-12) attribute to liquefaction and fluidization. Hatcher et al. (Reference 2.5.3-12) interpret crosscutting relationships of these structural and proposed paleoliquefaction and fluidization features as evidence for at least two strong paleoearthquakes in the ETSZ. Hatcher et al.(Reference 2.5.3-12) also suggest coseismic fracturing may have occurred along with expulsion of overpressured groundwater through bedrock fractures, as well as liquefaction and fluidization of sandy alluvium.

TI Team Observations, Interpretations, and Evaluation of Previous Work

At site DL-6 (Figures 2.5.3-10, 2.5.3-16, 2.5.3-17, 2.5.3-18, 2.5.3-19), a significant portion of Trench 2 presented in Reference 2.5.3-12 and Reference 2.5.3-13 had been re-excavated and cleaned by Dr. Hatcher's colleagues and students prior to field reconnaissance by the TI Team. The TI Team cleaned, logged, and photographed the east wall of Trench 2, and cleaned and photographed the west wall (Figure 2.5.3-17). Geomorphic and geologic mapping was

performed in the area of DL-6 to gain better perspective on the relationship of the slopes and bedding with possible paleoseismic features observed at the site (Figure 2.5.3-16).

The most conspicuous evidence for possible paleoseismic features among all the sites described by Hatcher and his colleagues along the Douglas Reservoir is located at Site DL-6. The two most prominent features include (1) a shallow-dipping shear plane, exposed in Trench 2 and visible at the ground surface for approximately 25 m on the shore of Douglas Reservoir; and (2) an alluvium-filled fracture also exposed in Trench 2 and at the ground surface that is truncated at depth by the shear plane (Figure 2.5.3-17).

The shear plane is marked by a relatively thin (0.5 – 1.5 cm) seam of reddish, soft, moist clay along a bedding plane within the Sevier Shale. No sand or Sevier Shale clasts were visible along the shear plane. The clay seam is probably derived from the Sevier Shale and has been oxidized by movement of meteoric water along the surface. The shear plane strikes N55°E and dips between 10 and 45 degrees, and is coincident with a gently dipping bedding plane in the Sevier shale and has apparent thrust motion (Figure 2.5.3-17). The shear plane becomes listric and steepens as it approaches the ground surface, but it is parallel to bedding lower in the trench and does not appear to cross cut the shale bedding. A small splay off the main shear plane accommodates minor displacement where the plane becomes listric. This splay also parallels bedding and does not appear to be rooted at depth to the main shear plane, which is inconsistent with the interpreted reverse motion. During field reconnaissance with Professor Hatcher and James Vaughn, no slickensides or rake marks on the shear plane were confidently identified. However, stress cutans were observed at several locations within the clay-rich shear plane. Where exposed at the ground surface and excavated to shallow depth, these stress cutans exhibited a dendritic or radial pattern which precludes their origin as fault or landslide slickensides or rake marks.

The shear plane in Trench 2 juxtaposes weathered sandy clay alluvial terrace materials and deeply to completely weathered (saprolite) Sevier Shale bedrock (Figure 2.5.3-17). Two near vertical, 15 to 40 cm wide alluvium-filled fissures occur in the hanging wall block above the shear plane (Figure 2.5.3-17). The fissures terminate at the shear plane 1 m below the ground surface, and do not occur in the footwall. The trench was subsequently deepened during field reconnaissance in an attempt to locate the basal portion of the purported offset filled fissure. However, no equivalent fissure material that might have been offset along the shear plane was found in the footwall. If the fissure fill is offset by approximately 1 m, as interpreted by Hatcher et al. (Reference 2.5.3-12) and Warrell (Reference 2.5.3-13), the offset equivalent in the footwall would have been uncovered. The base of the filled fissure and the shear plane are also visible at the ground surface, approximately 18 m southwest of Trench 2.

The apparent thrust displacement along the shear plane of about 1 m is based on the juxtaposition and apparent offset of the contact between the Sevier Shale bedrock and the terrace deposits (Figure 2.5.3-17). There are questions and fundamental concerns regarding this interpretation, including:

- If this fault is a secondary coseismic feature, how can ground motion from a deep earthquake thrust a block of material approximately 1m up a slope (as interpreted in Reference 2.5.3-12)? In particular, the downslope projection of the purported thrust fault would daylight in the canyon wall of the French Broad River. If the thrust fault post-dates formation of terrace T3, and thus daylights out of the canyon wall at the time of its purported displacement, there is no driving mechanism or lateral force to push this block of material up slope.

- If this thrust fault is the result of liquefaction (Reference 2.5.3-12), where is the liquefiable material that is reportedly stratigraphically beneath or within the Sevier Shale?

- What is the nature of the wide alluvium-filled fissure, and why is it not present in the footwall?

- If this fault is seismogenic, where does the relatively shallow, bedding plane parallel shear plane root to a more vertically oriented shear zone? If it does not, this feature should daylight further downslope, sub-aerially within Douglas Reservoir.

If the shear plane represents a thrust fault with a pure dip-slip vector parallel to the wall in Trench 2 (Figure 2.5.3-17) and the filled fracture predates the shear plane, then (1) the filled fracture should be found down-dip in the footwall and (2) the overlying material on the bedrock surface should match across the fault (Units 5 and 6c on Figure 2.5.3-17). The absence of the alluvium-filled fracture in the footwall does not support the hypothesis that this shear plane represents a thrust fault that offsets a pre-existing fracture as suggested by Hatcher et al. (Reference 2.5.3-12) and Warrell (Reference 2.5.3-13). Additionally, Units 5 and 6c appear to be different facies of the same material, which requires a significant component of lateral slip (out of the trench wall plane) to explain their spatial relationship exposed in Trench 2. These observations highlight the uncertainty regarding the proposed interpretations of thrust displacement at Site DL-6.

The geometry and sense of displacement of the offset bedrock is not well enough defined to provide a piercing point for accurate displacement measurements. The overlying material on the bedrock surface, as well as the character of the bedrock surface, do not match across the trench. The different material properties, such as grain size, sorting, and depositional structures of the overlying units (Units 5 and 6; Figure 2.5.3-17), indicate a significant component of lateral slip may have occurred, regardless of whether Unit 6c may have undergone potential fluidization. Lateral slip on a shallowdipping shear plane that is coincident to dip-slope bedding is more indicative of gravitational slope processes than compressional seismogenic processes.

Given the considerable uncertainty regarding the thrust-fault hypothesis for this feature, alternative explanations include in order of likelihood: (1) a lateral margin of a landslide (SE-directed movement) that locally juxtaposes the bedrock/alluvial contact in an apparent reverse separation in Trench 2 (Figure 2.5.3-18), (2) reverse movement at the toe of an ancient landslide within a paleo-landscape, and (3) deformation related to karst dissolution processes, as several closed depressions occur close to the site (Figure 2.5.3-19). Results from the TI Team assessment of the features observed at Site DL-6 are that they are likely the result of nontectonic processes and, therefore, do not represent paleo-earthquakes. The absence of the alluvium-filled fracture beneath the shear plane suggests it is either contemporaneous with or post-dates initial movement on the underlying shear plane (Figure 2.5.3-18). The filled fracture likely developed during extension of a pre-existing subvertical joint or fracture (striking N33°E) in the Sevier Shale that opened as a result of gravitational block sliding along the pre-existing, bedding parallel, basal shear plane. Subsequent infilling of the fracture with packages of alluvial material likely occurred shortly after extension (Figure 2.5.3-18). This interpretation is consistent with the orientation of the modern hillslope approximately parallel to the dip of bedding in the shale. Several linear features interpreted as slickenlines (Reference 2.5.3-13, their Figure 4-5) along the shear plane are oriented normal to the fissure, which also supports downslope movement of a gravitational block. To definitively determine the temporal relationship of the filled fracture, whether it postor pre-dates the shear plane, the basal portion of the fracture in the footwall should be located (if it exists below the floor of the trench that was

deepened during field reconnaissance) to resolve its origin and determine the possible sense and amount of slip along the shear plane.

The reported "boat structure" at site DL-6 was not observed during field reconnaissance, as Trench 1 had been backfilled and not re-excavated. Some evidence for paleofluidization-liquefaction was discussed at the north end of the exposed Trench 2 during the reconnaissance visit with Professor Hatcher and James Vaughn (Figure 2.5.3-17). This evidence included a poorly sorted alluvial deposit containing clasts of completely weathered Sevier Shale up to 1-2 cm in diameter, suspended in a mottled reddish brown clay matrix. The deposit does not exhibit the typical sedimentary characteristics of the well-established paleoliquefaction criteria, as defined in References 2.5.3-58, 2.5.3-59, and 2.5.3-60, and described in Subsection 2.5.3.2.6.1. Several diagnostic criteria that are critical to the interpretation of these features as a result of liquefaction are absent from these exposures, including sand sills, fining upward sand dikes, and flow structures. An alternative explanation for this poorly sorted deposit, supported by the absence of these key criteria, is that it is the result of a channelized debris flow of terrace sediments at some point in the past.

Hatcher et al. (Reference 2.5.3-12) postulate that the suspended Sevier Shale clasts visible in alluvium in the north side of Trench 2 (Units 6b and 6c; Figure 2.5.3-17) were expelled from the shear plane by the forceful expulsion of ground water. The soft clay within the shear plane does not resemble the matrix of the alluvium, nor are there any clasts of Sevier Shale within the clay-rich shear plane, which would be expected given this interpretation. The small shear splay in the footwall of the shear zone forms an acute angle, which graphically resembles a point of discharge (Figure 2.5.3-17). However, based on our detailed logging of the trench, the shear splay does not appear to connect with the main shear plane at depth (Figure 2.5.3-17). Additionally, the shear splay is clearly visible in the alluvium and, therefore, would have formed after any expulsion event (Figure 2.5.3-17).

2.5.3.2.6.3.7 Site DL-9

Warrell Observations and Interpretations

In addition to the six sites included in Reference 2.5.3-12, Warrell (Reference 2.5.3-13) includes observations at Site DL-9, located on the south side of Douglas Reservoir across from and ~1 km southwest of DL-6. Warrell (Reference 2.5.3-13) reports two OSL ages for this site: (1) DL-9-01, sampled from sediment filling a branching fissure, yielded an OSL age of 15,865 ± 1,735 y; DL-9-02, sampled from undisturbed terrace material near the site, yielded an OSL age of 21,765 ± 1,445 y.

TI Team Observations, Interpretations, and Evaluation of Previous Work

At site DL-9 (Figures 2.5.3-10, 2.5.3-20), numerous alluvium-filled fractures (similar to site DL-6) were observed on a moderately dipping slope within Sevier Shale bedrock. These alluvium-filled fractures are up to approximately 30 cm wide and strike in two conjugate orientations of about N35°E and N10°W. Bedrock at DL-9 dips gently to the southeast. T3 terrace deposits are located upslope and no fractures or deformation were observed in these deposits. The age of the terrace deposits at DL-9 is reported to be approximately 15 ka (Reference 2.5.3-13), based on the OSL age determined using alluvium sampled from the filled fractures. However, the terrace elevation is the same as site DL-6 (T3) and well-developed Fe-Mn soil concretions up to about 60 cm in diameter were observed in this same deposit several hundred meters west of site DL-9, which indicates much older age, possibly on the order of hundreds of thousands of years.

The relationship between the orientation of the alluvium-filled fractures, the modern slope aspect and dip, and the shallow dipping slope-parallel bedding indicates that these fractures likely developed along pre-existing planes of weakness (joints), which were subjected to extension during down-slope rotational block sliding (see Figure 2.5.3-20). This interpretation is consistent with the modern geomorphologic conditions. Similar to site DL-6, the fractures do not extend into the overlying terrace deposits and are confined to the Sevier bedrock.

As a result of the new Subsection 2.5.3.2.6, the following references are added at the end of Subsection 2.5.3.9:

2.5.3.9 References

2.5.3-57.   Obermeier, S.F., Vaughn, J.D., and Hatcher, R.D., Jr., Field Trip Guide – Paleoseismic Features in and Near Douglas Reservoir East Tennessee Seismic Zone, Northeastern Tennessee, Site Visit for the Nuclear Regulatory Commission and Other Agencies, University of Tennessee, 2010.

2.5.3-58.   Obermeier, S.F., Use of liquefaction-induced features for paleoseismic analysis - An overview of how seismic liquefaction features can be distinguished from other features and how their regional distribution and properties of source sediment can be used to infer the location and strength of Holocene paleo-earthquakes, *Engineering Geology*, Volume 44, pp. 1-76, 1996.

2.5.3-59.   Tuttle, M.P., The use of liquefaction features in paleoseismology: Lessons learned in the New Madrid seismic zone, central United States, *Journal of Seismology*, Volume 5, pp. 361-380, 2001.

2.5.3-60.   Counts, R. and Obermeier, S.F., Seismic signatures: Small-scale features and ground fractures: in Cox, R.T., Tuttle, M.P., Boyd, O.S., and Locat, J. (editors), *Recent Advances in North American Paleoseismology and Neotectonics East of the Rockies*, Geological Society of America Special Paper 493, pp. 203–219, 2013.

2.5.3-61.   Obermeier, S.F., Pond, E.C., Olson, S.M., Green, R.A., Stark, T.D., and Mitchell, J.K., Paleoliquefaction studies in continental settings: geologic and geotechnical factors in interpretations and back-analysis, *U.S. Geological Survey Open-File Report 01-29*, 72 pp, 2001.

2.5.3-62.   Heron, S.D., Jr., Judd, J.B., Johnson, H.S., Jr., Clastic dikes associated with soil horizons in the North and South Carolina Coastal Plain, *Geological Society of America Bulletin* Vol. 82, No. 7, pp. 1801-1810, 1971.

2.5.3-63.   Bechtel Power Corporation (Bechtel), Geologic Evaluation of Trench Exposure, Vogtle Nuclear Generating Plant, 1984.

2.5.3-64.   Abbott, J.C., Gelinas, R.L., and Amick, D.C., Investigation of suspect liquefaction features at the Savannah River Site, South Carolina, U.S. Nuclear Regulatory Commission, NUREG/CR-5503 Appendix A, p. A-3 to A-26, 1999.

2.5.3-65.   Obermeier, S.F., Liquefaction evidence for strong earthquakes of Holocene and latest Pleistocene ages in the states of Indiana and Illinois, USA, *Engineering Geology* 50, pp. 227-254, 1998.

2.5.3-66.   Hatcher, R.D., Jr., and Bridge, J., Geologic Map of the Jefferson City Quadrangle, Tennessee, *Tennessee Division of Geology Geologic Map*, GM-163-SW, Scale 1:24,000, 1973.

2.5.3-67   Nicholson, S.W., Dicken, C.L., Horton, J.D., Labay, K.A., Foose, M.P., Mueller, J.A.L., 2005. Preliminary integrated geologic map database for the United States: Kentucky, Ohio, Tennessee, and West Virginia, U.S. Geological Survey Open-File Report 2005-1324, version 1.1, available at http://pubs.usgs.gov/of/2005/1324/, accessed on September 22, 2016

As a result of the new Subsection 2.5.3.2.6, the following Figures are added at the end of Subsection 2.5.3:

Copies of the new Figures are provided on the following pages.

Legend:

T0 Modern (pre-reservoir floodplain) of the French Broad River (FBR) and youngest mapped; flooded by Douglas Reservoir year round in majority of locations.

T1 Geomorphically similar to and spatially associated with T0; flooded by Douglas Reservoir year round in majority of locations; ~20 to 40 ft above modern FBR.

T2 Often spatially associated with T1 and T3; appears more incised than T1; ~50 ft above modern FBR.

T2.5 Spatially associated with T2 and T3, though preserved in few locations; where preserved, appears more incised than T2; ~50 to 80 ft above modern FBR.

T3 Well-incised; most often preserved adjacent to T2 and less frequently adjacent to T2.5; ~80 ft above modern FBR.

T4 Dissected remnants concentrated along paleo-meanders; ~100 ft above modern FBR.

T5 Geomorphically similar to and often spatially associated with T4; in some locations, T5 is preserved near T3 without evidence for T4; ~120 ft above modern FBR.

QPT Undifferentiated Pleistocene terraces; incised and spatially limited; ~150-180 ft above modern FBR.

UT Undifferentiated terraces associated with tributaries of the FBR.
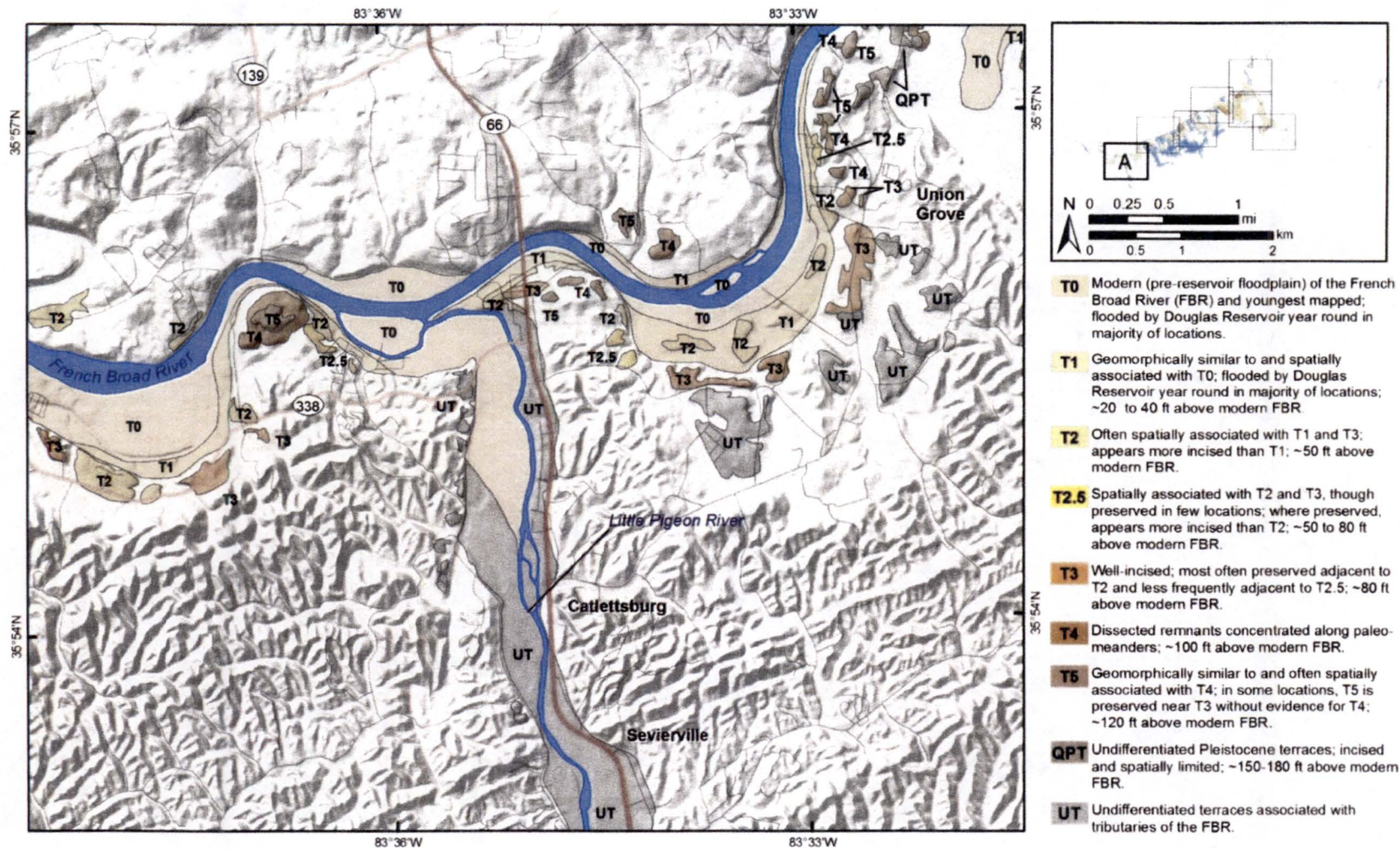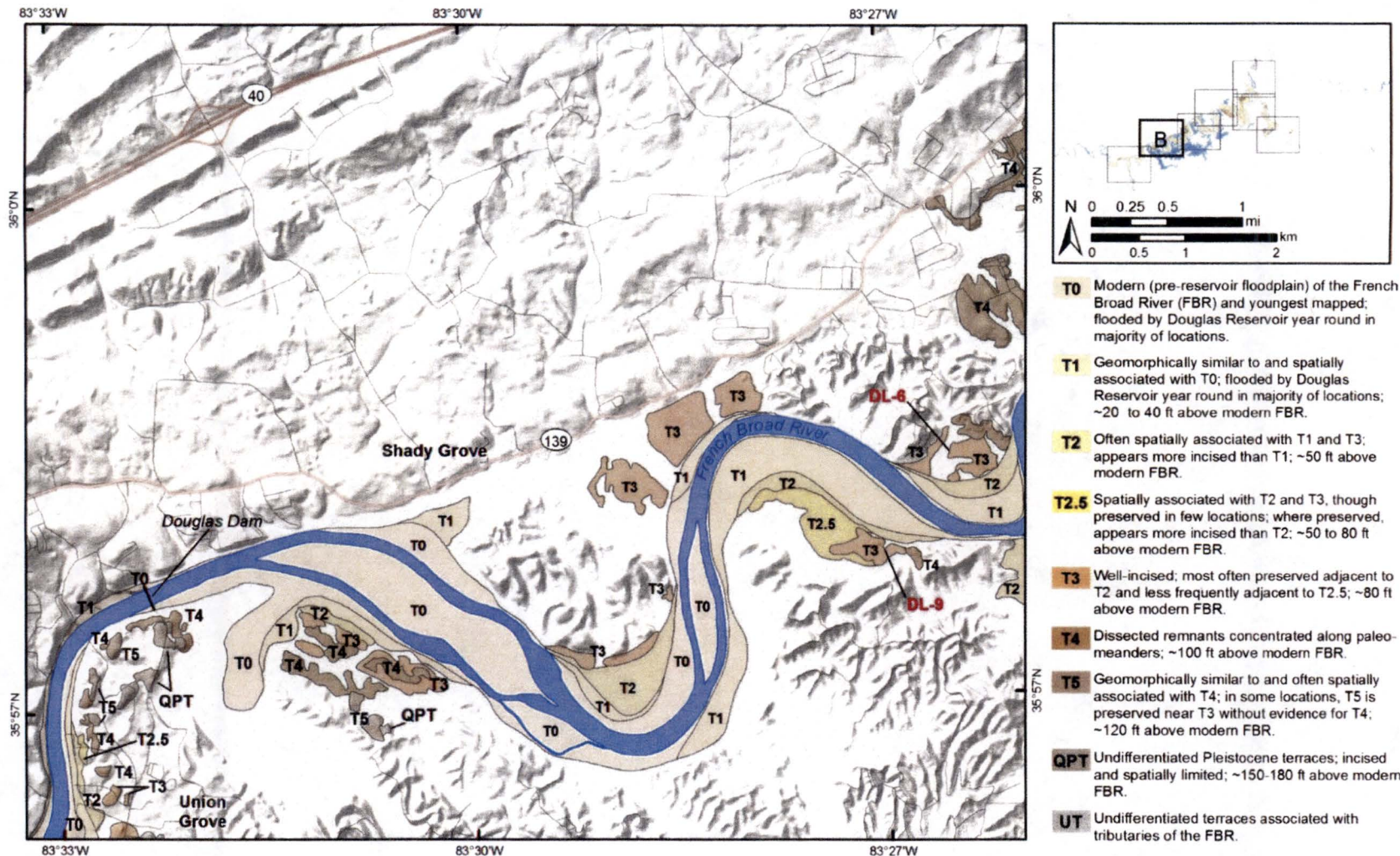
Figure 2.5.3-10. (Sheet 1 of 7), Quaternary Terrace Map of the Douglas Reservoir Area, Location A

Figure 2.5.3-10. (Sheet 2 of 7), Quaternary Terrace Map of the Douglas Reservoir Area, Location B

The legend for the map describes the following terrace units:

T0 Modern (pre-reservoir floodplain) of the French Broad River (FBR) and youngest mapped; flooded by Douglas Reservoir year round in majority of locations.

T1 Geomorphically similar to and spatially associated with T0; flooded by Douglas Reservoir year round in majority of locations; ~20 to 40 ft above modern FBR.

T2 Often spatially associated with T1 and T3; appears more incised than T1; ~50 ft above modern FBR.

T2.5 Spatially associated with T2 and T3, though preserved in few locations; where preserved, appears more incised than T2; ~50 to 80 ft above modern FBR.

T3 Well-incised; most often preserved adjacent to T2 and less frequently adjacent to T2.5; ~80 ft above modern FBR.

T4 Dissected remnants concentrated along paleo-meanders; ~100 ft above modern FBR.

T5 Geomorphically similar to and often spatially associated with T4; in some locations, T5 is preserved near T3 without evidence for T4; ~120 ft above modern FBR.

QPT Undifferentiated Pleistocene terraces; incised and spatially limited; ~150-180 ft above modern FBR.

UT Undifferentiated terraces associated with tributaries of the FBR.
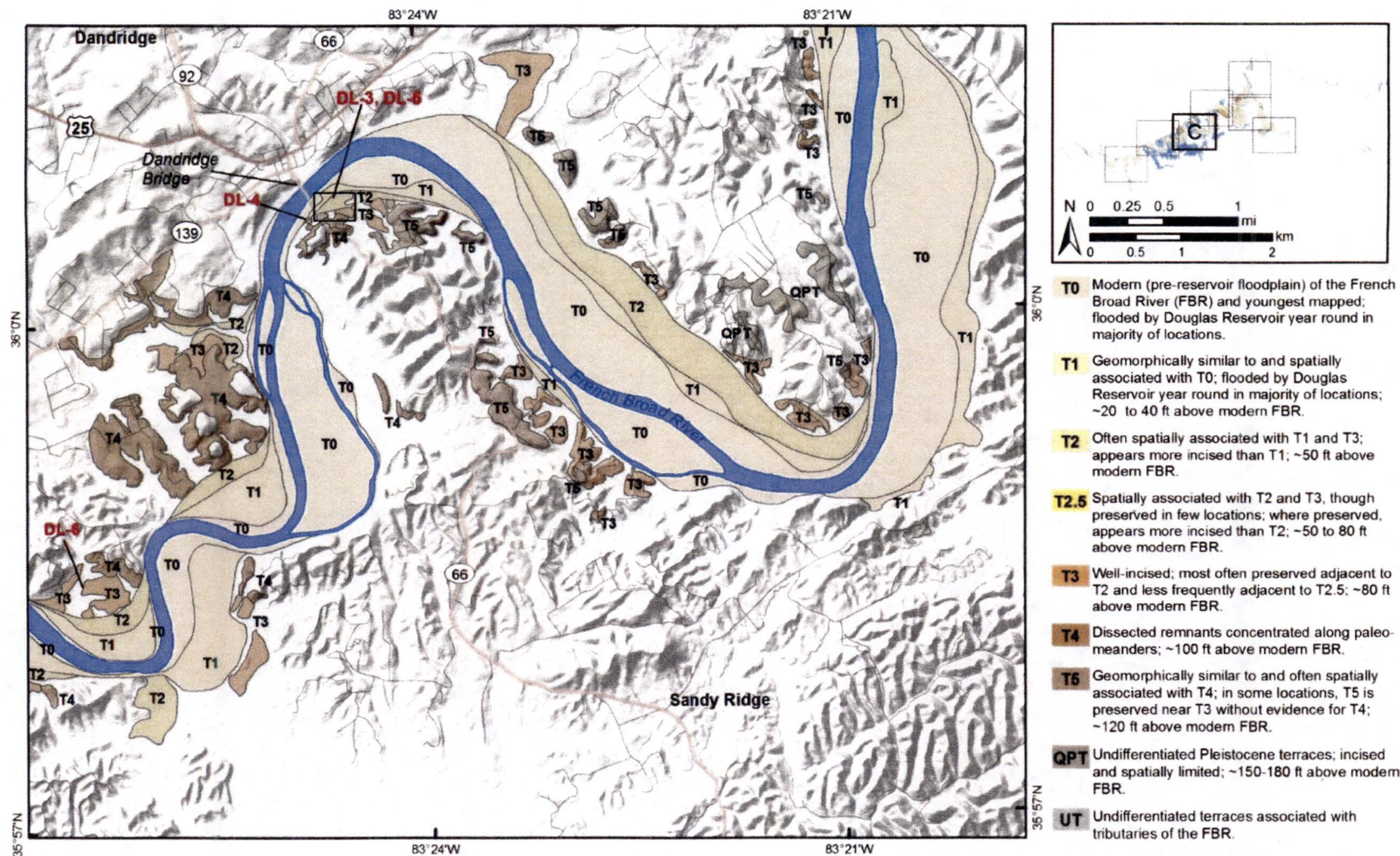
Figure 2.5.3-10. (Sheet 3 of 7), Quaternary Terrace Map of the Douglas Reservoir Area, Location C

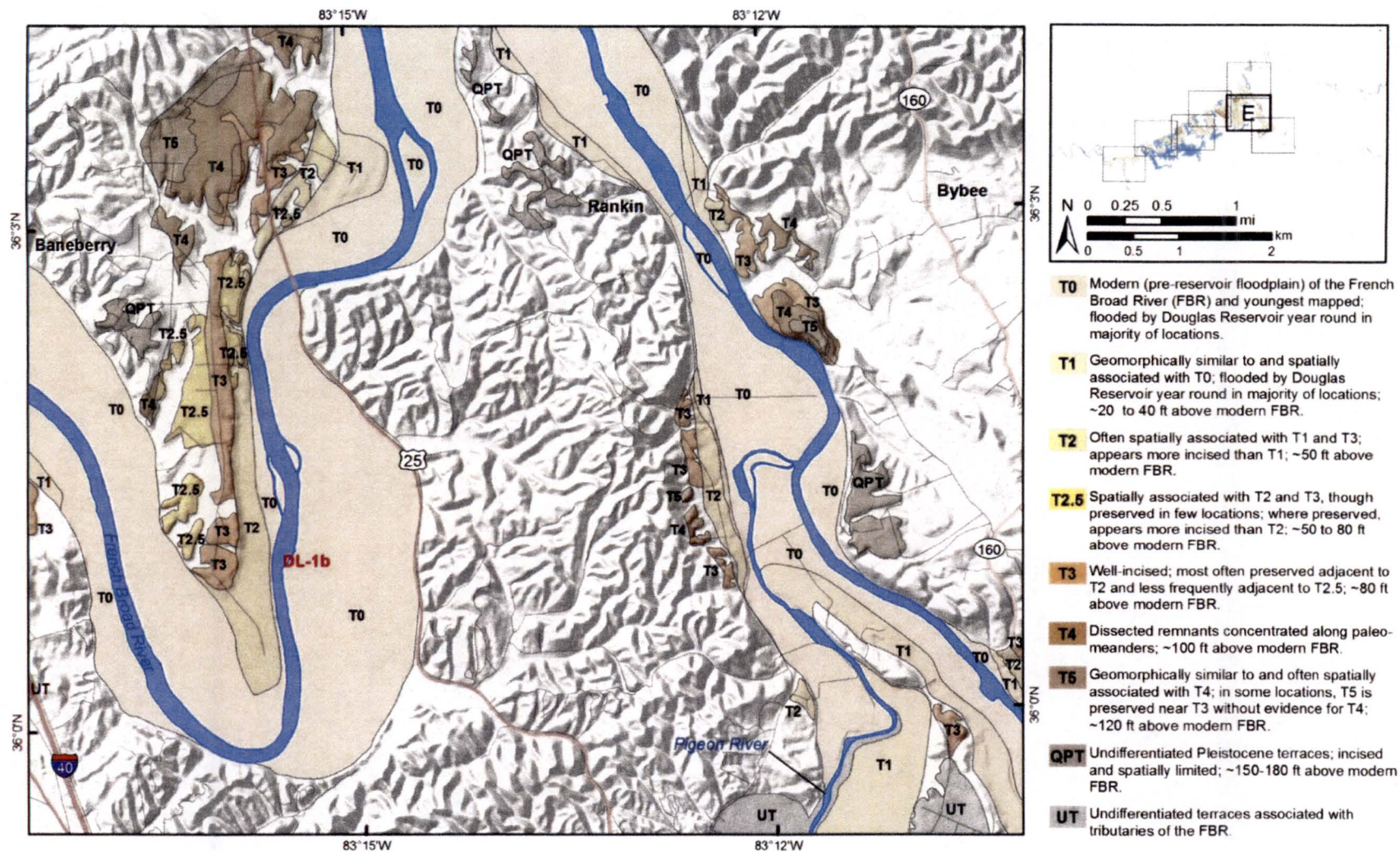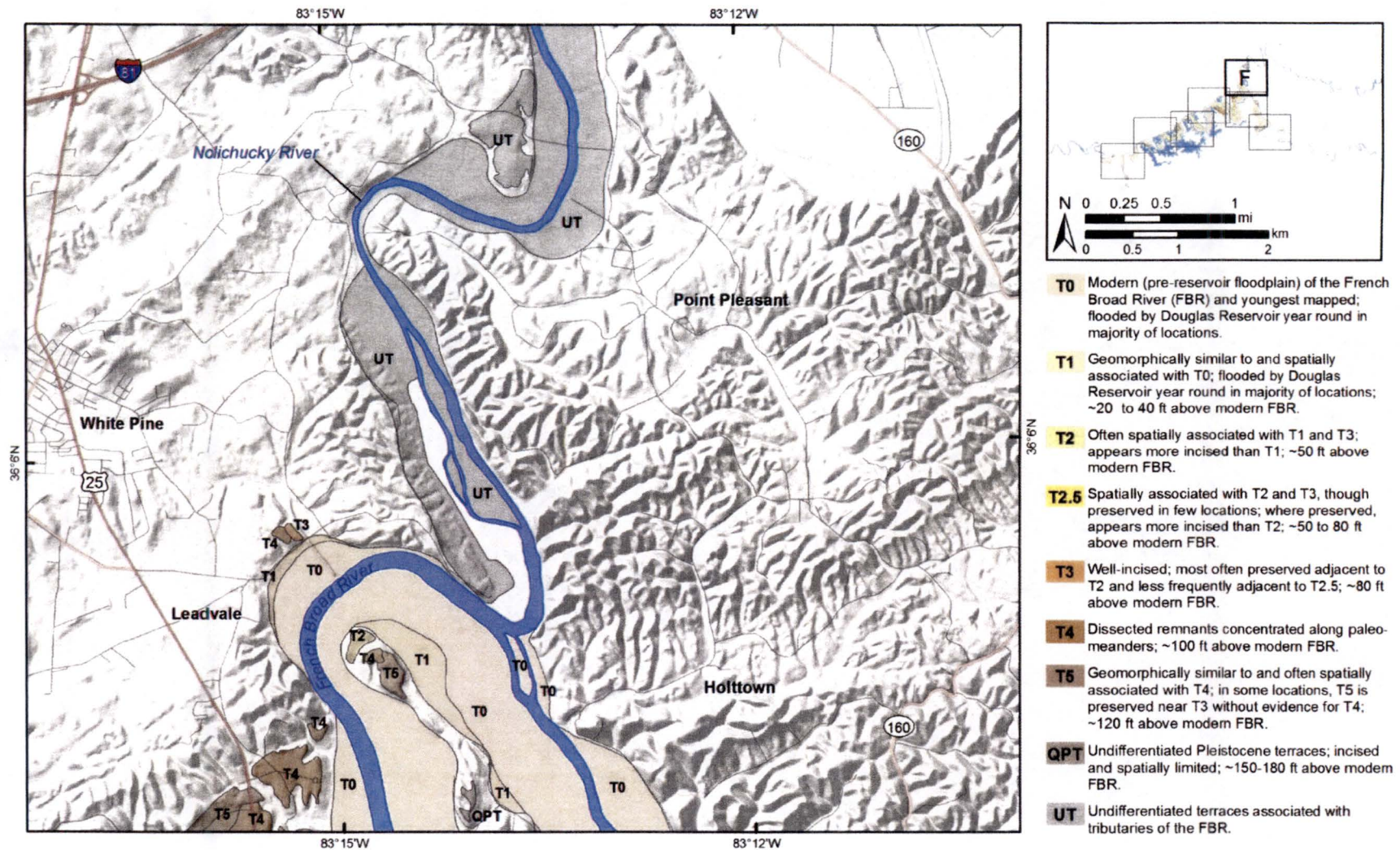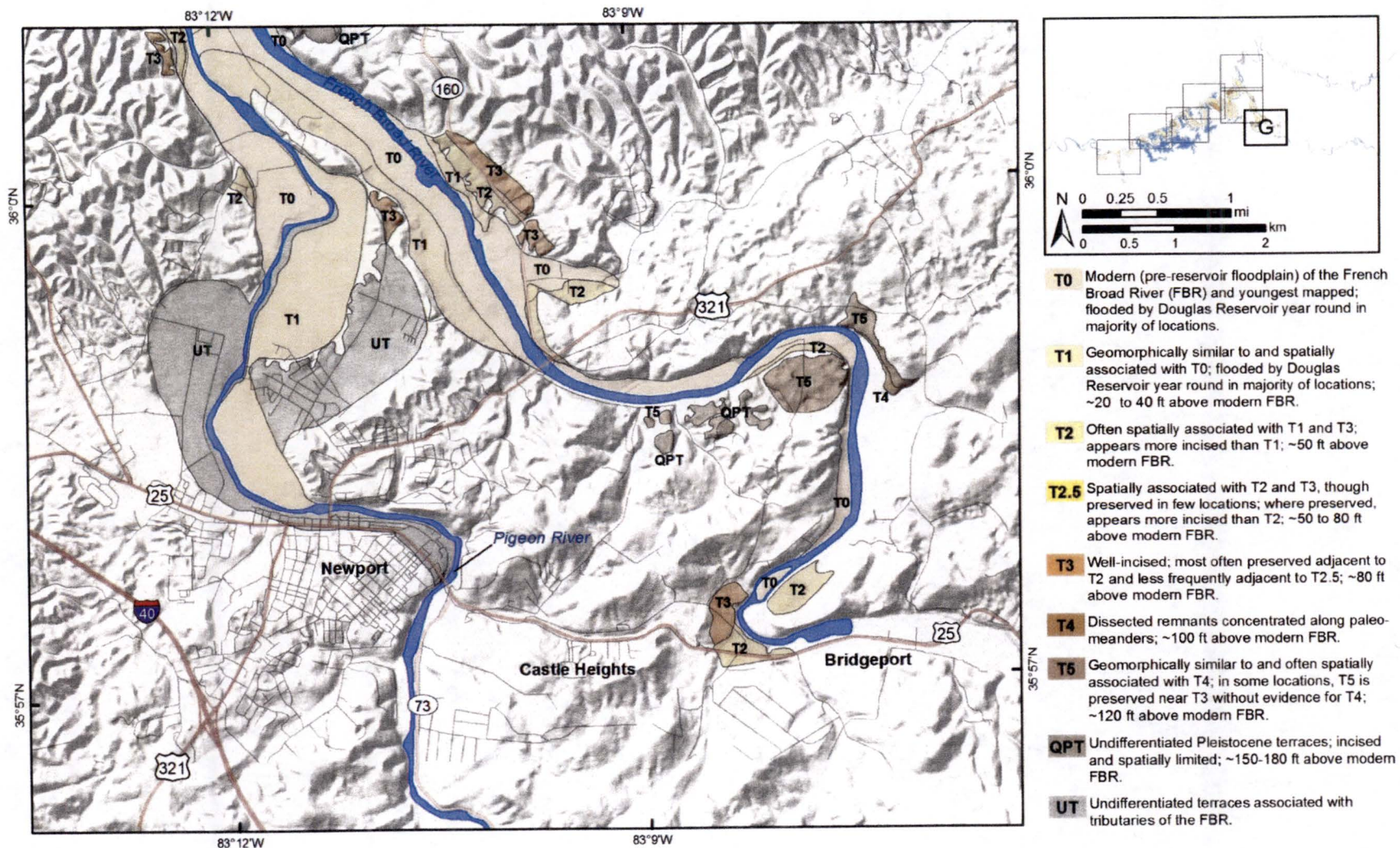Figure 2.5.3-10. (Sheet 4 of 7), Quaternary Terrace Map of the Douglas Reservoir Area, Location D

The legend of the figure contains the following descriptions:

T0 Modern (pre-reservoir floodplain) of the French Broad River (FBR) and youngest mapped; flooded by Douglas Reservoir year round in majority of locations.

T1 Geomorphically similar to and spatially associated with T0; flooded by Douglas Reservoir year round in majority of locations; ~20 to 40 ft above modern FBR.

T2 Often spatially associated with T1 and T3; appears more incised than T1; ~50 ft above modern FBR.

T2.5 Spatially associated with T2 and T3, though preserved in few locations; where preserved, appears more incised than T2; ~50 to 80 ft above modern FBR.

T3 Well-incised; most often preserved adjacent to T2 and less frequently adjacent to T2.5; ~80 ft above modern FBR.

T4 Dissected remnants concentrated along paleo-meanders; ~100 ft above modern FBR.

T5 Geomorphically similar to and often spatially associated with T4; in some locations, T5 is preserved near T3 without evidence for T4; ~120 ft above modern FBR.

QPT Undifferentiated Pleistocene terraces; incised and spatially limited; ~150-180 ft above modern FBR.

UT Undifferentiated terraces associated with tributaries of the FBR.

Legend:

T0 — Modern (pre-reservoir floodplain) of the French Broad River (FBR) and youngest mapped; flooded by Douglas Reservoir year round in majority of locations.

T1 — Geomorphically similar to and spatially associated with T0; flooded by Douglas Reservoir year round in majority of locations; ~20 to 40 ft above modern FBR.

T2 — Often spatially associated with T1 and T3; appears more incised than T1; ~50 ft above modern FBR.

T2.5 — Spatially associated with T2 and T3, though preserved in few locations; where preserved, appears more incised than T2; ~50 to 80 ft above modern FBR.

T3 — Well-incised; most often preserved adjacent to T2 and less frequently adjacent to T2.5; ~80 ft above modern FBR.

T4 — Dissected remnants concentrated along paleo-meanders; ~100 ft above modern FBR.

T5 — Geomorphically similar to and often spatially associated with T4; in some locations, T5 is preserved near T3 without evidence for T4; ~120 ft above modern FBR.

QPT — Undifferentiated Pleistocene terraces; incised and spatially limited; ~150-180 ft above modern FBR.

UT — Undifferentiated terraces associated with tributaries of the FBR.

Figure 2.5.3-10. (Sheet 5 of 7), Quaternary Terrace Map of the Douglas Reservoir Area, Location E

CNL-16-162

Figure 2.5.3-10. (Sheet 6 of 7), Quaternary Terrace Map of the Douglas Reservoir Area, Location F

CNL-16-162

Figure 2.5.3-10. (Sheet 7 of 7), Quaternary Terrace Map of the Douglas Reservoir Area, Location G
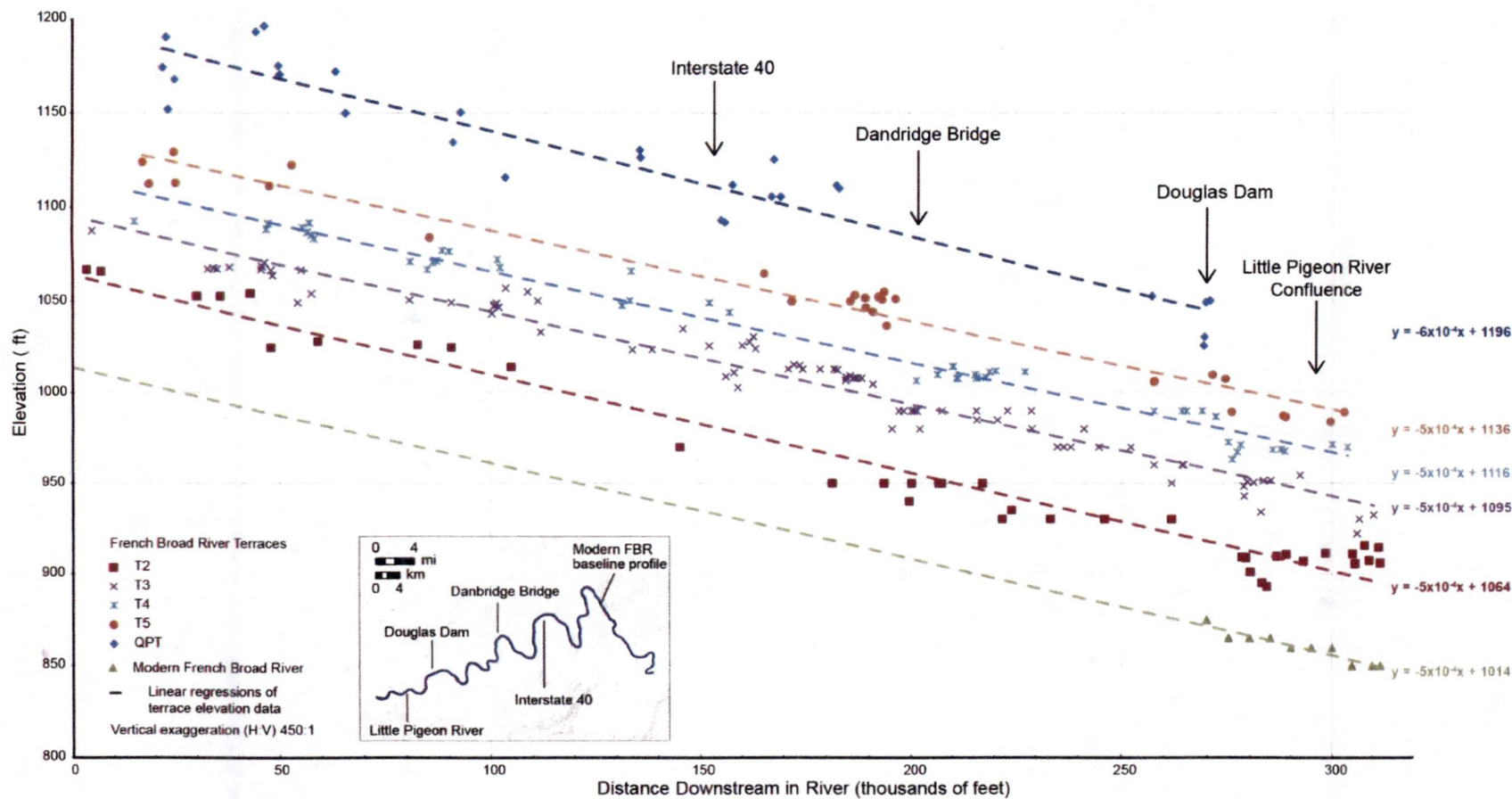
Figure 2.5.3-11. Longitudinal Profiles of Quaternary Terraces Along Douglas Reservoir
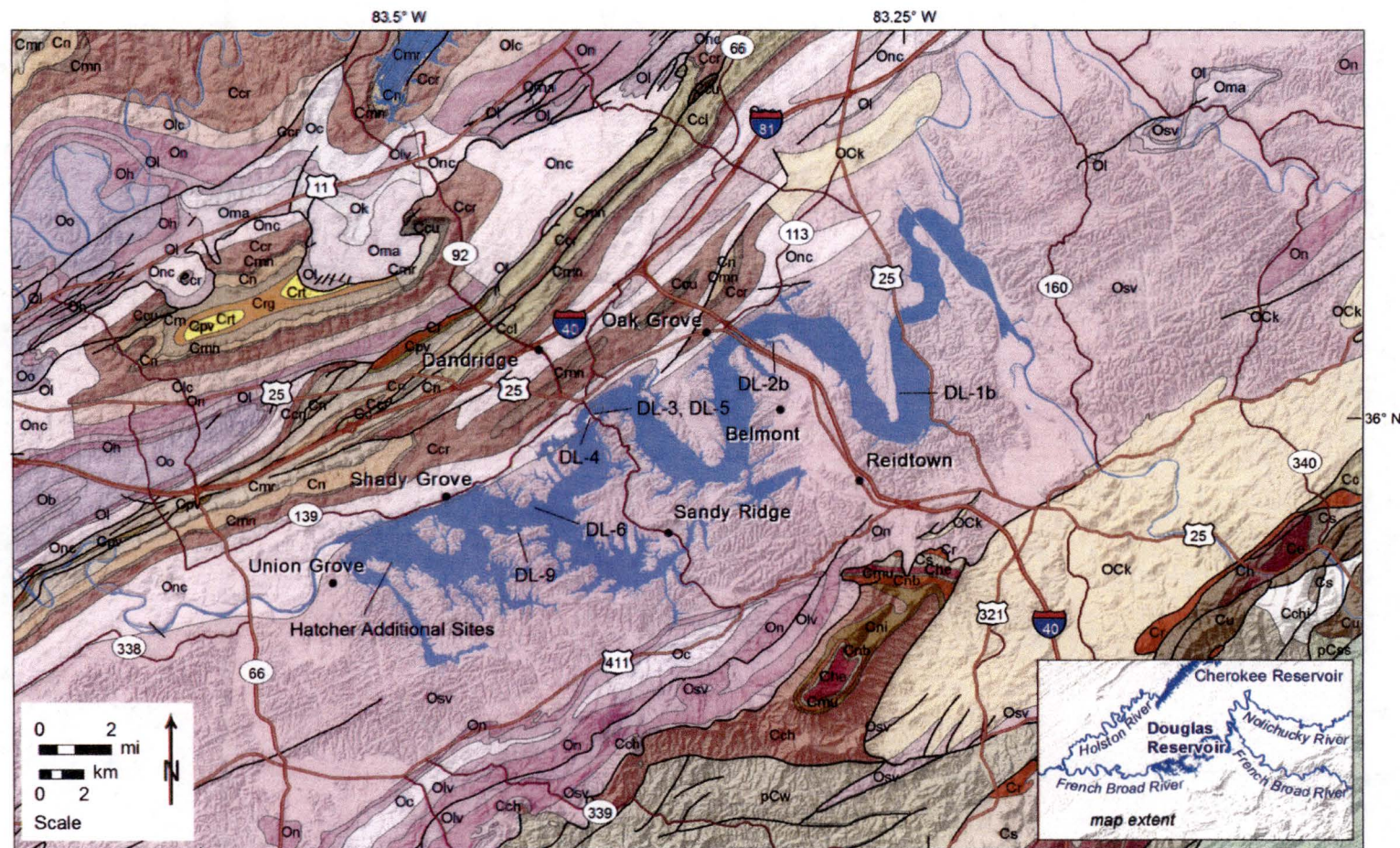
Notes:
Geologic map data from References 2.5.3-55 and 2.5.3-67.

**Figure 2.5.3-12, (Sheet 1 of 2). Geologic Map of the Douglas Reservoir Area**

CNL-16-162

Chickamauga Group

Ob	Bays Formation
Oo	Ottosee Shale
Oh	Holston Formation
Osv	Sevier Shale
Ol	Lenoir Limestone

Knox Group

Oma	Mascot Dolomite
Ok	Kingsport Formation
On	Newala Formation (Mascot Dolomite and Kingsport Formation)
Olv	Longview Dolomite
Oc	Chepultepec Dolomite
Olc	Longview and Chepultepec Dolomite
Onc	Mascot, Longview and Chepultepec Dolomite, and Kingsport Formation
Ccr	Copper Ridge Dolomite
OCk	Knox Group Undifferentiated

Ordovician

Conasauga Group

Cmn	Marynardville Limestone
Cn	Nolichucky Shale
Ccu	Marynardville Limestone and Nolichucky Shale

Cambrian

Conasauga Group (cont.)

Cc	Conasauga Group Undifferentiated
Cm	Maryville Limestone
Crg	Rogersville Shale
Crt	Rutledge Limestone
Cmr	Maryville and Rutledge Limestone, and Rogersville Shale
Cpv	Pumpkin Valley Shale
Cr	Rome Formation
Cs	Shady Dolomite

Chilhowee Group

Ce	Erwin Formation (Hesse and Nebo Sandstone, and Murry Shale)
Cnb	Nebo Sandstone
Che	Hessee Sandstone
Cmu	Murray Shale
Cni	Nichols Shale
Ch	Hampton Formation
Cu	Unicoi Formation
Cch	Cochran Conglomerate

Cambrian

Ocoee Supergroup

pCs	Snowbird Group
pCo	Ocoee Supergroup

Walden Creek Group

pCw	Walden Creek Group
pCss	Sandsuck Formation

Prcambrian

Contact

——— Fault

Figure 2.5.3-12, (Sheet 2 of 2). Explanation of Geologic Map of the Douglas Reservoir Area
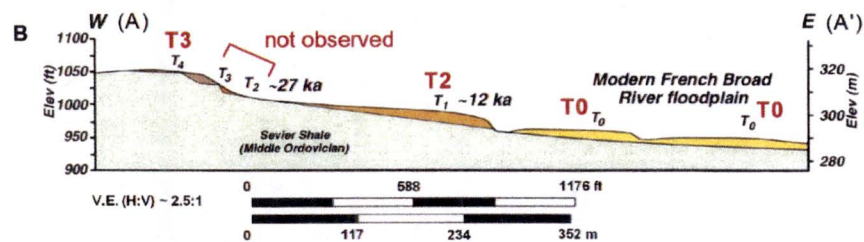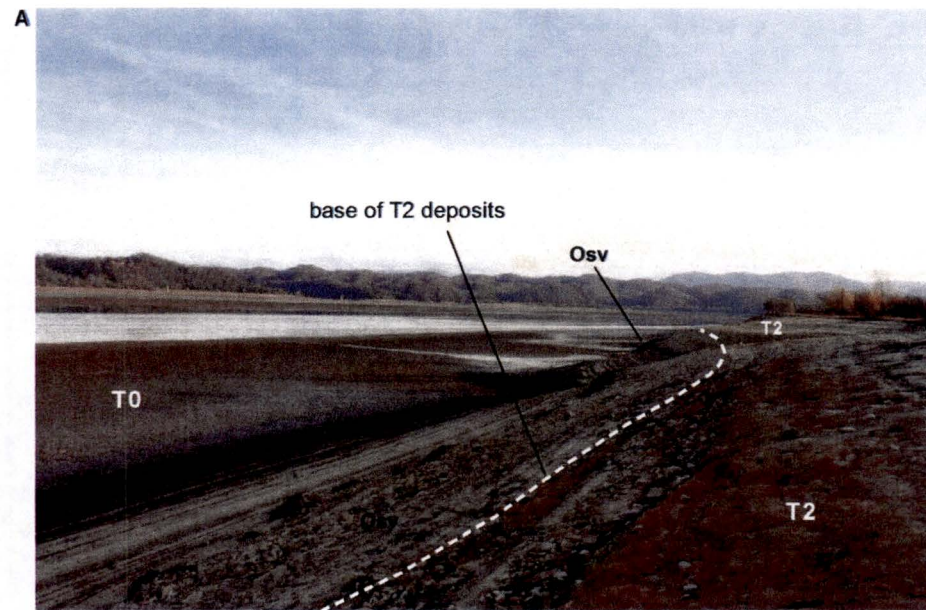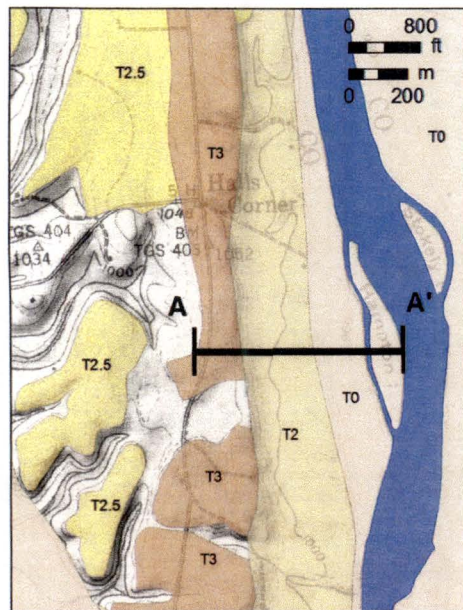
Notes:

A) Exposure of T0 and T2, as mapped in this report, and the base of T2 deposits overlying Sevier shale (Osv), viewed looking south.
B) Cross section A-A' modified from Reference 2.5.3-12: terrace interpretations in black from Reference 2.5.3-12; red from Quaternary terrace mapping presented in Figure 2.5.3-10 and shown in the location map.

Figure 2.5.3-13. Site DL-1
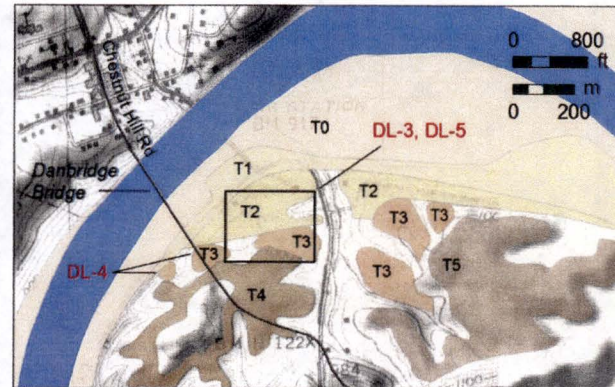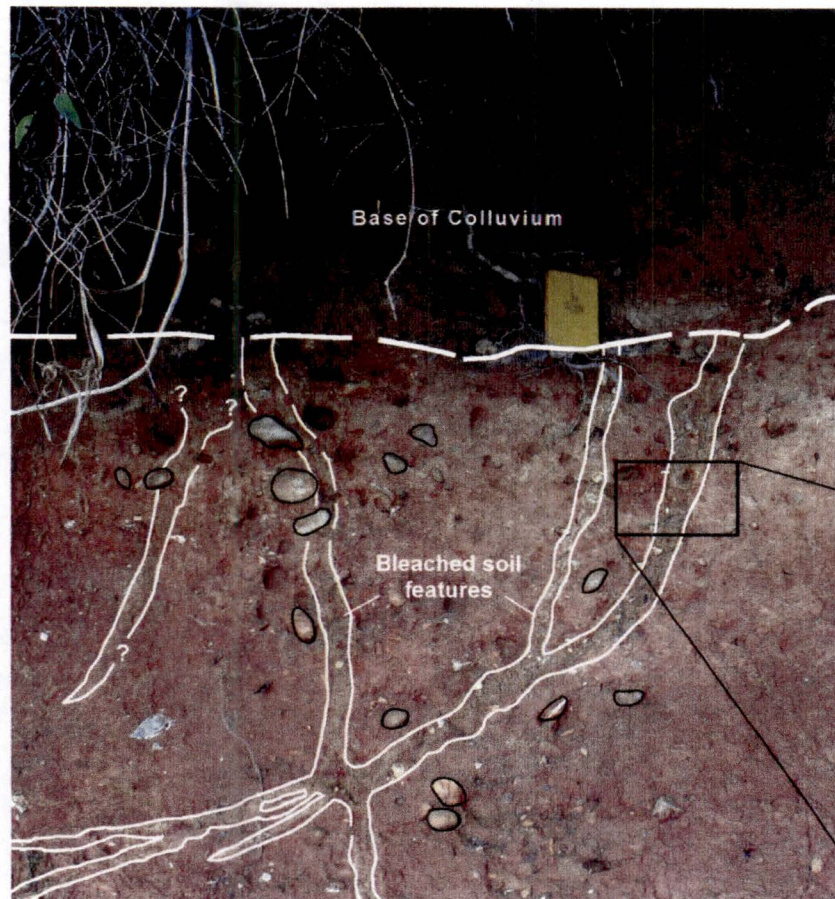
Notes:

A) Photo shows bleached rounded clasts (outlined in black) and bleached soil features truncated at the base of colluvium.

B) Detailed view of bleached soil features showing bleached rounded clasts and soil weathering.

Figure 2.5.3-14. Site DL-4
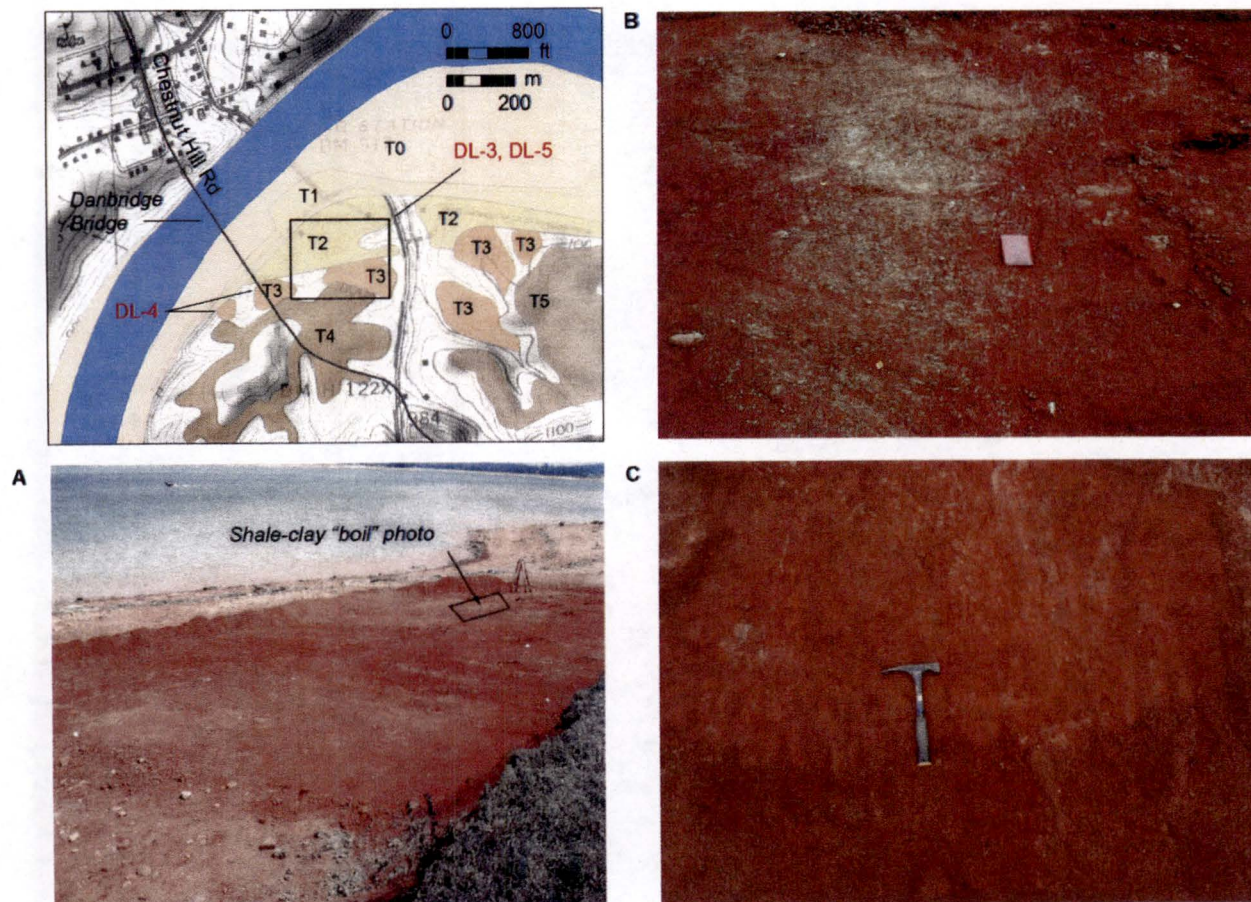
Notes:
A) and Bb) Images from Reference 2.5.3-12 show shale-clay "boil" exposed in the NE corner of DL-5b (not exposed during field reconnaissance).
C) Photo shows bleached fractures at the site (hammer for scale).

Figure 2.5.3-15. Site DL-5
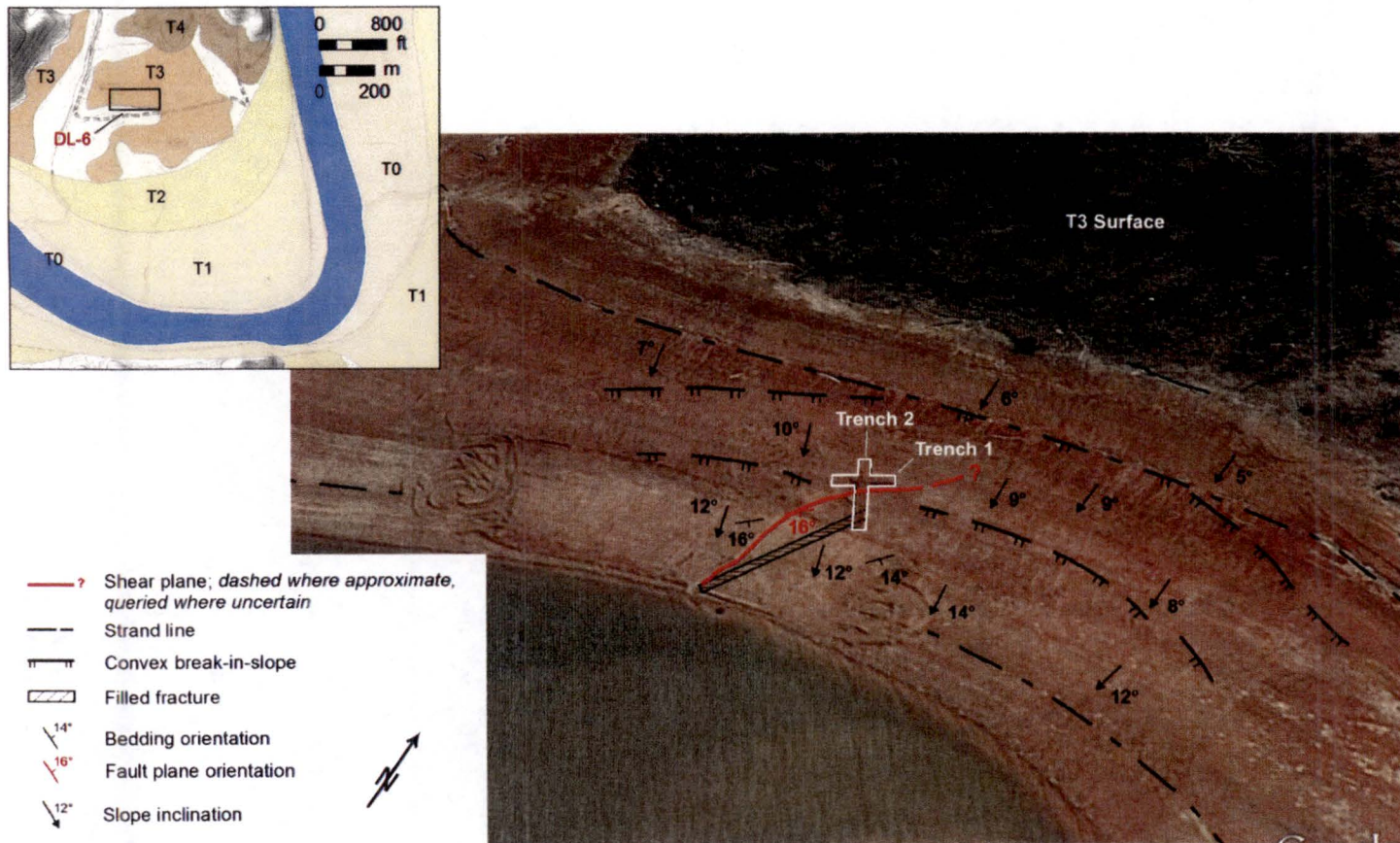
Notes:
Approximate locations of Reference 2.5.3-12 and 2.5.3-13 trenches, filled fractures, and shear planes below T3 surface. Trench 1 and the section of Trench 2 upslope of Trench 1 were not re-excavated during field reconnaissance. Figure 2.5.3-17 shows log of the NE wall of Trench 2. Bedding orientation and slope inclination as measured during field reconnaissance.

Figure 2.5.3-16. Aerial View of Site DL-6
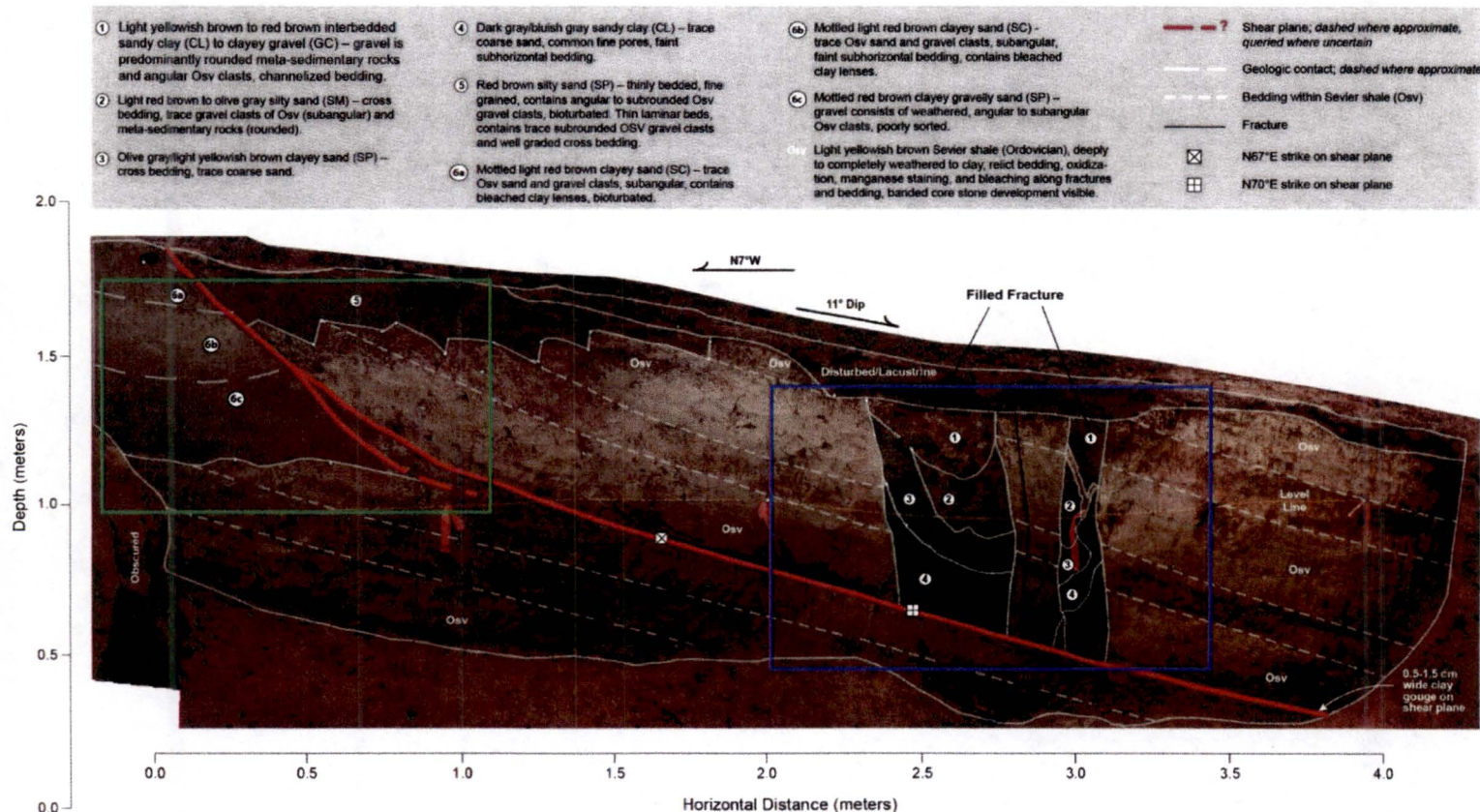
Notes:

White short dashed lines show relict bedding within deeply weathered Sevier shale (Osv) saprolite. Toward the southern end of the trench wall, filled fractures were observed above the shear plane only (blue box; Figure 2.5.3-17, Sheet 2 of 3). At the northern end of the trench wall, contact of Sevier shale with bioturbated silty sand (above shear plane) and mottled clayey and clayey gravelly sand (below shear plane) are observed (green box; Figure 2.5.3-17, Sheet 2 of 3).

Figure 2.5.3-17. (Sheet 1 of 3), Trench Log of Northeast Wall of Trench 2 at Site DL-6
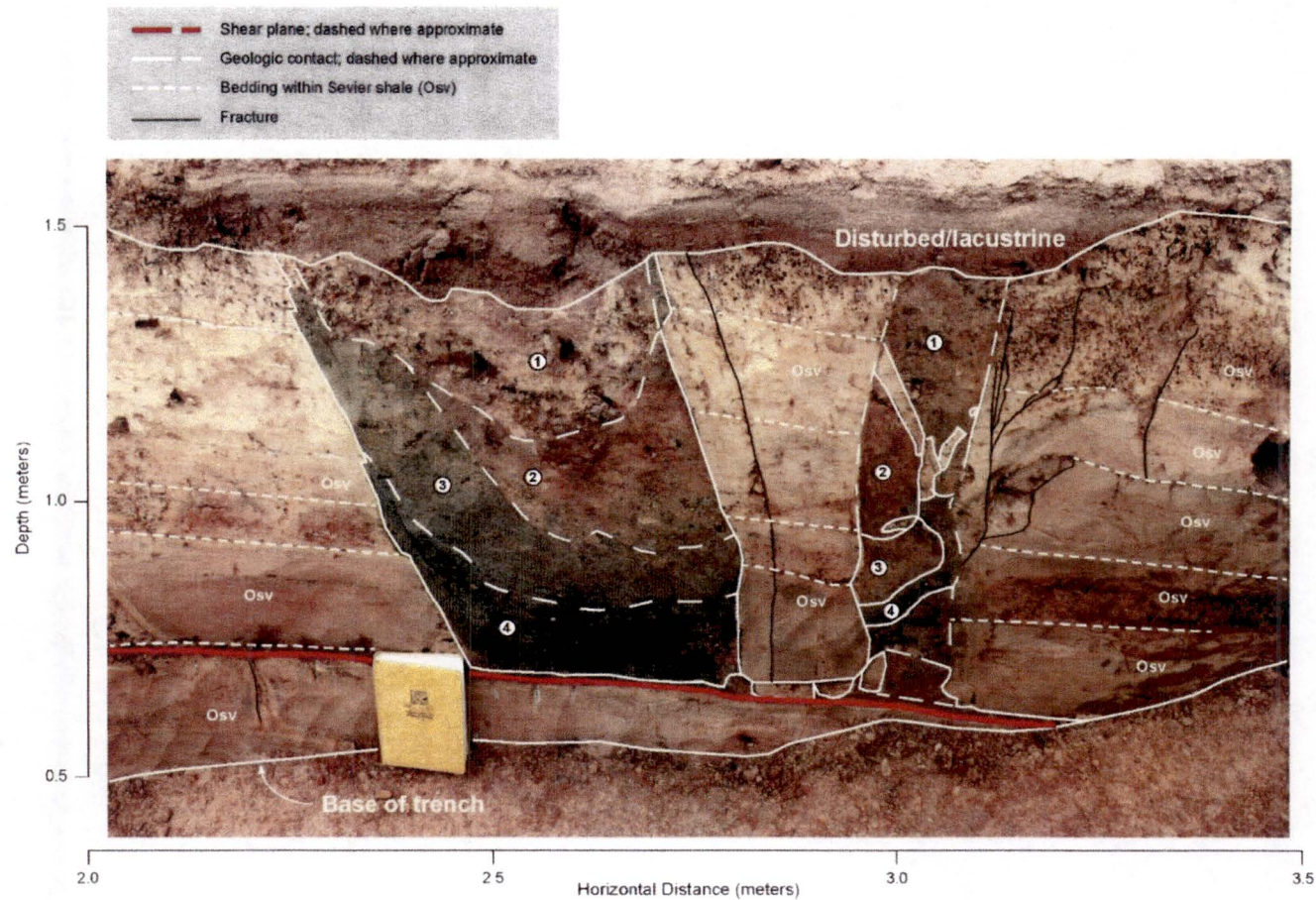
Notes:

Area of figure shown as blue box in Figure 2.5.3-17 (Sheet 1 or 3). Additional excavation below the shear plane did not reveal the potentially offset alluvium filled fracture.

Figure 2.5.3-17. (Sheet 2 of 3), Detailed View of Southern End of Northeast Wall of Trench 2 at Site DL-6

Legend:
- Shear plane; dashed where approximate
- Geologic contact; dashed where approximate
- Bedding within Sevier shale (Osv)
- Fracture
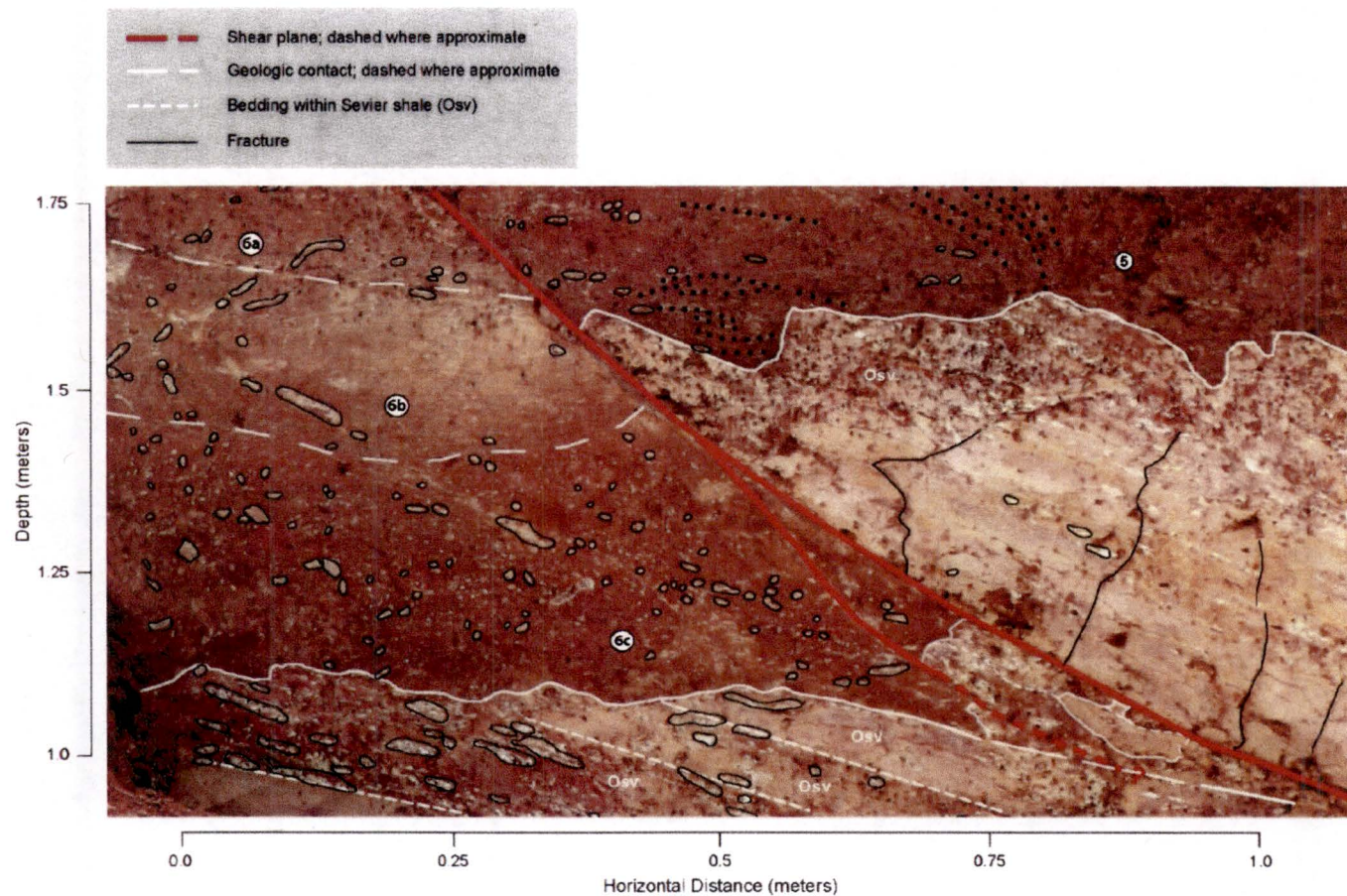
Notes:

Bleached Sevier shale fractures outlined in black. Black dots in Unit 5 show laminar cross bedding. Apparent reverse offset shows incompatibility between Units 5 and 6.

Figure 2.5.3-17. (Sheet 3 of 3), Detailed View of Northern End of Northeast Wall of Trench 2 at Site DL-6

A   Event 1 - Oblique downslope movement juxtaposes Sevier Shale above possible
         channel deposits as shown in Trench 2, East Wall.
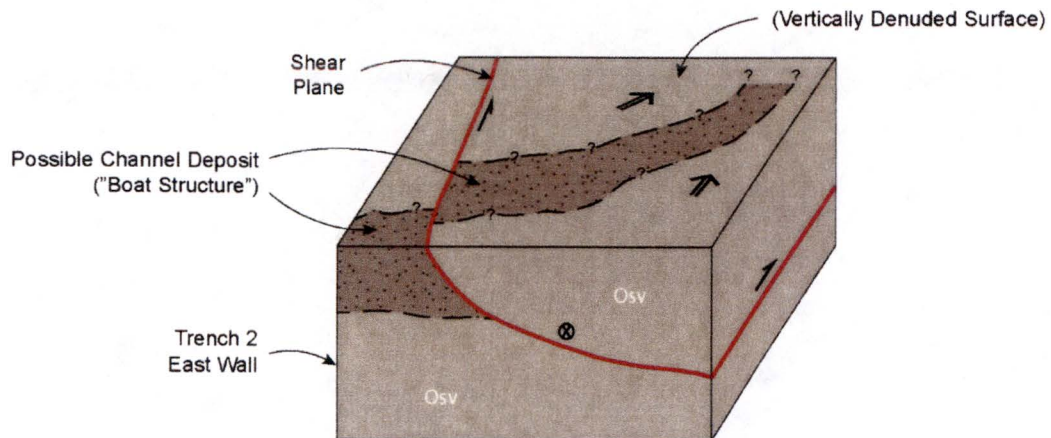
B   Event 2 - Later block sliding along pre-existing shear plane creates
         extensional fracture.
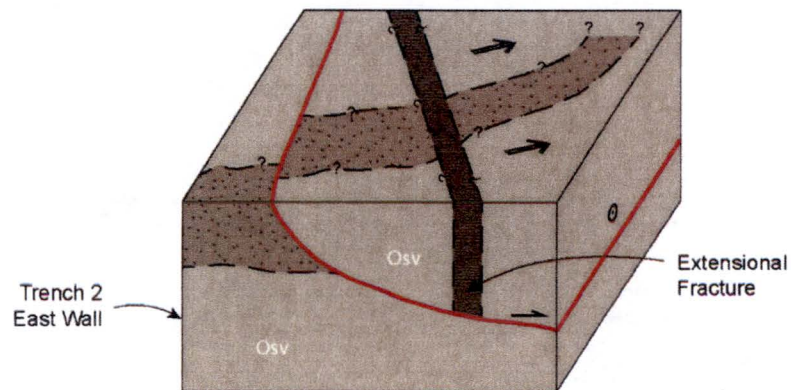
**Figure 2.5.3-18. Block Diagram Illustrating Alternative Hypothesis
Regarding Features in DL-6**
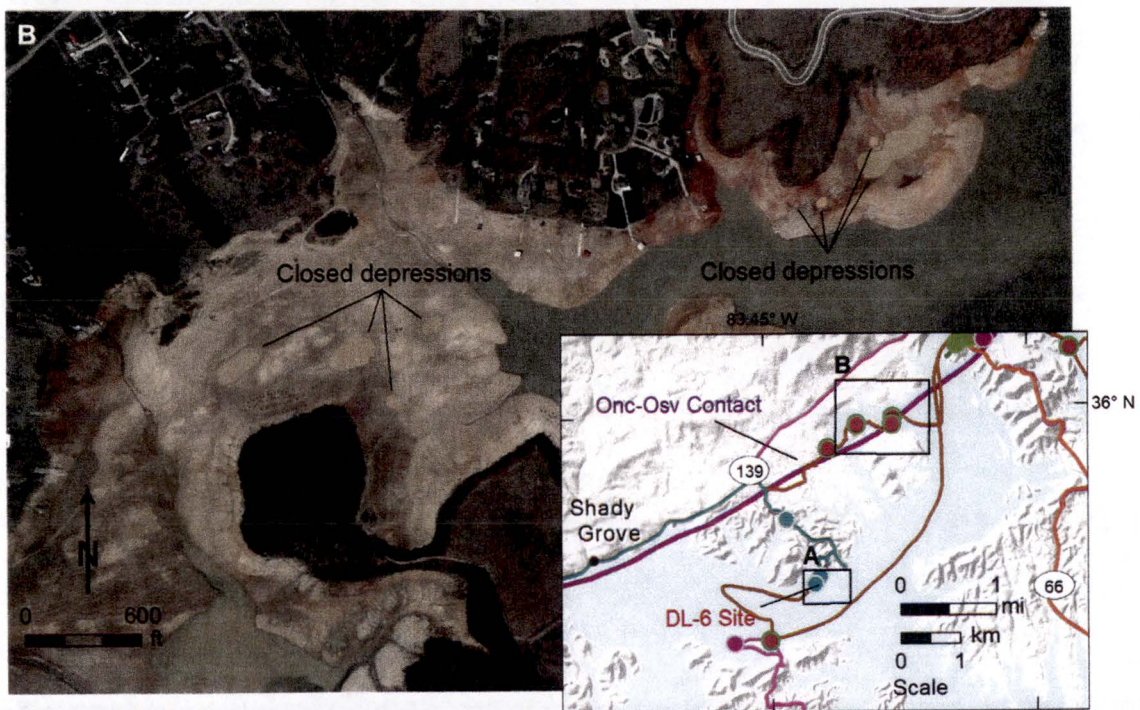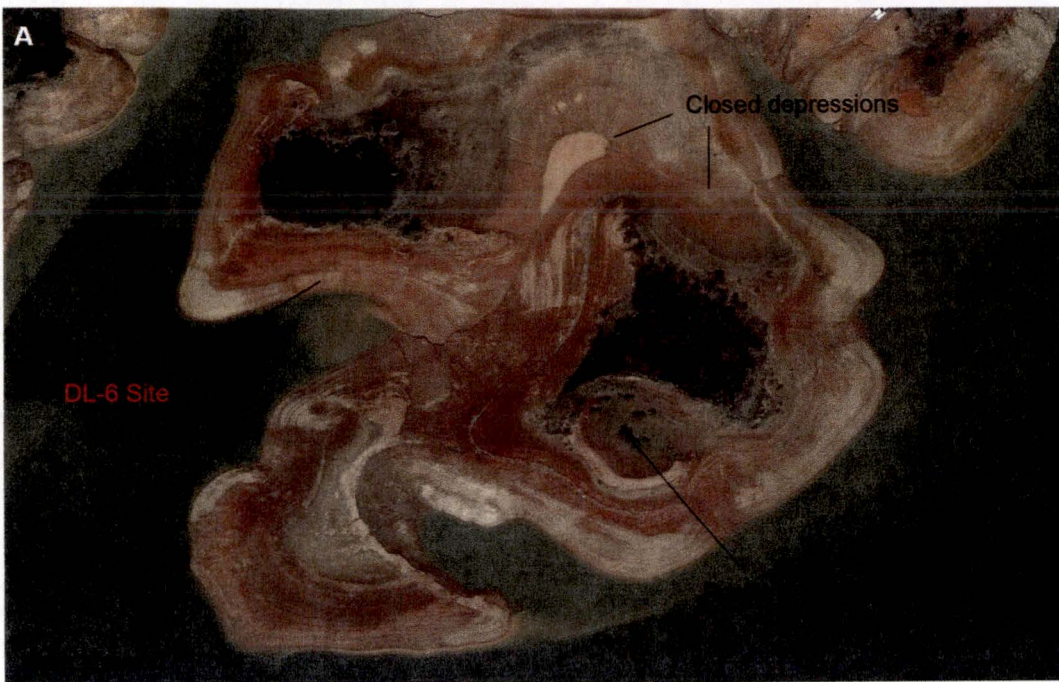
Figure 2.5.3-19. Examples of Closed Depressions Near Site DL-6
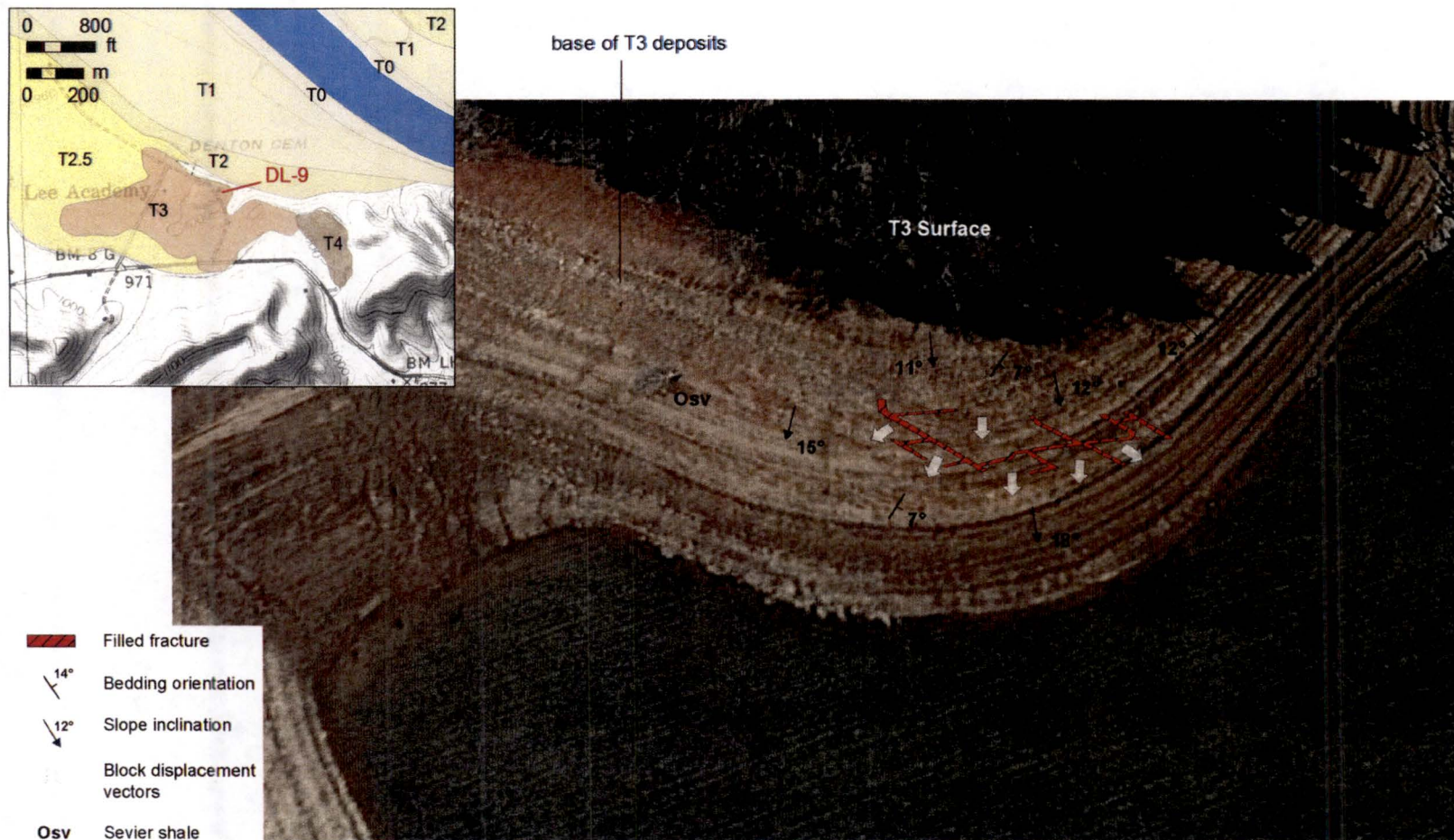
Notes:

Image includes a schematic of filled bedrock fractures mapped by Lettis Consultants International (LCI) and possible gravitational block displacement vectors shown below the T3 surface. Bedding orientation and slope inclination as measured during field reconnaissance.

Figure 2.5.3-20.   Aerial View of Site DL-9

ENCLOSURE 2

SUPPLEMENTAL INFORMATION RELATED TO
SURFACE DEFORMATION
OF THE EARLY SITE PERMIT APPLICATION FOR CLINCH RIVER NUCLEAR SITE

By letter dated May 12, 2016 (Reference 1), Tennessee Valley Authority (TVA) submitted an application for an early site permit for the Clinch River Nuclear (CRN) Site in Oak Ridge, TN. Subsequent to the submittal of the application, and consistent with interactions with NRC staff, TVA identified certain aspects of the application that it intends to supplement. By letter dated August 11, 2016 (Reference 2), TVA provided a plan for submitting the identified supplemental information.

This enclosure provides supplemental information related to Surface Deformation to support the NRC staff's review. This enclosure also includes proposed changes to the affected Site Safety Analysis Report (SSAR) sections. An Early Site Permit Application (ESPA) Change Request has been initiated to incorporate these changes into a future revision of the ESPA.

Supplement Item (Reference 2)

TVA will assess the potential for hypogenic karst development including the 2016 D. Doctor paper and the significance for surface and sub-foundation deformation at the CRN Site. TVA will provide a markup of the applicable ESPA sections that describe the results of this assessment.

Supplemental Information

To address the potential for hypogenic karst development and the significance for surface and sub-foundation deformation at the CRN Site, SSAR Subsection 2.5.1.1.1.3.1, "Karst in the Valley and Ridge Province," and Subsection in 2.5.1.2.5.1, "Karst Hazards," will be revised as shown below.

Note - deletions are shown as "~~strike-through~~" text and additions are shown as "underlined" text in the revised Subsections.

References:

1. Letter from TVA to NRC, CNL-16-081, "Application for Early Site Permit for Clinch River Nuclear Site," dated May 12, 2016

2. Letter from TVA to NRC, CNL-16-134, "Schedule for Submittal of Supplemental Information in Support of Early Site Permit Application for Clinch River Nuclear Site," dated August 11, 2016

SSAR Subsection 2.5.1.1.1.3.1 is revised as indicated:

2.5.1.1.1.3.1   Karst in the Valley and Ridge Province

Karst in the Valley and Ridge province, which includes the CRN Site, forms in folded and faulted Paleozoic carbonate rocks, labeled FFC on Figure 2.5.1-4. These rocks form a linear band running southwest to northeast through the states of Alabama, Georgia, Tennessee, Kentucky, Virginia and West Virginia, Maryland, Pennsylvania, New Jersey, and New York. Karst landscape features in the Valley and Ridge include sinkholes, caves, springs, seeps, and sinking streams.

Shofner, et al., (2001 Reference 2.5.1-25) (Figure 2.5.1-5) shows the general distribution of sinkholes in the Valley and Ridge province of Tennessee. Cover-collapse sinkholes are the most common in this province. Cover-collapse and cover-subsidence sinkholes are a primary cause of damage to homes and infrastructure in the region (Reference 2.5.1-27). Loss of material at the bedrock-soil interface results in soft or loose soils and voids. However, as the authors indicate, "...although similar geologic conditions appear to favor both sinkhole development and cave formation, the actual processes involved in the development of these two types of features seems to be only weakly related."

Weary (Reference 2.5.1-26) notes, "Where carbonates are thick and extensive, cave systems may be long and complex. Where thin and interbedded with non-carbonates, caves are small and short." In this province, caves are common, but tend to be relatively small (less than a few kilometers in length), as the carbonate strata are folded and interbedded with siliciclastic strata. ~~The geometry of cave passages shows conspicuous structural control, with passages oriented along bedding strike, joints, or joint-bedding plane intersections. A karst model for the Valley and Ridge province of Tennessee illustrates the~~ The tectonic history of the region has produced a series of imbricate thrust sheets that repeat stratigraphy and results in a lack of horizontal continuity ~~in the carbonate units, especially~~ perpendicular to strike. ~~(Figure 2.5.1-4). As a result, most cave passages are oriented parallel to strike~~ Consequently, most cave passages are oriented parallel to strike with their geometries exemplifying structural control, such as passages oriented along bedding strike, joints, or joint-bedding plane intersections. ~~Based exclusively on~~ According to Sutherland's (Tennessee Cave Survey) cave count ~~by physiographic provinces, not the total number of caves indicated in the map explanation,~~ about ~~1,850~~ 9,839 caves are known in ~~the Valley and Ridge of~~ Tennessee, ~~comprising~~ of which approximately 15 percent are located in the Valley and Ridge province ~~of all caves in the state~~ (Reference 2.5.1-28).

SSAR Subsection 2.5.1.2.5.1 is revised as indicated:

2.5.1.2.5.1   Karst Hazards

In this section, karst processes and features in the site vicinity and area are reviewed, and site-specific geologic and geotechnical data relevant to the assessment of <u>potential</u> karst hazard within the site location are presented. The presence of karst features is documented at the CRN Site, and a thorough examination of the nature, origin, occurrence, and potential hazards posed by karst features and processes is made.

Karst Conceptual Models

<u>To provide background and context, and enable the eventual development of a site-specific karst model, the section begins with a review of conceptual karst models. All karst models entail the same basic principle, that karst landscapes and features are dominantly formed by the dissolution of bedrock by water (Reference 2.5.1-35).</u>

<u>Karst models can be classified by whether they invoke *epigenic* dissolution, *hypogenic* dissolution, or both. Epigenic dissolution occurs as meteoric water descends and flows along a hydrologic gradient underground through the rock, eventually discharging to springs in nearby valleys (Reference 2.5.1-35). Hypogenic dissolution occurs when groundwater ascends from below, independent of recharge from the overlying or immediately adjacent ground surface (Reference 2.5.1-289).</u>

<u>Most of the published literature on karst focuses on *epigenic* karst, formed by descending groundwater. Epigenic karst is formed by water moving from the ground surface down into soluble rock formations, then through them along the hydraulic gradient. Permeability of the regolith and/or rock formations governs the extent to which water is able to penetrate to varying depths. As discussed in Subsection 2.5.1.1.1.3, epigenic karst features develop from a self-accelerating process of water flow along well-defined pathways. As the water flows through the rock, it dissolves and enlarges the pore or fracture space through which it flows. These pathways include bedding planes, joints, fractures, and faults. Enlarging the fracture allows it to carry more water, which increases the dissolution rate, eventually forming a conduit. The location and geometry of dissolution conduits are controlled by the rock composition, rock structure, porosity, amount of fractures and voids, amount of recharge, the hydraulic gradient, and other factors (Reference 2.5.1-290).</u>

<u>Early models of epigenic karst formation view the style of dissolution as a function of the hydrologic zone of formation (Reference 2.5.1-291). *Vadose* dissolution occurs as descending water flows through the unsaturated (vadose) zone from the ground surface down toward the water table, resulting in vertical and steeply pitched dissolution channels. Deep *phreatic* dissolution takes place below the water table in the phreatic zone, from groundwater first descending, moving laterally, then ascending along a hydraulic gradient, resulting in deep caves that follow joints, faults, fractures, and/or bedding planes. Water table dissolution takes place at and just below the water table, resulting in horizontal cave passages.</u>

<u>Ford and Williams (Reference 2.5.1-290) presented a model that accounted for the variation in the depth of dissolution in epigenic phreatic cave formation (Figure 2.5.1-53) as a function of rock properties. They proposed that in rock with abundant fractures and pathways for water flow, dissolution is concentrated in the zone of mixing of meteoric and groundwater at the top of the groundwater table, resulting in an "ideal water table cave" with dominantly horizontal passageways. In rock with few, tight, or widely spaced fractures, water is forced to descend</u>

CNL-16-162

along available fractures before it can continue laterally or upward to follow the hydraulic gradient, forming the deeper and more complex "deep phreatic or *bathyphreatic* cave."

Later research by Worthington (Reference 2.5.1-302) proposes that depth of phreatic dissolution is dependent on additional hydraulic, structural, and solubility factors, which can combine to form conduits at very great depths. The decrease in the viscosity of water with depth as temperature increases along the geothermal gradient facilitates efficient flow, an effect that favors deep dissolution in settings with long flow paths and steeply dipping strata.

Studies of karst aquifers by the U. S. Geological Survey (Reference 2.5.1-292) led to the development of a general karst model for the Valley and Ridge province of Tennessee. In this model, shown in Figure 2.5.1-69, epigenic karst processes lead to dissolution throughout the vadose and phreatic zones. Dissolution is most intense in the near surface, and proceeds downward along bedding planes and joints. Phreatic dissolution occurs in both the shallow and deep phreatic zones, with the dominant direction of flow parallel to strike. Dissolution may extend to depths greater than 180 m (600 ft).

Over the last few decades, research on *hypogenic* karst, has expanded greatly and hypogenic features are increasingly recognized in karst environments. The understanding and the definition of hypogenic karst has evolved and been refined over this timeframe. Early definitions of hypogenic speleogenesis linked the process to very specific examples and characteristics, mostly through a geochemical framework associated with hydrothermal waters or oxidation of hydrocarbons (References 2.5.1-290, 2.5.1-293). Hill (Reference 2.5.1-294) demonstrated that large caves in New Mexico such as Carlsbad Caverns were formed by acidic waters charged with hydrogen sulfide derived from hydrocarbons at depth. Defining hypogene speleogenesis has evolved with increasing research on the subject, but the common theme was that dissolution occurred at depth, essentially decoupled from surficial processes and hydrologic conditions. This theme has persisted and, the following definition presented by Reference 2.5.1-289 is now generally applied. Hypogenic speleogenesis is "the formation of caves by water that recharges the soluble formation from below, driven by hydrostatic pressure or other sources of energy, independent of recharge from the overlying or immediately adjacent surface."

Hypogene dissolution requires a structural setting in which waters can descend to great depths, and then rise up through the soluble formation. Klimchouck (Reference 2.5.1-289) presents a model of an open basin in which both hypogene and epigene dissolution may take place (Figure 2.5.1-70). More often, however, a confining layer forces the water to great depths and creates the opportunity for hypogene dissolution. The rising water is often aggressive i.e. having the ability to dissolve rocks. Water becomes aggressive, for example, through geochemical interaction with deeper strata rich in hydrocarbons, dissolution of carbonates to form carbonic acid, or at increased temperatures.

The mixing of fresh water and salt water in coastal settings can also result in hypogene dissolution. Cunningham and Walker (Reference 2.5.1-41) describe multistoried vertical sag features evident in high resolution seismic reflection profiles from Biscayne Bay, Florida. They interpreted these stacked sag features as evidence for coalesced, collapsed paleocave systems. Cunningham and Walker (Reference 2.5.1-41) proposed two hypogene mechanisms to explain these broad structural sags. They postulate upward flow driven by Kohout convection with dissolution by mixed fresh and saline groundwaters and/or upward ascension of hydrogen-sulfide-charged groundwater derived from dissolution and reduction of calcium sulfates in deeper strata. Additionally, the faults associated with these collapse features may serve as pathways for upward ground water flow. This setting is highly susceptible to both epigenic and

hypogenic karst processes due to the high porosity and permeability of Florida limestones and the frequent mixing of salt water and fresh water in groundwaters near the coast (Reference 2.5.1-295).

Within the Valley and Ridge, Doctor and Orndorff (Reference 2.5.1-296) identify multiple hypogenic characteristics in caves within the central Appalachian Great Valley (AGV) of Virginia. Here, rocks are stratigraphically similar in age, composition, and structure to those at the CRN Site. Steeply dipping strata, folds, and faults account for the availability of deep flow paths and allow for rising of thermal and geochemically altered waters (Reference 2.5.1-297). Doctor and Orndorff (Reference 2.5.1-296) propose that the caves initially formed by hypogene dissolution, were significantly enlarged by deep phreatic dissolution, then selectively modified by water table and vadose dissolution as erosion and landscape lowering gradually exposed them.

The major lines of evidence Doctor and Orndorff present for hypogene dissolution and deep phreatic dissolution of caves in the AGV are (1) the random landscape position of the caves, (2) the complex geometry of cave passages, (3) the presence of many thermal and travertine springs, and (4) the observation of cavities in water wells to depths of more than 1,000 ft. Caves appear to be randomly distributed beneath the landscape without regard for the modern stream networks. Cave elevations do not cluster about stream terrace elevations, nor do they cluster at any elevation that might reflect pauses in regional downcutting. Passages are not related to positions of modern trunk streams. Instead, cave passages are maze-like with vertical extents of over 20 m. They follow joints, faults, and bedding planes, and have phreatic features such as cupolas and feeder tubes. Caves are known to occur in isolated hills with no inlets or outlets, far from base level streams. In an interview (Reference 2.5.1-298) Doctor also noted the presence of exotic mineral deposits, including dog-tooth spar, gypsum, iron, or fluorite, as evidence of hypogene processes. Present-day thermal and travertine springs indicate that hypogene conditions likely still exist at depth, and the presence of very deep dissolution cavities in water wells supports hypogene dissolution as an ongoing process. Figure 2.5.1-71 shows Doctor and Orndorff's (Reference 2.5.1-296) model of how the interaction of a fault and a fold can result in hypogene dissolution by waters rising along a fault.

In summary, karst models show that dissolution occurs in a variety of hydrogeologic settings. Epigenetic dissolution, by descending and circulating meteoric water, can occur in the vadose zone, in the shallow phreatic zone, and in the deep phreatic zone. Dissolution begins along fractures, faults, and bedding planes, and proceeds to form voids and conduits capable of rapid transmittal of water. Hypogenic dissolution, by water ascending from below, forms conduits and voids with characteristic geometry and mineralogy. These voids can be later modified by epigenetic processes. Either epigenic or hypogenic processes are capable of creating voids and conduits at significant depth below the water table. A karst model for the CRN Site, informed by the above discussions, is presented at the conclusion of Subsection 2.5.1.2.5.1.2.

SSAR Subsection 2.5.1.2.5.1.1 is revised as indicated:

2.5.1.2.5.1.1   Karst in the Site Vicinity and Area

The site vicinity includes portions of the Valley and Ridge physiographic province and the Appalachian Plateaus province of eastern Tennessee (Subsection 2.5.1.2.1). The Valley and Ridge province of the site vicinity is underlain by northeast-striking folded and faulted sedimentary strata of Cambrian through Silurian age (Figures 2.5.1-27 and 2.5.1-34) as previously described in Subsection 2.5.1.2.3. Karst features are abundant and well-documented in carbonate strata of the Valley and Ridge province. By contrast, very few karst features lie within the Appalachians Plateau province within the 25-mi CRN Site radius. Pennsylvanian clastic rocks, rather than carbonate rocks, underlie this portion of the Appalachian Plateau province (Figure 2.5.1-4).

Karst development in the Valley and Ridge Province within the 25-mi radius site vicinity is similar to development within the 5-mi radius site area as stratigraphy and geologic structure are consistent through the province. Therefore, the following detailed discussions of karst development focus on the site area.

The 5-mi radius site area falls entirely within the Valley and Ridge physiographic province of Tennessee (Subsection 2.5.1.2.1). Paleozoic strata, folded and faulted during the Alleghanian orogeny, are eroded into a series of parallel ridges and valleys striking northeast as described in Subsection 2.5.1.1.3. The strata are Cambrian to Ordovician in age and include sandstone, siltstone, limestone, and dolomite. Some strata are dominated by a single lithology and others include significant interbeds of other lithologies. Karst development is observed to vary strongly with stratigraphic unit. In general, the thickest and ~~most pure~~ most pure carbonate units host the largest and most abundant karst features. All carbonate units host some karst features. Dissolution rates are variable and are dependent on a number of factors, including, but not limited to: (1) bedrock geochemistry; (2) location of rock relative to water table; (3) fracture density; or localized anthropogenic effects (e.g., acid mine drainage). According to White (Reference 2.5.1-30), estimates of the rate of denudation of karst surfaces by dissolution of carbonate bedrock in the Appalachians is in the range of 30 millimeters per kiloannum.

This section begins with a review of karst-related studies in the site area, much of which has focused on the ORR, owned by the Department of Energy, which adjoins the Tennessee Valley Authority (TVA) CRN Property (Figure 2.5.1 39). These previous studies provide a robust framework and conceptual model for the local karst setting. To extend this understanding to the CRN Site area, a detailed mapping and inventory of karst features of the site area was conducted based on interpretation of high resolution LiDAR-based topographic data obtained in 2013. Presentation of the mapping results is followed by analysis of the distribution of karst features with respect to stratigraphic unit, and a discussion of the influence of bedrock lithology and structure on karst development in the site area.

Previous Karst-related Studies in the Site Area

Understanding of the local karst setting was advanced significantly by karst characterization efforts within the ORR. The ORR ~~property adjoins the TVA CRN Property and~~ comprises most of the northern half of the 5-mi radius site area (Figure 2.5.1-39). Studies conducted in the 1980s and 1990s include: Reservation-wide geologic studies and a karst inventory, contaminant fate and transport, ground failures, or site characterization. Primary organizations involved in these studies include ORNL, its contractors, and the University of Tennessee.

CNL-16-162

A Reservation-wide synthesis of ORR geology was completed by Hatcher et al. (Reference 2.5.1-9). This comprehensive report is composed of nine chapters, each summarizing a different aspect of the geology of the ORR. Relevant to the understanding of karst are chapters on stratigraphy, soils, geologic structure, and hydrogeology. Chapter 3.5 establishes the stratigraphic framework and lithology of the units of the Chickamauga Group which underlie the CRN Site as described in Subsection 2.5.1.2.3. This stratigraphy was based on rock core borings drilled at ORNL, and these unit names and descriptions are applied to the CRN SMR Project rock core. Chapter 4 describes the formation and characteristics of soils. The carbonate units are mantled by mature soils composed of the residuum of the underlying bedrock and colluvium. In addition, flat-bottomed dolines often contain layers of Pleistocene loess, interbedded with colluvium. Geologic structure is summarized in Chapter 5. Faults and joints, along with bedding planes, control the location and orientation of dissolution conduits. Major joint sets are oriented northeast and northwest, with minor north-south and east-west trending sets.

Chapter 7 of Hatcher et al. (Reference 2.5.1-9) describes a conceptual model for groundwater flow developed for the ORR (see Subsection 2.4.12.1.3 for more discussion). In the model the stormflow zone, or soil above rock approximately down to 0.3 to 6.5 ft below the ground surface, accounts for 90 percent or more of water moving through the subsurface (Figure 2.5.1-72). The water table zone, an area 3 to 16 ft thick below the vadose zone, takes up the remaining 10 percent of subsurface flow. Water deeper than this likely moves, if at all, on a scale of thousands of years or more. Separate models are developed for aquitards, dominated by non-carbonate strata, and the Knox aquifer, dominated by carbonate strata. The model notes that in the Knox aquifer a few hydrologically dominant cavity systems control groundwater movement in the saturated zone.

A comprehensive karst inventory of the ORR was conducted by Lemiszki et al. (Reference 2.5.1-239) to help understand the extent of and controls on the karst systems in the Oak Ridge area. Sinkholes, cave entrances, and springs were identified using 1942 aerial photography, detailed field mapping, reviews of existing reports, maps, drilling records, and word-of-mouth. The data were compiled on a topographic base map, as shown in the excerpt in Figure 2.5.1-40. The study concluded that most of the sinkholes occur in the Knox Group, followed by the Chickamauga Group, and the Conasauga Group. Lemiszki et al. (Reference 2.5.1-239) estimated that about 16 percent of the 555 sinkholes mapped were active. Caves occur only in the Knox Group, or the Maynardville Limestone of the Conasauga Group.

Most of the published literature on karst focuses on epigenic karst formed by descending groundwater. Hypogenic karst forms as a result of ascending groundwater. Hypogenic speleogenesis is defined with reference to the source of fluid recharge to the cave-forming zone, and type of flow system. Confined aquifer settings are the principal hydrogeologic environment for hypogenic speleogenesis. These hydrogeologic settings may evolve through geologic time and lose their confinement due to uplift and denudation (Reference 2.5.1-40). Cunningham and Walker (Reference 2.5.1-41) described multistoried vertical features clearly observed on high resolution seismic reflection survey profiles from Biscayne Bay, Florida. They interpreted these stacked sag features as compelling evidence for coalesced, collapsed paleocave systems. The seismic reflection profiles indicated deformation associated with collapse and subsequent burial by undeformed late Miocene and Holocene rocks and sediments. The authors proposed two hypogene mechanisms to explain these broad structural sags. It is possible that the faults associated with these collapse features served as pathways for upward groundwater flow and subsequent carbonate dissolution by mixed fresh and saline groundwaters. Regardless of the precise dissolution mechanism, the types of stacked sag structures and associated steeply dipping faults clearly visible on the seismic reflection profiles

Cave development in the ORR was found to be strongly controlled by geologic structure and stratigraphy. Rubin and Lemiszki (Reference 2.5.1-240) synthesize a number of datasets, including karst inventory, cave survey, lithologic, and drilling data, to develop a model for cave development in the Oak Ridge area. Lithology is found to be a major factor; the thicker and more pure purer limestone and dolomite units feature the larger and more extensive solution conduits. Figure 2.5.1-41 shows generalized geology with typical joint and bedding orientations within the ORR. Site-specific characterization of the karst susceptibility of lithologic units is presented in Subsection 2.5.1.2.5.1.2.

In the Chickamauga Group of the White Oak Mountain Trust Sheet, where the CRN Site is located, Rubin and Lemiszki (Reference 2.5.1-240) find that the Rockdell, Benbolt, and Witten formations are the purest and thickest limestones, and the Fleanor Shale is a major potential barrier to down-dip conduit development. Chert beds, because of their thin bedding and closely spaced fractures, do not tend to inhibit dissolution. Bedding dip, faults, and fractures in the carbonates act as infiltration pathways and sites for potential dissolution. Groundwater flow is constrained by the presence of noncarbonate units, resulting in strike-parallel cave systems.

Downcutting due to fluvial erosion and karstification since the Pliocene has resulted in the preservation of large relict cave segments in resistant carbonate ridges of the Knox Group (Rubin and Lemiszki (Reference 2.5.1-240). Copper Ridge Cave (Figure 2.5.1 40) and Cherokee Caverns, located along strike about 10 mi. (16 km) northeast of Copper Ridge Cave, are good examples (Figure 2.5.1-41). The master passages are strike-parallel and approximately horizontal, reflecting their formation in a phreatic environment. coincident with a former groundwater table. Vadose passages, formed above the water table, are oriented down-dip or along joints. A conceptual model for karst systems in the Oak Ridge area (Figure 2.5.1-42) illustrates the relationships among bedding dip, caves, other subsurface conduits, and surface topography (Reference 2.5.1-240). No evidence for hypogene karst processes has been documented in the caves of the Oak Ridge, Tennessee area, although thorough studies have yet to be conducted.

A detailed study of the West Chestnut Ridge site for a proposed waste disposal facility provides insights into the nature of the weathering profile, karst processes, and groundwater flow (Reference 2.5.1-241). West Chestnut Ridge adjoins the northeast boundary of the CRN Site (Figure 2.5.1-39), and is underlain by the Conasauga and Knox Groups. Ketelle and Huff (Reference 2.5.1-241) identify five karst zones that are stratigraphically controlled, each mapped as lines of features along strike. Karst features include dolines (sinkholes or closed depressions), solution pans (gentle sunken areas with no topographic closure), open karst throat (funnel where water disappears, also swallow hole and swallet), and a hummocky slope attributed to possible raveling of soil into bedrock cavities. They postulate that some gullies initiate where laterally flowing soil water emerges.

The West Chestnut Ridge site is mantled by thick residuum in which mature soils, classified as paleudults, have developed. The residuum is generally devoid of carbonate minerals, except at its base near the bedrock contact. Based on 10 boreholes, residual soil of variable thickness overlies a zone of cavitose carbonate bedrock with mud and gravel-filled cavities. The cavitose zone ranges in thickness from 0 to more than 100 ft. Vertical cavity dimensions varied from 1 to 16 ft (Reference 2.5.1-241).

CNL-16-162

Groundwater flow in the West Chestnut Ridge site is strongly affected by karst porosity. Field permeability tests in the soil, bedrock, and weathered bedrock, found that the range in permeability values spanned four orders of magnitude. Dye injected into a swallow hole was detected at three locations along the Clinch River arm of the Watts Bar Reservoir, yielding a flow rate of 790 to 1250 ft/day (240 to 380 m/day), thought to represent the upper bound of groundwater movement for the West Chestnut site (Reference 2.5.1-241). The dye test suggests that subsurface flow may follow strike-parallel conduits during low flow conditions and well-up and rise to additionally flow beneath the surface drainage channels during high flow conditions.

In a separate dye tracing study, conducted in response to a sewer pipe break between buildings 3019 and 3074 at the ORNL (site X-10 on Figure 2.5.1-41), dye was injected into a seven-foot high cavity found beneath the ruptured pipe (References 2.5.1-242 and 2.5.1-243). The cavity had formed in limestone of the Chickamauga Group. Dye moved primarily to the east or northeast, along strike, consistent with a model of groundwater movement controlled by solution cavities, joints, and fractures.

Evidence of deep groundwater flow has been documented within the ORR. Nativ and others (References 2.5.1-300 and 2.5.1-301) point to the presence of ancient brine at depths of more than 300 ft having geochemical signatures of partial recharge by recent waters, and to the presence of post-bomb contaminants at a depth of approximately 880 ft. Observed temperature and salinity anomalies in shallow groundwater system at ORR may be attributed to upward flow from the deep system. Nativ (References 2.5.1-300 and 2.5.1-301) also postulates that while the frequency of fractures and dissolution conduits generally decrease with depth, there are likely spatial variations where local fracture density increases and that these provide pathways for connectivity between the shallow and deep systems.

Hydrogeologists at the Tennessee Department of Environment and Conservation (TDEC) have noted evidence for connections between the shallow and deep aquifers at the ORR (Reference 2.5.1-299). Contaminants from the ORNL site are observed to flow southwest along strike through the deep aquifer.

The detection of shallow subsurface karst features using geophysical methods was studied by Doll et al., (References 2.5.1-244 and 2.5.1-245). The 1999 study examined the ability of different geophysical methods to detect a mud-filled void extending from 59 to 98 ft (18 to 30 m) depth discovered during installation of monitoring wells near the ORR Y-12 plant. Both microgravity and resistivity methods were able to detect the void. Seismic refraction data were not able to detect the void, but did detect two depressions in the bedrock surface beneath the soil. The Doll et al. (Reference 2.5.1-245) 2005 study evaluated both seismic reflection and seismic refraction data at the ORR. Seismic refraction surveys were conducted to assess the depth to bedrock and identify buried sinkholes, and were used successfully for these applications. Seismic reflection was less successful at detecting voids within the bedrock and was used primarily for mapping geologic structures. Conventional procedures for analyzing the data have inherent assumptions about the nature of the seismic velocity structure that conflict with the typical structures at karst sites, therefore they do not accurately represent the structure of the karst features. Seismic reflection studies were conducted to image bedrock structures such as faults. Karst was found to significantly influence the quality of stacked seismic reflection profiles. Doll et al. (Reference 2.5.1-245) note that similar to seismic refraction, attributes of karst structures, such as steeply dipping boundaries, rough interfaces, and laterally discontinuous interfaces are in conflict with the assumptions inherent in seismic reflection analysis.

The following text under subheading "Cave Development" of SSAR Subsection 2.5.1.2.5.1.1 is revised as indicated:

Cave Development

Caves in the study area are segments of underground dissolution passages that can be entered from the surface. The observed features of caves can provide information on the extent and patterns of subsurface dissolution that can be applied to passages that may be too small to be explored or that do not intersect the surface. The presence of extensive underground drainage systems is indicated by the presence of surface depressions, springs, and other karst features. As described in Subsection 2.5.1.2.5.1.2, cavities encountered in exploratory boreholes drilled at the site are further evidence of the presence of an underground drainage system.

Cave passages in the region can be placed into two categories based on the groundwater setting (Reference 2.5.1-35). Vadose passages form above the water table by water moving downward from the surface toward the groundwater table. Vadose passages tend to follow the steepest available openings such as vertical joints and dipping bedding planes. Their geometry can be described as slots, chimneys, shafts, pits, or canyons. Phreatic passages form at or just beneath the water table where groundwater flows laterally in the direction of the hydraulic gradient. The ideal phreatic passage is a tube-shaped conduit, reflecting dissolution on all sides in a water-filled passage. This shape is often modified by the geometry of joints and bedding planes, and the presence of less soluble strata.

As stream incision and landscape lowering proceeded during the late Tertiary and Quaternary, former phreatic passages were abandoned and left as dry cave passages beneath the hills (Reference 2.5.1-31). New phreatic passages formed at the present water table, along with vadose passages that reflect the new subsurface geometry. As the non-active solution passages, vadose or phreatic, come closer to the ground surface, they may partially fill with cave formations such as flowstone and stalagmites, or with soil from the ground surface above. The ceiling or walls may spall, forming breakdown blocks on the cave floor.

Twenty-four caves were identified in the 5-mi site radius, all of which formed in the Copper Ridge Dolomite, Chapultepec Dolomite, or Maynardville Limestone (Figure 2.5.1-47, Table 2.5.1-8). Descriptions of local caves were provided by Peter Lemiszki and Bruce Zerr. In November of 2013, TVA geologists accompanied by Mr. Zerr inspected the entrances of six caves, and conducted a geologic traverse of the interior of one cave (Figure 2.5.1-48). Brief descriptions of these caves and their genesis follow.

Cave Creek Cave is a small cave in the Mascot Dolomite that contains an active stream. Its entrance is located at the base of a bedrock wall at the margin of the valley, where the stream emerges to join the creek that flows through the valley bottom. The main passage extends horizontally northeast along strike beneath the hill of Mascot Dolomite. Several large sinkholes on the hill above probably discharge downward through enlarged vertical joints, the water exiting through Cave Creek Cave. Active stream flow and sediment transport is indicated by the presence of alluvial sand, silt, and fine gravel covering the floor of the cave, and the presence of the stream itself. The ceiling shows fresh dissolution features (Figure 2.5.1-48). This cave is a good example of an active stream passage developed along bedding strike.

Copper Ridge Cave, the largest cave in the site area, begins in a deep sinkhole on a hillside in the Copper Ridge Dolomite (Figure 2.5.1-40). The entrance passage is a stream-carved canyon that takes local water collected on the hillside then flows underground down-dip for approximately 700 ft (Figure 2.5.1-48). A 400 ft-long linear segment of the entrance passage follows a prominent northwest-oriented joint set. The wall of the entrance passage shows evidence of small-scale dissolution at the intersection of joints and bedding planes (Figure 2.5.1-48). The passage eventually intersects a 40-ft diameter, 700-ft long tube-shaped passage extending along strike (Reference 2.5.1-240). This passage, now more than one hundred feet above the level of the Clinch River, is interpreted to be a relict phreatic passage formed when base level was higher (Reference 2.5.1-253). The passage is closed off by rubble at both ends where it intersects the present ground surface at the margins of two ravines.

Flashlight Heaven Cave is a smaller segment of a similar abandoned horizontal phreatic passage. The cave is a single flattened tube-shaped passage entered from the hillside, approximately 20 ft wide and 100 ft in length (Reference 2.5.1-254). ~~The inside contains cave formations.~~ Based on its close proximity to Copper Ridge Cave, this cave may represent a segment of the same system.

Smith Cave, located on the west bank of the Clinch River arm of the Watts Bar Reservoir across from the CRN Property, is also an abandoned segment of a phreatic passage. The entrance is 35 ft above the river where fluvial incision has cut across the passage, exposing it in the bluff. The cave, formed in the Chapultepec Dolomite, extends approximately 350 ft horizontally along strike, and ends in rubble. The passage is 20 to 30 ft wide and its original phreatic shape has been modified by the deposition of flowstone and breakdown of slabs of rock from the ceiling (Figure 2.5.1-48).

Other caves in the area show similar patterns of development. Three small caves at the north margin of the CRN Property occur in the Maynardville Limestone near the contact with the Copper Ridge Dolomite, and a fourth within the Copper Ridge Dolomite. These four caves are small, each less than 300 ft in length. Two are described as relict horizontal phreatic passages oriented along strike. Passage cross-sections are influenced by the dipping bedding planes, and by the partial sediment fill on the floor. The other two caves show passage development both along strike and down-dip. In the vicinity of Melton Hill Dam, a 400 ft-long cave appears to be developed along a northwest-striking joint. This cave passage is fairly linear, oriented northwest. It follows the dip of the bedding, rising gradually from its entrance at the base of the hill, and shows signs of ceiling collapse at the uppermost end.

The following text under subheading "Summary of Local Karst Development" of SSAR Subsection 2.5.1.2.5.1.1 is revised as indicated:

Summary of Local Karst Development

Field inspection and descriptions of local caves in the 5-mi site area support the geologic model of cave development presented by Rubin and Lemiszki (Reference 2.5.1-240) for the Oak Ridge area. Cave development is strongly controlled by geologic structure and stratigraphy. Lithology is found to be a major factor; the thicker and purer limestone and dolomite units feature the larger and more extensive solution conduits, and the less-pure beds serve as barriers affecting passage size and network geometry. The orientation of the cave passages is influenced by bedding strike and dip, and joint orientation. The larger cave passages are typically relict phreatic passages that formed at the intersection of bedding and the groundwater table, and therefore are parallel to strike. A smaller number of passages are observed to follow northwest-striking joints. Vadose passages are steep to gently dipping and follow both dipping joints and bedding planes as water moves downward through these passages toward the water table.

Due to the long history of landscape lowering, abandoned or relict segments of cave passages are found at various levels beneath the hills of the site area. After abandonment, passages are divided into segments by surface erosion, and may partially fill with sediments, cave formations, and collapsed rock from the ceiling. Presently active phreatic cave passages are generally not accessible due to their position at and below the groundwater table.

The extent to which formation of these caves was initiated under deep phreatic conditions, including hypogenic conditions is not known. The generally horizontal orientation of the major phreatic passages in the caves documented suggests shallow phreatic dissolution may have played a significant major role in their formation. However, the presence of deep cavities in water wells (Reference 2.5.1-292) suggests that deep phreatic dissolution is also taking place, and may have played a role in the inception of cave formation. No clear evidence of hypogene dissolution has been documented in the site area. Cave passage geometry is consistent with either phreatic or vadose dissolution. Secondary minerals characteristic of hypogene processes, such as travertine springs or exotic minerals in caves, are not documented. Most springs in the Oak Ridge Reservation have water chemistry typical of meteoric water (Reference 2.5.1-299).

SSAR Subsection 2.5.1.2.5.1.2 is revised as indicated:

2.5.1.2.5.1.2   Karst Processes and Features at the Clinch River Nuclear Site

Documentation of karst features at the site provides the technical basis for the development of a site-specific karst model. This section begins with discussion of the properties of the geologic units expected to influence the occurrence of karst dissolution, including carbonate content, bedding characteristics, and jointing. Karst features at the site are then documented. Features consist primarily of karst depressions (also known as sinkholes or dolines) observed on the ground surface (Figure 2.5.1-37), and cavities encountered in boreholes. The data are based on geologic mapping and field reconnaissance, and on geotechnical investigations conducted for the CRBRP (Reference 2.5.1-100) and the CRN Site. Finally. the site-specific karst model is presented.

Karst Susceptibility of Site Stratigraphic Units

The susceptibility of a stratigraphic unit to karst development is strongly dependent on its properties, especially composition, bedding, and jointing characteristics. The following section presents data on the chemical and mineralogic composition of the stratigraphic units present at the site, and describes their bedding and jointing.

Rock Composition

The stratigraphic units of the Chickamauga Group that underlie the site are composed of varying proportions of calcite, dolomite, sand, silt, clay, and chert. The stratigraphic column presented in Figure 2.5.1-37, provides general lithologic descriptions. Within each unit are compositional variations among the different beds. During the 2013 geotechnical investigation, samples were taken from representative beds of each unit for mineralogic, chemical, and petrographic testing. The results of these tests, presented in Table 2.5.1-9, provide information on the percent carbonate (calcite and dolomite), a primary indicator of the susceptibility of a rock type to karst dissolution. Additional mineralogic data from rock core samples drilled for the CRBRP (Table 2.5.1-10) (Reference 2.5.1-100) are incorporated into the analysis.

The data show a range of composition in the site strata tested (Table 2.5.1 9, Sheet 1 and 2.5.1-9, Sheet 2). Significant differences in carbonate content are noted among the stratigraphic units and within each unit, shown graphically in Figure 2.5.1-49. Geologic units with the highest carbonate content are the Mascot Dolomite, the Eidson Member (included in the Blackford Formation in Figure 2.5.1-37), and the Rockdell and Benbolt Formations. The Fleanor Shale, Blackford and Bowen Formations have relatively lower carbonate contents. Regardless, carbonate is a significant component of every stratigraphic unit tested. The variability in carbonate content within any given unit (Figure 2.5.1-49) reflects the alternating interbeds of carbonate-rich and clastic-rich strata observed in the core, and typical of the Chickamauga Group within Bethel Valley (Reference 2.5.1-9). Mineralogic analyses show that the non-carbonate component is dominated by quartz, including silt, sand, and chert, with minor mica, feldspar, iron oxide, and clay.

Bedding and Jointing

Bedding planes, joints, and fracture zones constitute the initial pathways for water to penetrate the rock and begin the process of dissolution. An understanding of their orientations and spacing can help predict likely dissolution patterns. Detailed descriptions of bedding, jointing, and fracture zones are provided in Subsection 2.5.1.2.4.

Borehole contacts show that bedding is consistently oriented N52°E33°SE (Reference 2.5.1-100). Data from borehole contacts also show generally planar bedding contacts between formations within the Chickamauga Group. In contrast, the contact between the Knox Group (Mascot Dolomite) and the Chickamauga Group (Blackford Formation) is irregular at the site scale, reflecting a major erosional unconformity (Figure 2.5.1-73).

Joints encountered in the core are consistent with regional joint sets and with joint orientations recorded in boreholes drilled for the CRBRP (Reference 2.5.1-100). The CRBRP reported primary joint orientations of N52°E37°SE, N52°E58°NW, N25°E80°SW, and N65°W75°N (Reference 2.5.1-100). Discontinuity orientation data from borehole ATV and outcrop measurements collected for the CR SMR Project show that Joint set 1, oriented N60°E59°NW, is the dominant joint set at the site. Joint set 2 has an average orientation of N60°E38°SE. Minor high angle joint sets are oriented at N60°E73°SE, N40°W74°SW, and N38°W73°NE.

Karst-Related Surface Features at the Site

Karst-related surface features at the site include large funnel-shaped and dish-shaped sinkholes, and small holes in the ground. Surface features were identified by both the CRBRP and CRN Site investigations. Inspection of the CRBRP site topographic map (Figure 2.5.1-46) reveals several closed depressions, identified as sinkholes and delineated on the CRBRP site geologic map (Figure 2.5.1-46). Two major sinkhole clusters are identified, one in the Knox Group (at the contact between the Kingsport Formation and Mascot Dolomite) and the other in the Chickamauga Group (Witten Formation) (Figure 2.5.1-45). The CRBRP investigation drilled nine exploratory holes (B-60 through B-68) in the Knox Group sinkhole cluster. Soil thickness was found to vary markedly, from 2 ft at the margin of the sinkholes, to as much as 78 ft within a sinkhole. Solution voids up to four feet high were encountered below the top of rock. The sink area was found to be aligned along a high-angle northeast striking (N52°E) joint set (Reference 2.5.1-100).

The CRBRP map (Figure 2.5.1-50) also shows a line of small holes in the Unit B limestone (Rockdell Formation) along the contact with the Unit A siltstone (Fleanor Shale). The holes are described as one to two feet in diameter and three to ten feet deep, and were interpreted to represent raveling of material into solution-widened joints (Reference 2.5.1-100). One 15-ft-wide sinkhole in the Rockdell Formation was investigated by four boreholes. The top of rock illustrated the irregularity of the limestone rock surface due to solutioning along joints. Soil seams and voids up to three feet in height were encountered in the limestone. No solution, weathering or drilling water losses occurred below the contact with the Fleanor Shale (Reference 2.5.1-100).

Mapping of surface features for the Clinch River ESPA CR SMR Project using high resolution LiDAR topographic data identified the same two major sinkhole clusters, along with several additional sinkholes. Compare Figure 2.5.1-50 and Figure 2.5.1-37. Field reconnaissance shows that the large sinkhole complex in the Witten Formation consists of a large dish-shaped closed depression approximately 800 ft long by 300 ft wide, elongated along strike. The eastern end of this depression contains a steep-sided swallet with a vertical bedrock wall, corresponding to the prominent joint set striking N52°E. Based on field observations, water appears to collect and sink rapidly into the ground at this location. The western end of the larger depression is dish-shaped with a flat floor (Figure 2.5.1-45). At the time of inspection, it was covered with a thin film of silt, evidence of recent standing water. A small swallet was located at the margin of this depression. Fill now covers the southern portion of the depression.

Grading of the site during the 1980s removed some surface karst features identified by the CRBRP. A complete set of sinkholes identified by both projects is overlain on the 1973 site topographic map in Figure 2.5.1-46.

Karst-Related Subsurface Features at the Site

Karst subsurface features consist of dissolution features formed from movement of vadose and phreatic groundwater along bedding planes and joints within the rock. The primary documentation of these dissolution features comes from boreholes, Boreholes, however, provide a poor indication of the actual extent and geometry of dissolution. Due to their small diameters and the large distances between borings compared to the likely geometry of the dissolution network, boreholes show only a small fraction of the dissolution features present. However, the presence of cavities is a positive indication of the presence of a dissolution network. An understanding of the expected patterns of dissolution must be relied on to complete the picture. The occurrence of cavities in boreholes is analyzed and discussed with respect to elevation and lithologic unit.

Seismic refraction tomography surveys are useful to image near-surface karst features such as an irregular top of bedrock and shallow cavities (References 2.5.1-255 and 2.5.1-256). This method and other geophysical methods are often used in karst terrain to complement borehole analysis. A seismic refraction tomography survey, consisting of six lines, each 500 to 600 ft in length, was conducted at the site to map depth to rock (Reference 2.5.1-214). These surveys were conducted primarily in areas that had been graded as part of CRBRP construction activities. The soil and rock under the high points had been removed, and fill had been emplaced in the low points to create a planar ground surface. The resulting tomography models, therefore, primarily delineate the margins of the fill. No features were observed in the seismic refraction data that could clearly be attributed to karst phenomena.

Additionally, two seismic reflection survey lines were completed at the site during the CRN Site field investigation (Figure 2.5-36, Subsection 2.5.1.2.4.2.1). Both seismic reflection profiles show planar beds of uniformly dipping strata. The types of large-scale karst-related stacked sag structures and associated small faults observed in the Biscayne Bay, Florida, seismic reflection profiles (Reference 2.5.1-41) are not visible in the CRN lines, nor on a seismic reflection profile along Tennessee route 29 on the ORR in the CRN Site vicinity. The uniformity of the planar beds imaged by these seismic reflection profiles is evidence for the lack of any large-scale karst collapse or stacked sag features along these survey lines .

An additional source of subsurface information is documentation of the condition of the rock exposed during the 1983 excavation for the CRBRP foundation. The Fleanor Shale and Rockdell Formation strata were exposed during the excavation. Continuous exposure of rock provides a more robust picture of the dissolution network than borehole data. However, few records of the excavation were located. Those available are summarized below.

Karst Features Observed in Boreholes

Soil borings show an irregular top-of-rock beneath the soil mantle. The soil-rock interface, termed the epikarst zone (Reference 2.5.1-7, p. 120) is characterized by an irregular bedrock surface. The epikarst zone represents the dissolution weathering front, where downward penetrating water encounters soluble bedrock. The CRBRP PSAR (Reference 2.5.1-100) reports that the soil-rock contact is typically quite irregular, exhibiting rock pinnacles and intervening gaps. These irregularities are developed by solution-widening along joints and to a lesser degree along bedding planes. The wide range of soil depths over the top of rock reflects

these irregularities. Due to grading of the site during the 1980s, the irregular bedrock surface is best expressed in the CRBRP soil borings and in the CRN Site soil borings outside the graded areas. In a few of these CRN Site soil borings, blow counts are observed to decrease with depth consistent with dissolution of the rockhead and loss of the deepest horizons of the soil into slots and cavities in the rock.

Cavities, both open and clay-filled, were encountered in rock core borings drilled at the site. A total of 238 cavities, defined as being at least 0.1 ft in height in the core, were logged in rock core borings, including borings from the CRBRP drilling program (Reference 2.5.1-100) and the CRN Site drilling program (Table 2.5.1-11). Of the 180 rock core borings drilled at the site (104 for the CRBRP and 76 for the CRN Site), 75 borings, or 42 percent, encountered one or more cavities (Table 2.5.1-11). This number should be considered a minimum as not all possible solution features were logged as cavities. The CRBRP borings encountered clay intervals up to 8 ft thick in five borings (Reference 2.5.1-100). The clay was described as similar to the overburden residual soils and interpreted to represent in situ weathering. Alternatively, these intervals could represent cavities that have been filled with soil washed in from above. Weathered and fractured zones were encountered in some CRN Site borings where core losses of 1 to 3 ft took place. Dissolution is likely to have played a role in the weathering of these zones, as the lithologies are calcareous.

The frequency and size of cavities generally decrease with depth, and are observed to be greater in units with higher carbonate content (Figure 2.5.1-49, Figure 2.5.1-51). Cavity size is inferred from the observed height of that cavity in the borehole; cavity height yields no information regarding the lateral extent of that cavity. Cavities were encountered in boreholes drilled in every stratigraphic unit within the footprint of the proposed excavation, including the Blackford Formation, Eidson Member, Fleanor Shale, Rockdell Formation, and Benbolt Formation (Table 2.5.1-11). The number of borings in each unit varied and therefore the number of apparent karst features per unit may not be representative. Regional surface expression of karst is a better indicator of unit susceptibility (Plate 1; Figure 2.5.1-37; Table 2.5.1-7). The greatest number and the apparently largest cavities were encountered in borings in the Rockdell Formation, where over one hundred cavities were encountered, ranging up to 16.5 ft in height. In the Eidson Member, which is similar in composition to the Rockdell Formation but one-third the thickness, 56 cavities were encountered ranging in size up to 11 ft in height. In the interbedded siltstone and limestone of the Blackford Formation 30 cavities were encountered up to 2.5 ft in height. Finally, in the Fleanor Shale, with the lowest carbonate content of the group, 19 cavities were encountered up to 1.4 ft in height.

The distribution of cavities in cross-section illustrates the influence of lithology and bedding planes on karst development (Figure 2.5.1-51). Boreholes from both the CRBRP and the CRN Site are projected onto a plane oriented perpendicular to strike, with cavities indicated by red flags. The largest and most numerous cavities are observed in the Rockdell Formation and Eidson Member. Smaller and fewer cavities were encountered in the Blackford Formation, Fleanor Shale, and Benbolt Formation. Within the Rockdell Formation, the larger cavities appear to be aligned along bedding, suggesting the influence of bedding planes and lithologic variability among individual limestone beds. In two boreholes, the cavities occur within a pure limestone bed of Rockdell subunit D above the contact with a calcareous siltstone bed at the top of Rockdell subunit C (Figure 2.5.1-51). Here, dissolution appears to be localized in the subunit D limestone as water flows down-dip along the less soluble bed of subunit C. Natural gamma radiation downhole logs show a strong contrast in gamma-ray signal across the subunit C/D contact, suggesting the calcareous siltstone bed has significant clay content, increasing its effectiveness as an impermeable layer.

The frequency of cavities encountered in boreholes increases with increasing elevation, consistent with the generally surface-intensive nature of karst processes. Figure 2.5.1-52 plots the elevation of each cavity encountered by both the CRBRP and CRN Site borehole programs against its length, and shows the percent cavities encountered in the rock core in 50-ft elevation intervals from 600 to 900 ft elevation. The cavity percentage decreases from 9.3 percent between 850 and 900 ft to 0.2 percent between 650 and 700 ft (Figure 2.5.1-51). No cavities were encountered below 650 ft. Most cavities occur above the level of the Watts Bar Reservoir (740 ft). The concentration of cavities in this zone is consistent with karst dissolution taking place both above the water table (vadose dissolution) and at the water table (shallow phreatic dissolution). Long-term landscape lowering will have raised former phreatic conduits into the vadose zone through time. Thus, some cavities encountered in the present vadose zone may be originally phreatic in origin.

A few important cavities were encountered below the level of the reservoir, as low as 660 ft elevation (Table 2.5.1-10, Figure 2.5.1-52). Assuming that the pre-reservoir groundwater level had been no lower than the bed of the Clinch River, 719 to 720 ft (Reference 2.5.1-100), these cavities formed more than 60 ft below the groundwater table; (i.e., the piezometric surface beneath the hills would have been higher and inclined toward the water surface of the river). The presence of these cavities suggests that deeper groundwater circulation is taking place. (Reference 2.5.1-7) present a conceptual model that shows a continuum between a bathyphreatic cave and an ideal watertable cave (Figure 2.5.1-53), dependent on the degree of fracturing present in the rock. Where fractures are few, dissolution must follow the few available pathways, which may result in deep dissolution, forming bathyphreatic passages (panel 1 of Figure 2.5.1-53). Where there are many fractures, dissolution may proceed along more direct routes, forming the ideal watertable cave (panel 4 of Figure 2.5.1-53). Based on the observed distribution of cavities encountered in boreholes at the site, dissolution conduits at the site may best fit a model having a mixture of phreatic and watertable leveled components (panel 3 in Figure 2.5.1-53).

Trends in the frequency of cavities seen in the boreholes at the CRN Site show good correlation with observation well data. The occurrence and size of open fractures is greatest within the first hundred feet of the ground surface approximately (Figure 2.5.1-51, Figure 2.5.1-52). Packer tests at the site indicate that hydraulic conductivity decreases at depths greater than 100 to 150 ft below ground surface (see Subsections 2.4.12.1.4.1, 2.4.12.2.4.1 for additional details) consistent with a decrease in cavity frequency with depth. Additionally, precipitation events result in increased water levels in some observation well clusters in all screened intervals, from the upper screened intervals (15 to 105 ft below ground surface) down to the deep screened intervals (up to 297 ft below ground surface). These data indicate that meteoric water is able to permeate vertically through the formation, suggesting zones of high connectivity in the near surface, but also deeper. These data also suggest that the rate of flow at depth is likely much lower than in near surface elevations, consistent with regional trends.

A number of the cavities encountered in the boreholes were partially to completely filled with clay or soil. Drilling procedures allowed for the collection of soil samples from these cavities. Selected samples were examined visually in the field to gain insights into the origin of this material. At issue was whether the soil constituted residual material derived from dissolution of the adjacent rock, or foreign material transported into the cavity through either a horizontal conduit system or a vertical system of enlarged joints and dipping bedding planes. Most soil samples appeared to be derived either from the residuum of the rock in which they were found, or from the residual soil overburden that may have washed down through a vertical dissolution system.

CNL-16-162

In a single boring drilled for the CRBRP in the large sinkhole complex in the Knox Group, rounded grains were found in the cavity fill, suggesting possible alluvial transport (Reference 2.5.1-100). This sinkhole complex is aligned with a linear valley that extends across much of the peninsula (Figure 2.5.1-46). The sinks and the linear valley may be relict expressions of a former a phreatic conduit system extending across the peninsula along a strike-parallel vertical joint. If so, the rounded grains could represent Clinch River alluvium transported through this system.

Fifteen boreholes penetrated shear-fracture zones during the subsurface investigation (Reference 2.5.1-214; see Table 2.5.1-17). Core recovered from 100- and 200-series borings in shear-fracture zones is commonly described as calcite-healed, with rock quality generally described as high with moderate to high core recovery (Reference 2.5.1-214; see Subsection 2.5.1.2.6.4). Shear fracture zones do not appear to be loci for accelerated dissolution relative to adjacent rock.

Karst Features in the CRBRP Excavation

A potential source of information regarding subsurface karst development would be geologic documentation of the CRBRP nuclear island excavation made in 1983 (Figure 2.5.1-54). This excavation extended to an elevation of 712.5 ft primarily in the Fleanor Shale and partly in the Rockdell Formation, with 75-ft high near-vertical faces on the north, east, and south sides, and a 26-degree slope on the west side (References 2.5.1-100, 2.5.1-246, and 2.5.1-257). The CRN plant excavation may extend down through and bear on these same units. Continuous foundation exposures are the best way to evaluate the density, size and shape, and continuity of potential dissolution features, as well as the variability in the depth, severity, and lateral persistence of weathering. The CRBRP PSAR (Reference 2.5.1-100) proposed a program of geologic mapping and photography to document the condition of the rock units with respect to weathering, fractures, and dissolution, and Kummerle and Benvie (Reference 2.5.1-257) mention that geologic mapping was conducted. However, geologic records of the CRBRP excavation were not available to the CR SMR Project.

A brief statement by geologists Rubin and Lemiszki (Reference 2.5.1-240) provides some insight into the geologic conditions exposed in the CRBRP excavation:

> "...during foundation construction a number of cavities were revealed with average diameters of 0.5 to 1 m. The largest cavities occur in the thick to massive limestone beds of the Rockdell Formation."... "In addition a surprising number of small cavities are present in the mudstone-rich Fleanor Shale."

An example of similar small cavities may be the dissolution-enlarged joints observed in thin interbeds of limestone of the Blackford Formation in a road cut exposure in the City of Oak Ridge, Tennessee (Figure 2.5.1-55). Dissolution is restricted to the approximately 1 ft-thick limestone beds, which are bounded between adjacent beds of calcareous siltstone. The cavities are now filled with soil.

Karst Model for the Site

The conceptual model for karst development at the CRN Site, presented below, is developed to be consistent with concepts, observations and data derived from regional, local, and site-specific studies. The model is <u>partially illustrated in Figure 2.5.1-73 and</u> described by the following points:

1. The bedrock surface beneath the mantle of residual soil is undergoing dissolution from downward penetrating <u>meteoric</u> rainwater, resulting in an irregular top of rock with pinnacles and intervening dissolution slots<u>, or cutters</u>, formed along vertical joints. Soil can be washed down the slots into dissolution passages within the rock, creating voids which can stope upwards through the soil and eventually collapse.

2. The soil-bedrock interface, termed the epikarst (Reference 2.5.1-7, p. 120), is characterized by soft soils, cavities, and shallow groundwater. Rainwater <u>(stormflow)</u> is temporarily stored in the epikarst zone, draining both laterally along the top of bedrock, and downward through enlarged bedrock joints into the deeper karst system.

3. <u>Major</u> ~~Primary~~ phreatic dissolution pathways are strike-parallel. Groundwater flow is constrained by low-carbonate units, resulting in strike-parallel drainage systems. Phreatic conduits are localized in the high-carbonate beds, often near the intersection of the groundwater table with a bedding plane or high angle-strike-parallel joint.

4. ~~Secondary~~ <u>Additional</u> dissolution pathways occur ~~both~~ down-dip following bedding planes and lithologic contacts, and along joints.

5. The thicker and purer carbonate beds have larger and more numerous cavities and sinkholes. The Rockdell, Eidson (member), Benbolt, and Witten formations, the most carbonate-rich units in the Chickamauga Group, have relatively higher numbers of sinkholes and borehole cavities than other units. The Fleanor, Blackford, and Bowen formations the most carbonate-poor units in the Chickamauga Group, have no mapped sinkholes and smaller and fewer borehole cavities than other units.

6. Cavities in the carbonate-poor units occur within thin carbonate interbeds. The siltstone itself is calcareous and weathers primarily by dissolution; however, it leaves a silty residuum which inhibits the development of continuous conduits.

7. Long-term erosion, stream incision, and landscape lowering have resulted in older dissolution passages formed near or below the groundwater table being abandoned, segmented, filled with sediment and flowstone, and ultimately collapsed. Rock above the present groundwater table may contain any combination of active vadose passages and abandoned and/or filled vadose and phreatic passages.

8. <u>Borehole data show that</u> subsurface dissolution is most intense near the surface and decreases steadily with depth. Small numbers of cavities <u>are observed</u> below the water table. <u>This is consistent with observations of decreased fracturing frequency and groundwater flow rates with depth in the ORR studies (Reference 2.5.1-9).</u>

9. <u>Evidence of hypogene processes is not documented at the CRN Site. Fracture frequency as well as dissolution cavities significantly decrease with depth based on analyses of borehole logs (Reference 2.5.1-214). Seismic reflection profiles across the site show continuous, uninterrupted bedding at depth beneath the site suggesting that large hypogenic karst collapse features are not present, at least along the two dimensional profile lines. However, groundwater studies in the ORR area indicate some</u>

deep phreatic groundwater circulation may be occurring in the Chickamauga carbonate rock beneath the ORR area, and dissolution conduits and cavities may be present to depths of more than 800 ft (Reference 2.5.1-213).

In summary, karst was characterized at the CRN Site by an initial review of regional and local karst literature and data, followed by collection of new data for the site area and the site itself. A number of subsurface investigations were performed at the CRN Site to evaluate the presence or absence of karst. These studies included (1) geotechnical boreholes to a minimum elevation of approximately 260 ft (540 ft depth) and angled boreholes specifically for karst evaluation, (2) two seismic reflection lines, (3) field reconnaissance and mapping of surficial karst features in the site area, (4) consideration of observations from the previous CRBRP excavation, (5) evaluation of hydrothermal activity in the site region, (6) mineralogy and geochemistry of karst features, (7) review of karst models provided by others for the AGV of Virginia, and (8) comparison of karst features at the CRN Site to potential karst analogues in Florida.

At the CRN Site, evidence of both vadose and phreatic dissolution is present and appears to be controlled by the structure of the subsurface strata (i.e. bedding planes, joints, and fractures). Karst dissolution is clearly evident in the cavities encountered in boreholes, and in sinkhole features at the site. The extent of deep phreatic dissolution, below the water table, could not be evaluated based on the limits of subsurface data. However, deep phreatic dissolution likely occurs based on local groundwater studies, and the presence of favorable factors such as long flow paths, steeply dipping bedding, faults and/or fractures, rock types that are susceptible to dissolution, and locally confined and/or semi-confined aquifers.

No exhumed paleo-hypogenic karst features have been observed in the site area. Evidence for paleo-hypogenic karst including secondary or exotic minerals in caves, and hydrothermal or travertine springs are not documented in the site area. No saline water was encountered in wells to 300 ft depth at the CRN Site. Most springs in the Oak Ridge Reservation have water chemistry typical of meteoric water (Reference 2.5.1-299). Cave passage geometry in the site area is consistent with formation by vadose or phreatic epigenic processes. Isolated maze caves typical of hypogenic processes are not common in the site vicinity. These observations do not rule out the possibility that paleo-hypogenic karst features may have been modified by more recent epigenic processes.

To provide a more detailed delineation of karst features below the floor of the proposed excavation, a surface geologic mapping and subsurface exploration program will be implemented during site excavation as described in Subsection 2.5.1.2.6.10.

CNL-16-162

SSAR Subsection 2.5.1.2.5.1.3 is revised as indicated:

2.5.1.2.5.1.3 Potential Karst Hazard at the CRN Site

The CRN plant structures may be placed in deep excavations that <u>will likely</u> extend below the level of the Watts Bar Reservoir.~~, to an elevation of approximately 681 ft. The northern portion of the power block area will bear on the Fleanor Shale and Eidson Member; the southern portion of the power block area will bear on the Benbolt and Rockdell Formations.~~ Overburden soils and cavities associated with dissolution near the top of rock will be removed during the excavation process. Therefore, there is little hazard of a cover-collapse or subsidence sinkhole, the most common sinkhole type in the site area. However, cavities have been observed in boreholes as deep as 660 ft elevation (Table 2.5.1-11). <u>A complete understanding of the extent and spatial distribution of these cavities or other potential karst cavities contains some uncertainty, however, the significant amount of data collected at the CRN Site during this investigation, as well as during past investigations and excavations, provides a comprehensive understanding of the karst setting within approximately 300 ft of the ground surface.</u>

These cavities pose three types of <u>potential karst</u> hazards to the proposed structures.

First, the potential presence of cavities in the excavation walls below the groundwater table may pose a hazard to the safety of the excavation; Groundwater may discharge from the cavities, making it difficult to maintain a dry excavation, and the water may affect slope stability during construction. If the cavities are small or discharges are small, they may be mitigated, for example, by grouting. If they are large or are discharging large volumes of water, grouting may be difficult or ineffective. A large cavity with a high discharge may represent a segment of an active phreatic passage. The CRBRP (Reference 2.5.1-100) anticipated this potential hazard. However, documentation from the CRBRP excavation into the Fleanor Shale show the excavation to have been relatively dry (Reference 2.5.1-257).

Second, the presence of cavities below the base of the foundation may require mitigation to ensure foundation stability. Small cavities that are exposed in the excavation floor or wall can be mitigated, for example by grouting. Slightly deeper cavities that cannot be seen may be detected using geophysical methods or boreholes in the finished excavation. If detected, engineering analyses can determine the appropriate mitigation for these cavities. <u>Additional measures to confirm understanding of karst hazard at the CRN Site are discussed in Subsection 2.5.1.2.6.10.</u> Final conclusions regarding karst hazard ~~are~~ <u>will be</u> based on detailed geologic mapping of the excavations and geophysical surveys at foundation level.

Third, the presence of cavities can enable rapid movement of an accidental release. Accidental releases are evaluated in Subsection 2.4.13.

As a result of the revised text in Subsection 2.5.1.2.5.1, the following references are added at the end of SSAR Subsection 2.5.1.3:

References   2.5.1.3

2.5.1-289.   Klimchouk, A. B. 2007. *Hypogene Speleogenesis: Hydrogeological and Morphogenetic Perspective. Special Paper no. 1*, National Cave and Karst Research Institute, 106 pp.

2.5.1-290.   Ford, Derek C., and Williams, Paul W., *Karst geomorphology and hydrology*, "Chapter 1, Introduction to karst,", p. 1-9, and "Chapter 7, Cave systems," p. 242-315, Unwin Hyman Ltd., London, 1989.

2.5.1-291.   Bretz, J.H., 1942, *Vadose and phreatic features of limestone caves: The Journal of Geology*, v. 50, no. 6, p. 675-811.

2.5.1-292.   Wolfe, W. J., Haugh, C. J., Webbers, A., and Diehl, R. H., *Preliminary conceptual models of the occurrence, fate, and transport of chlorinated solvents in karst regions of Tennessee*, U. S. Geological Survey, Water Resources Investigations Report 97-4097, 1997.

2.5.1-293.   Worthington, S.R.H., and Ford, D.C., 1995, *High sulfate concentrations in limestone springs: An important factor in conduit initiation?*,: Environmental Geology, No. 25 Vol. 1, p. 9-15.

2.5.1-294.   Hill, C.A., 2000, *Sulfuric acid hypogene karst in the Guadalupe Mountains of New Mexico and West Texas*, in Klimchouk, A.B., Ford, D.C., Palmer, A.N., and Dreybrodt, W., eds., Speleogenesis: *Evolution of karst aquifers: Huntsville, Alabama*, National Speleological Society, p. 309-316.

2.5.1-295.   Klimchouk, A.B., 2014, *The Methodological Strength of the Hydrogeological Approach to Distinguishing Hypogene Speleogenesis*, in Klimchouk, A., Sasowsky, I., Mylroie, J., Engel, S.A., and Engel, A.S., Eds., Hypogene Cave Morphologies. Selected papers and abstracts of the symposium held February 2 through 7, 2014, San Salvador Island, Bahamas. Karst Waters Institute Special Publication 18, Karst Waters Institute, Leesburg, Virginia, p. 4-12.

2.5.1-296.   Doctor, D. H., and Orndorff, W., 2016, *Deep phreatic influence on the origin of caves and karst in the central Appalachian Great Valley*, in: Chavez, T., and Reehling, P., eds., Proceedings of DeepKarst 2016: Origins, resources, and management of hypogene karst, National Cave and Karst Research Institute, Symposium 6, p. 89-104.

2.5.1-297.   Doctor, D.H., Weary, D.J., Brezinski, D.K., Orndorff, R.C., and Spangler, L.E., 2015, *Karst of the Mid-Atlantic region in Maryland, West Virginia, and Virginia, Geological Society of America*, Field Guide 40, p. 425-484.

2.5.1-298.   Doctor, Daniel H., 2016, *Personal communication regarding hypogene karst, telephone interview conducted September 7, 2016*, by Janet Sowers, Kevin Clahan, Dave Fenster, Mike Buga, Alan Troup, Rebecca Carr, Matt Huebner, and Walter Justice.

2.5.1-299.   Davies, Gareth, Jones, Sidney, and Gephart, Thomas, 2016, *Personal communication regarding evidence for deep karst dissolution at the Oak Ridge Reservation, telephone interview conducted September 9, 2016*, by Janet Sowers, Kevin Clahan, Mike Buga, Alan Troup, Rebecca Carr, Matt Huebner, Hillol Guha, and Walter Justice.

2.5.1-300.   Nativ, R., 1996, *The Brine Underlying the Oak Ridge Reservation, Tennessee, USA: Characterization, Genesis, and Environmental Implications*, Geochimica et Cosmochimica Acta, Vol. 60, No. 5, p. 787-801.

2.5.1-301.   Nativ, R., Halleran, A., Hunley, A., 1997, *Evidence for Ground-Water Circulation in the Brine-Filled Aquitard, Oak Ridge, Tennessee, Ground Water*, Vol. 35, No. 4. P 647-713.

2.5.1-302.   Worthington, S. R. H., 2001, *Depth of conduit flow in unconfined carbonate aquifers: Geology*, v. 29, no. 4, p. 335-338.

As a result of the revised text in Subsection 2.5.1.2.5.1, the following Figures are added at the end of SSAR Subsection 2.5.1:

Figure 2.5.1-69.   Karst Hydrogeologic Model for the Valley and Ridge Region, Tennessee

Figure 2.5.1-70.   Epigenetic and Hypogenetic Karst in Basinal Groundwater Flow

Figure 2.5.1-71.   Isolated Phreatic Maze Cave Development in and Anticline Near a Fault

Figure 2.5.1-72.   Schematic Vertical Relationships of Groundwater Flow Zones in the ORR

Figure 2.5.1-73.   Karst Model of the CRN Site

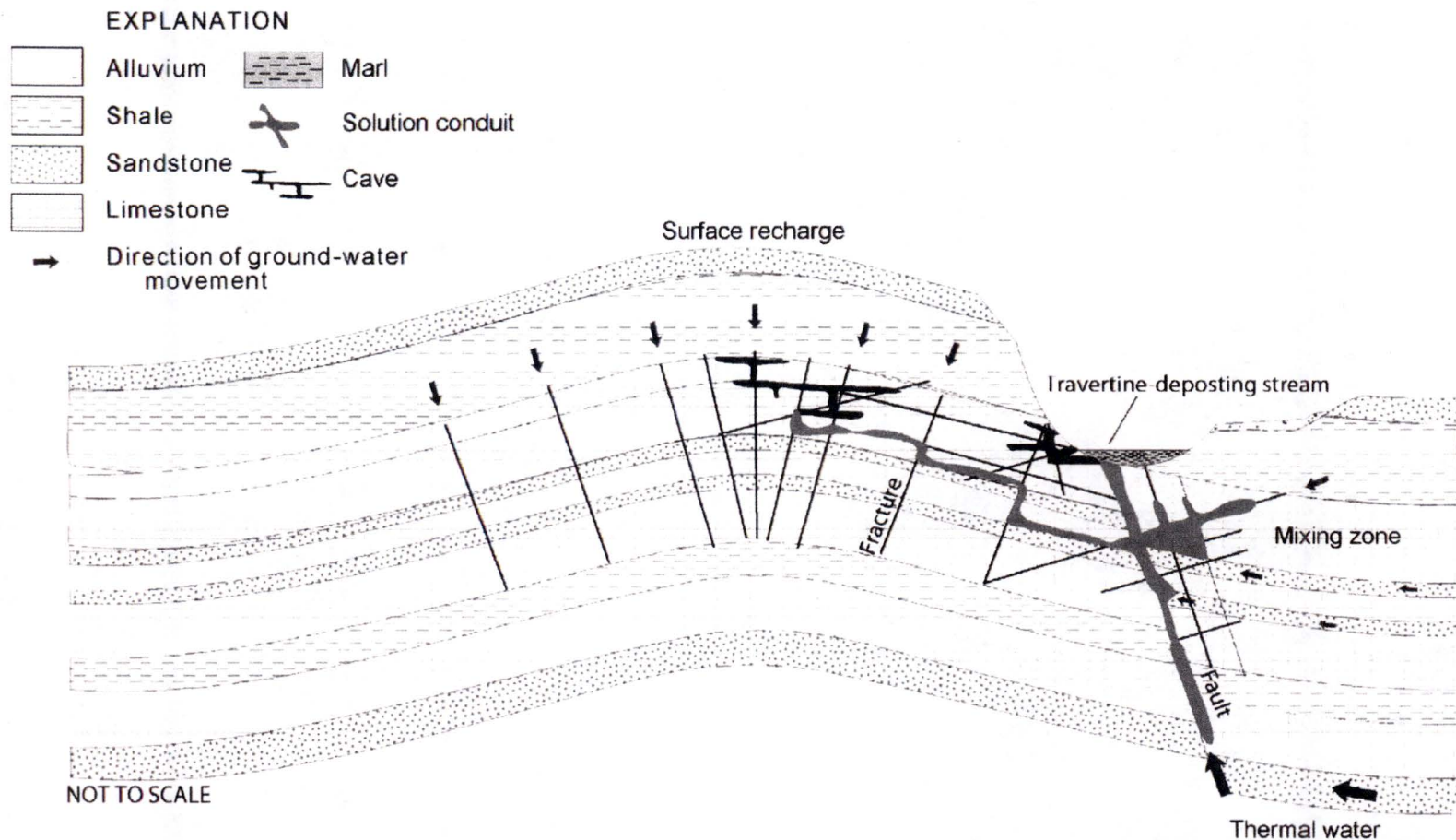**Copies of the new Figures are provided on the following pages.**
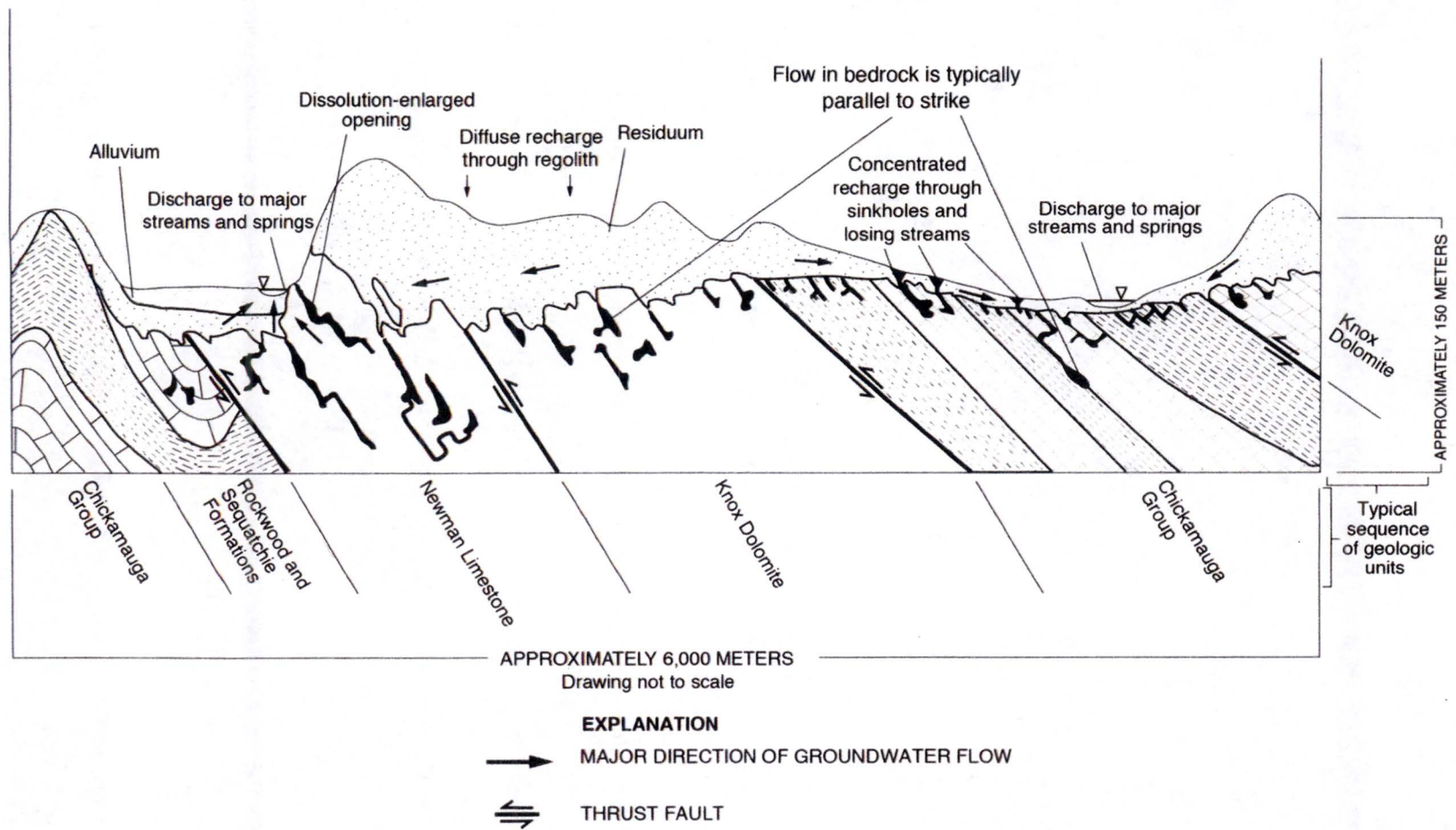
Figure 2.5.1-69. Karst Hydrogeologic Model for the Valley and Ridge Region, Tennessee
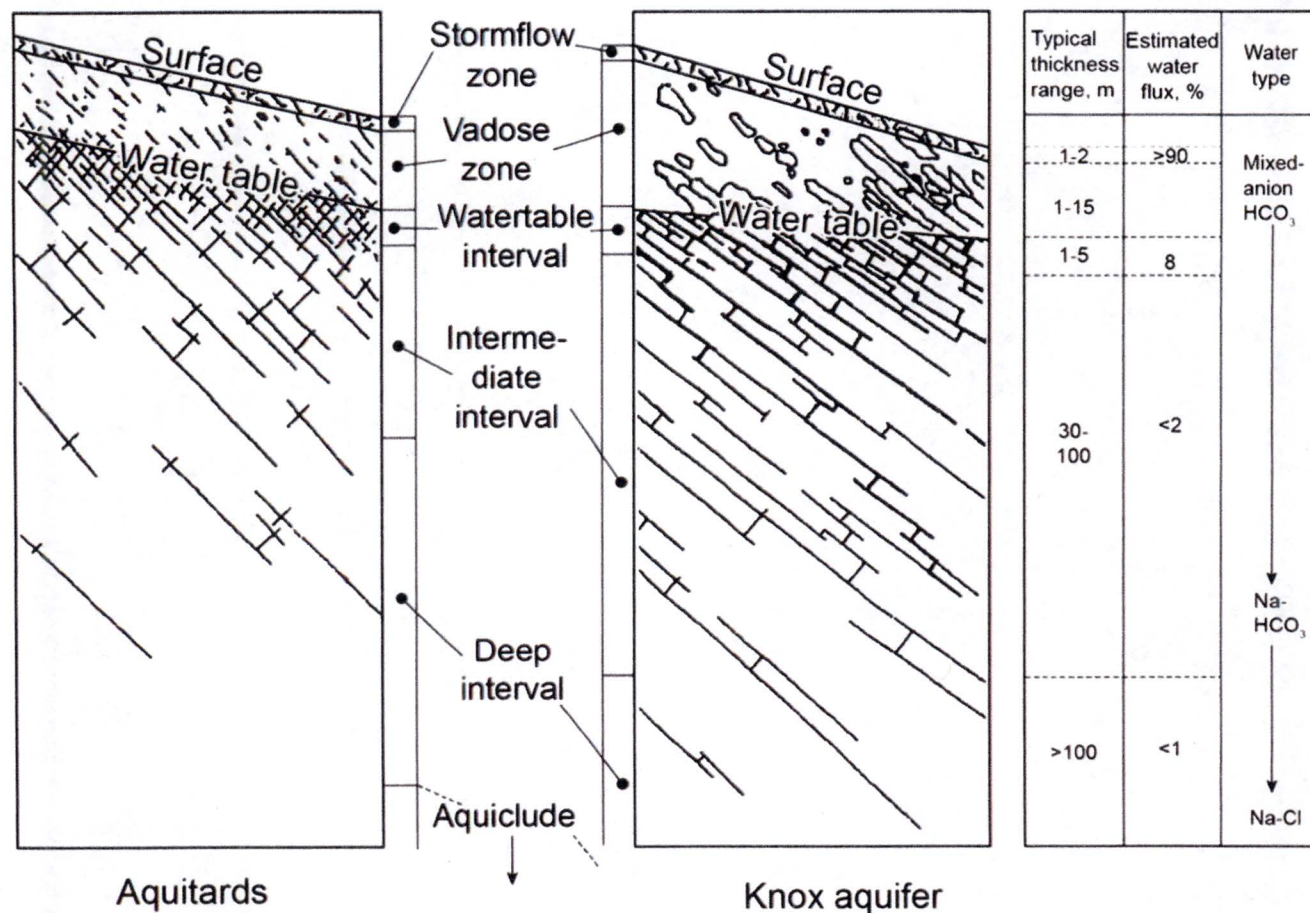
From Reference 2.5.1-292.

CNL-16-162
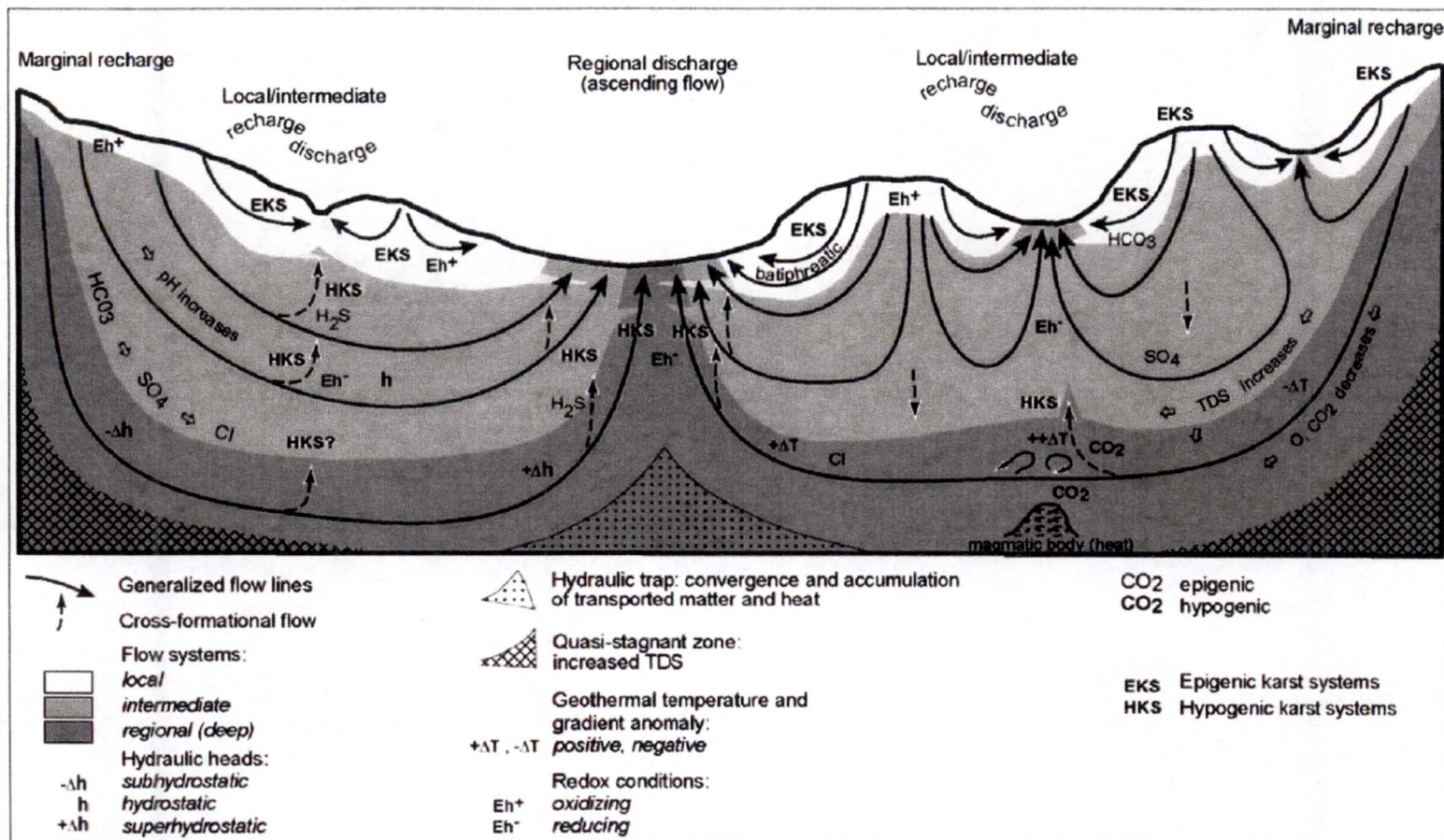
Epigenic and hypogenic karst in the context of basinal groundwater flow. The figure shows mainly gravity-driven flow in an idealized homogenous basin. In reality, most sedimentary sequences are highly heterogeneous, and gravity-driven flow interacts with other flow mechanisms. From Reference 2.5.1-289.

Figure 2.5.1-70. Epigenetic and Hypogenetic Karst in Basinal Groundwater Flow

EXPLANATION

Alluvium Marl

Shale Solution conduit

Sandstone Cave

Limestone

→ Direction of ground-water movement

Surface recharge

Travertine-deposting stream

Fracture

Fault

Mixing zone

Thermal water

NOT TO SCALE

Schematic illustration of isolated phreatic maze cave development within a mixing zone localized near to a fault. Rising water along the fault intersects the shallow karst aquifer, and creates cavernous porosity in the mixing zone. If rising fluids were initially hydrothermal, alteration of the bedrock along fractures may result in slightly more resistance to weathering, and result in a cave located within a hill on the land surface. From Reference 2.5.1-296.

Figure 2.5.1-71. Isolated Phreatic Maze Cave Development in and Anticline Near a Fault

Schematic vertical relationships of flow zones of the ORR, estimated thicknesses, water flow, and water types. From Hatcher et al. (Reference 2.5.1-9), Chapter 7

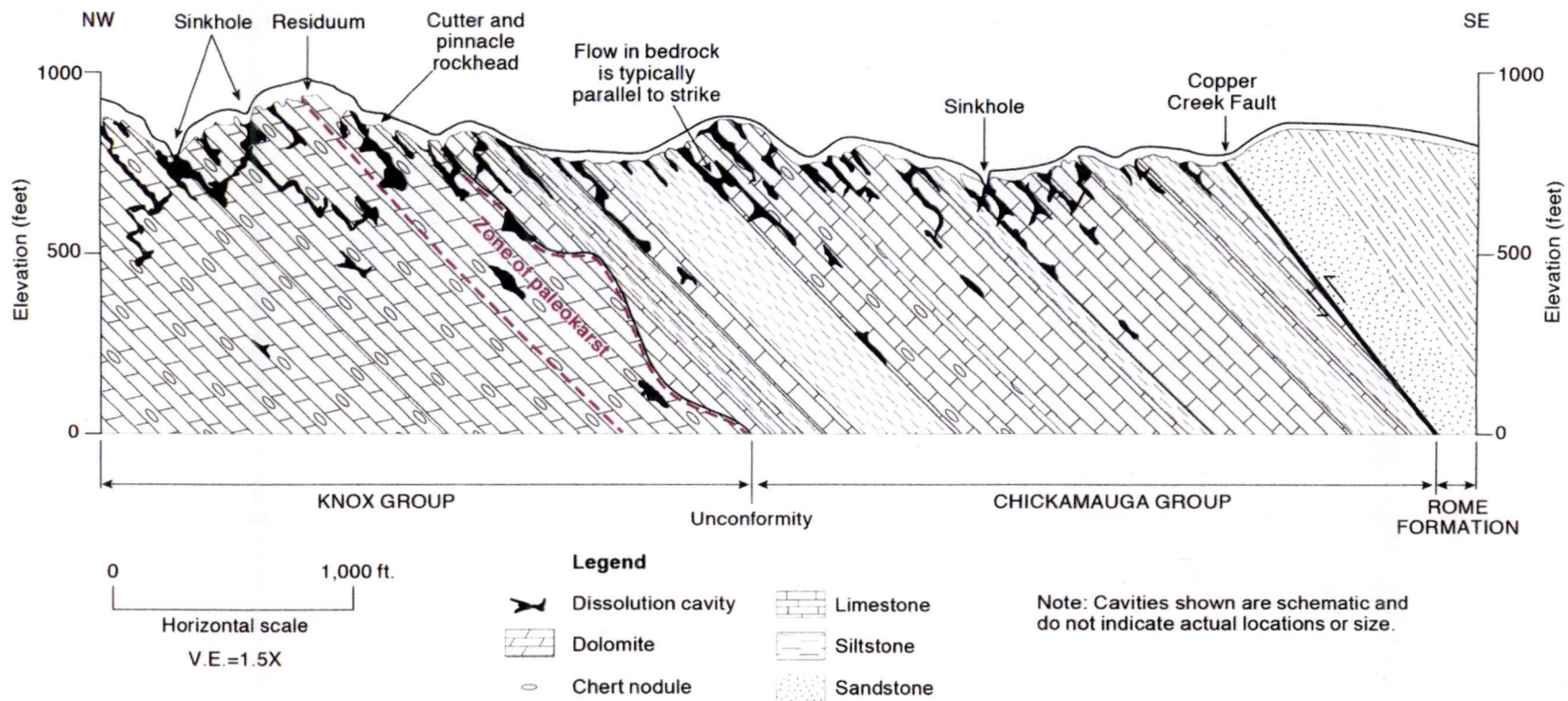**Figure 2.5.1-72. Schematic Vertical Relationships of Groundwater Flow Zones in the ORR**

Figure 2.5.1-73. Karst Model of the CRN Site

ENCLOSURE 3

SUPPLEMENTAL INFORMATION RELATED TO
STABILITY OF SUBSURFACE MATERIALS AND FOUNDATION
OF THE EARLY SITE PERMIT APPLICATION FOR CLINCH RIVER NUCLEAR SITE

By letter dated May 12, 2016 (Reference 1), Tennessee Valley Authority (TVA) submitted an application for an early site permit for the Clinch River Nuclear (CRN) Site in Oak Ridge, TN. Subsequent to the submittal of the application, and consistent with interactions with NRC staff, TVA identified certain aspects of the application that it intends to supplement. By letter dated August 11, 2016 (Reference 2), TVA provided a plan for submitting the identified supplemental information.

This enclosure provides supplemental information related to Stability of Subsurface Materials and Foundation to support the NRC staff's review.

Supplement Item (Reference 2)

TVA will provide a markup of the applicable ESPA sections to include additional information for "Karst Features," regarding:

- *the size (both in vertical and horizontal directions) and spatial distribution of subsurface voids at the site, and;*
- *a plan for additional geophysical studies and a preliminary grouting program to evaluate and address the voids within the sub-foundation area (zone of influence) are large enough to affect the stability of foundations and structures during the life time of a planned nuclear power plant.*

Supplemental Information

Subsequent to August 11, 2016, TVA conducted a comprehensive review of the applicable ESPA sections to identify where additional information for "Karst Features" would be useful. As described in more detail below, based on that review, TVA has concluded that site characterization information included in the ESPA meets or exceeds applicable regulations and guidance, such that no additional or revised information is necessary.

Consistent with regulatory guidance in the NUREG 0800, "Standard Review Plan for the Review of Safety Analysis Reports for Nuclear Power Plants, LWR Edition," and Regulatory Guide 1.206, "Combined License Application for Nuclear Power Plants," Site Safety Analysis Report (SSAR) Section 2.5.1.2.5.1.1 discusses karst features in the region and vicinity of the Clinch River Nuclear (CRN) Site, while SSAR Section 2.5.1.2.5.1.2 discusses karst features at the CRN Site. Information specific to the CRN Site subsurface investigations is provided, as well as information gathered during excavation of the foundation for the Clinch River Breeder Reactor Project (CRBRP) at its location adjacent to the CRN Site.

A catalog of potential karst cavities encountered during subsurface investigation (i.e., borings) for both the CRBRP and CRN Site is provided in SSAR Table 2.5.1-11. This catalog includes the length of the cavity (vertical extent of rod drop) and provides the data for the distribution of depth and size of karst features depicted in Figure 2.5.1-52. Figure 2.5.1-51 is a cross section that depicts the spatial relationship of the cavities, indicated in borings associated with the CRN

Site subsurface investigation, with example Reactor Building Locations A and B and depth associated with the plant parameter envelope (PPE). For the ESPA, no specific reactor building footprint is provided, but rather a reactor building area is designated. The reactor building area is the area, considering the different small modular reactor technologies, in which the reactor buildings would likely be sited.

Although much information has been gathered about the CRN Site, a quantitative estimate of the horizontal extent of the potential karst cavities or the spatial distribution of these cavities is not practical, beyond that which is described currently in the SSAR, absent additional characterization that requires design-specific information. Accordingly, SSAR Section 2.5.1.2.6.10 currently outlines actions to be detailed in the combined license application (COLA) and completed as a part of excavation and construction to confirm the current understanding of karst at the CRN Site, to ensure that the size, distribution, and extent of karst cavities are identified commensurate with the potential impact of karst on safety-related structures. These actions include:

- performing detailed geologic mapping of excavation walls during excavation/construction, allowing documentation of the characteristics of dissolution features in the near-surface carbonate rock units and verification of the decrease in cavity size and abundance with depth, as predicted by the subsurface investigation and geological mapping

- performing a PLAXIS, or similar, analysis in support of COLA to provide information about the minimum size of a potential undetected cavity that could adversely affect foundation performance for a given range of depths below safety-related structures

- designing and conducting additional surface geophysical surveys during excavation/construction to detect cavities below the foundation elevation that are larger than the minimum postulated by the PLAXIS analysis that could adversely affect foundation performance

- performing confirmatory drilling or borehole testing during excavation/construction to characterize the source of geophysical anomalies, if detected

- developing a grouting program, based upon the information obtained by the geologic mapping, geophysical surveys and PLAXIS (or similar analysis), to mitigate the effect of voids or cavities on foundation performance at and below the foundation levels of safety-related structures.

Duke Energy Florida and Florida Power and Light Company have addressed the potential for karst and have developed associated plans for its mitigation in the COLAs for Levy County (Reference 3) and Turkey Point Units 6 and 7 (Reference 4), respectively. These applications include plans for excavation mapping at the time of construction and grouting programs based upon postulated void size and the building/foundation design for the NRC-certified AP1000.

Accordingly, this information is best provided/developed during the COLA/Construction stage for the following reasons:

- Currently, the floor of the excavation, based on the surrogate plant defined by the PPE, would be located greater than 138 feet below ground surface. Resolution of geophysical surveys generally decreases with depth. Accordingly, geophysical surveys performed at ground surface (at the time of ESPA), rather than at the excavation floor (at the time of

excavation/construction), will have a significantly decreased ability to assess the size and extent of karst at locations below the foundation.

- Karst dissolution characteristics and stratigraphy vary with location throughout the site and with depth. The specific locations and foundation depths of safety-related buildings depend upon the reactor technology, which has not yet been selected.

- Other parameters (such as foundation loads, foundation dimensions, foundation thickness, deformation limits [e.g., angular distortion or differential settlement], and elastic modulus of foundation) are required to perform a PLAXIS, or similar analysis to determine the minimum size of an undetected cavity that could adversely affect foundation performance. These parameters are dependent upon the technology, which has not yet been selected.

- Because the size and distribution of karst dissolution features vary with depth and stratigraphic unit, a site-specific grouting program should be developed based on excavation size, foundation depth, and building location associated with the chosen technology and the results of the PLAXIS analysis. For the detailed grouting program to be effective, it would be informed by the mapping of the excavation, results of surface geophysical surveys conducted on the floor of excavations, and the maximum acceptable undetected void size versus depth, as determined in the PLAXIS analysis. In addition, a grout testing program would be developed to determine the grout mix to be used, grouting pressures, and closure criteria.

- Performance of additional geophysical surveys or analyses to support ESPA would not eliminate the need for those actions currently proposed in SSAR Subsection 2.5.1.2.6.10 to support COLA/construction after the reactor technology has been chosen.

During the January 13, 2016, public meeting on seismic and geotechnical topics and subsequent discussions regarding the ESPA, NRC asked TVA about the possibility of performing additional surveys to determine suitability of the site. In consideration of the information above, TVA evaluated the option of performing additional geophysical surveys to provide additional information about the vertical and horizontal extent of karst features and their spatial distribution at the site. Three methods of surface geophysical survey were evaluated: electrical resistivity imaging (ERI), multi-channel analysis of surface waves (MASW), and high-resolution shear wave seismic reflection. The ERI method would detect variations in earth resistivity (inverse of electrical conductivity) that could indicate the presence of karst-related bedrock voids significant to foundation performance. The MASW and high-resolution shear wave reflection surveys would detect changes in shear wave velocity (Vs) within the rock mass that could be related to the presence of karst voids and solution cavities significant to foundation performance. A surface-based geophysical survey and the proposed geophysical surveys proposed at the foundation during construction would not provide sufficient information to eliminate uncertainty regarding the spatial distribution and sizes of dissolution features to the extent needed for the COLA. However, a site-specific grouting program based on results of the additional analysis performed for the chosen reactor technology and geophysical surveys will constrain the potential sizes of subsurface voids and greatly reduce or eliminate that uncertainty.

Accordingly, sufficient characterization of the site for karst features has been completed for the regulatory requirements of the ESPA. TVA has outlined future actions, in SSAR Subsection 2.5.1.2.6.10, which include performing additional detailed excavation mapping and analyses, as stated previously in this response.

References:

1. Letter from TVA to NRC, CNL-16-081, "Application for Early Site Permit for Clinch River Nuclear Site," dated May 12, 2016

2. Letter from TVA to NRC, CNL-16-134, "Schedule for Submittal of Supplemental Information in Support of Early Site Permit Application for Clinch River Nuclear Site," dated August 11, 2016

3. Duke Energy Florida, LLC, Levy Nuclear Plants COL Application, Rev. 9, April 6, 2016.

4. Florida Power and Light Company, Turkey Point Units 6 and 7 COL Application, Rev. 7, October 14, 2015.

ENCLOSURE 4

CD ROM, REVISED SITE VICINITY GEOLOGIC MAP PLATES

CNL-16-162